

UNCLASSIFIED

AD NUMBER

AD907816

NEW LIMITATION CHANGE

TO

**Approved for public release, distribution
unlimited**

FROM

**Distribution authorized to U.S. Gov't.
agencies only; Test and Evaluation; 29 DEC
1972. Other requests shall be referred to
Air Force Flight Dynamics Laboratory,
Attn: PTB, Wright-Patterson AFB, OH 45433.**

AUTHORITY

AFWAL ltr, 11 Feb 1980

THIS PAGE IS UNCLASSIFIED

AD 907816

AFFDL-TR-72-147 - VOL. III

**PROPULSION SYSTEM
INSTALLATION CORRECTIONS**

**VOLUME III:
SAMPLE CASES**

W. H. BALL
THE BOEING COMPANY

1 D D C
PROPR 1972
MAR 6 1973
RIGBY E

**TECHNICAL REPORT AFFDL-TR-72-147 - VOL. III
DECEMBER 1972**

Distribution limited to U.S. Government agencies only.
test and evaluation; statement applied 28 December 1972.
Other requests for this document must be referred to Air
Force Flight Dynamics Laboratory (PTB), Wright-Patterson
Air Force Base, Ohio 45433

**AIR FORCE FLIGHT DYNAMICS LABORATORY
AIR FORCE SYSTEMS COMMAND
WRIGHT-PATTERSON AIR FORCE BASE, OHIO 45433**

NOTICE

When Government drawings, specifications, or other data are used for any purpose other than in connection with a definitely related Government procurement operation, the United States Government thereby incurs no responsibility nor any obligation whatsoever; and the fact that the Government may have formulated, furnished, or in any way supplied the said drawings, specifications, or other data, is not to be regarded by implication or otherwise as in any manner licensing the holder or any other person or corporation, or conveying any rights or permission to manufacture, use, or sell any patented invention that may in any way be related hereto.

Copies of this report should not be returned unless return is required by security considerations, contractual obligations, or notice on a specific document.

**PROPELLION SYSTEM
INSTALLATION CORRECTIONS
VOLUME III:
SAMPLE CASES**

W.H. RALL

Distribution limited to U.S. Government agencies only.
test and evaluation, statement applied 29 December 1972.
Other requests for this document must be referred to Air
Force Flight Dynamics Laboratory (PTB), Wright-Patterson
Air Force Base, Ohio 45433

FOREWORD

This report was prepared by the Research and Engineering Division, Aerospace Group, of The Boeing Company under Air Force Contract F33615-72-C-1580, "Propulsion System Installation Corrections", Project 1366. The program was conducted under the direction of the Prototype Division, Air Force Flight Dynamics Laboratory, Air Force Systems Command. Mr. Gordon Tamplin was the Air Force Program Monitor.

The program was initiated on 31 December 1971 and draft copies of the final reports were submitted for approval on 31 October 1972.

Dr. P. A. Ross was Program Manager and Mr. W. H. Ball was principal investigator during the program. Significant contributions to the program were made by the following individuals: Mr. Joe Zeeben, engine performance; Dr. Franklin Marshall, inlet and exhaust system technology; Mr. John Petit, nozzle internal performance and nozzle/afterbody drag; and Mr. Gary Shurtleff, programming.

This report contains no classified information extracted from other classified reports.

Publication of this report does not constitute Air Force approval of the report's findings or conclusions. It is published only for the exchange and stimulation of ideas.

Ernest J. Cross Jr.

Lt. Col. Ernest J. Cross, Jr.
Chief, Prototype Division
Air Force Flight Dynamics Laboratory

ABSTRACT

This report presents the results of a research program to develop a procedure for calculating propulsion system installation losses. These losses include inlet and nozzle internal losses and external drag losses for a wide variety of subsonic and supersonic aircraft configurations up to Mach 4.5. The calculation procedure, which was largely developed from existing engineering procedures and experimental data, is suitable for preliminary studies of advanced aircraft configurations. Engineering descriptions, equations, and flow charts are provided to help in adapting the calculation procedures to digital computer routines. Many of the calculation procedures have already been programmed on the CDC 6600 computer. Program listings and flow charts are provided for the calculation procedures that have been programmed. The work accomplished during the program is contained in four separate volumes. Volume I contains an engineering description of the calculation procedures. Volume II is a programmer's manual containing flow charts, listings, and subroutine descriptions. Volume III contains sample calculations and sample input data. Volume IV contains bookkeeping definitions and data correlations.

TABLE OF CONTENTS

SECTION	Page
I INTRODUCTION	1
II LIGHTWEIGHT FIGHTER SAMPLE CASE	5
2.1 Configuration	5
2.1.1 Inlet	5
2.1.2 Nozzle/Afterbody	5
2.2 Predicted Performance Characteristics	5
2.2.1 Inlet	5
2.2.2 Nozzle/Afterbody	27
2.3 Comparison of Predicted and Test Data	28
2.4 Summary of Input Data for Lightweight Fighter	36
III F-4J SAMPLE CASE	37
3.1 Configuration	37
3.1.1 Inlet	37
3.1.2 Nozzle/Afterbody	37
3.2 Predicted Performance Characteristics	44
3.2.1 Inlet	44
3.2.2 Nozzle/Afterbody	44
3.3 Comparison of Predicted and Test Data	44
3.4 Summary of Input Data for F-4J	56
3.5 Sample Input Data and Output Data	57
REFERENCES	77

LIST OF ILLUSTRATIONS

Figure No.	Title	Page
1	General Arrangement Drawing of Lightweight Fighter Study Configuration	2
2	General Arrangement, F-4J	3
3	Two-Dimensional Inlet Details	6
4	Subsonic Diffuser Internal Lines	7
5	LWF Subsonic Diffuser Area Variation	8
6	LWF Nozzle/Afterbody External Lines	9
7	Local Mach Number vs. Free-Stream Mach Number for LWF	14
8	LWF Recovery vs. Mass Flow	15
9	Matched Inlet Recovery	16
10	Matched Mass Flow	17
11	Buzz Limit	18
12	Distortion Limit	19
13	Reference Mass Flow	21
14	K_{ADD} Factors for LWF Spillage Drag Prediction	22
15	Spillage Drag for LWF	23
16	Boundary Layer Bleed Airflow	24
17	Boundary Layer Bleed Airflow Total Pressure Recovery	25
18	Boundary Layer Bleed Drag	26
19	Nozzle Boattail Pressure Drag Coefficients as $f(\beta)$	29

LIST OF ILLUSTRATIONS (Continued)

Figure No.	Title	Page
20	Boattail Drag Correction for Nozzle Pressure Ratios Other Than $P_T/P_\infty = 2.5$	30
21	LWF Reference Drag for Nozzle/Afterbody	31
22	Comparison of Predicted and Measured Inlet Recovery	32
23	Comparison of Predicted Data and Test Data for LWF Spillage Drag	33
24	Comparison of Predicted and Test Data for Nozzle/Afterbody Drag	34
25	Comparison of Predicted and Test Data for Subsonic Nozzle/Afterbody Drag as a Function of Nozzle Pressure Ratio	35
26	Basic F-4J Fuselage, Canopy, and Duct Configuration	38
27	F-4 Inlet Ramp Orientation	39
28	Inlet Geometry for $M_\infty = 0-1.20$	40
29	Inlet Geometry for $M_\infty = 1.60-2.0$	41
30	Model F-4J/B Nozzle & Shroud Arrangement	42
31	Nozzle Geometry and Operating Conditions	43
32	Local Mach Number vs Free-Stream Mach Number	45
33	Total Pressure Recovery vs Mass Flow Ratio	46
34	Matched Inlet Recovery	47
35	Matched Inlet Mass Flow Ratio	48
36	Buzz Limit	49

LIST OF ILLUSTRATIONS (Continué)

Figure No.	Title	Page
37	Distortion Limit	50
38	Reference Mass Flow Ratio	51
39	Inlet Spillage Drag	52
40	Boundary Layer Bleed Drag	53
41	Boundary Layer Bleed Airflow	54
42	Reference Nozzle Drag for F-4J	55

SYMBOLS AND NOMENCLATURE

A	Area, in ²
A_C	Inlet capture area, in ²
A_0	Local stream tube area ahead of the inlet, in ²
A_{0_I}	Free-stream tube area of air entering the inlet, in ²
R	Aspect ratio, dimensionless
B	Velocity decay exponent, dimensionless
C	Sonic velocity, ft/sec.
C_D	Drag coefficient, $\frac{D}{qA_{REF}}$, dimensionless
C-D	Convergent-divergent
$C_{D_{ADD}}$	Additive drag coefficient, $C_{D_{ADD}} = \frac{D_{ADD}}{qA_C}$, dimensionless
C_{D_A} _{MAX}	Afterbody drag coefficient, $\frac{DRAG}{qA_{MAX}}$, dimensionless
$C_{D_{Base}}$	Base drag coefficient $\frac{(P_b - P_\infty) A_{BASE}}{qA_{MAX}}$, dimensionless
C_{D_S}	Scrubbing drag coefficient, $\frac{DRAG}{qA_{MAX}}$, dimensionless
C_f _g	Thrust coefficient, $\frac{F}{\frac{W}{g} (V_{cp})}$, dimensionless
C_S	Stream thrust coefficient, dimensionless, (defined by Figure 48 of Volume IV)
C_V	Nozzle velocity coefficient, dimensionless
Conv.	Convergent
D	Drag, lb.; Hydraulic Diameter, $\frac{4A}{P}$, in., diameter, in.

SYMBOLS AND NOMENCLATURE (Continued)

F	Thrust, lb.
F_{g_i}	Ideal gross thrust (fully expanded), lb.
f/a	Fuel/air ratio, dimensionless
g	Gravitational constant, ft/sec^2
h	Enthalpy per unit mass, BTU/lb.; height, in.
h_{fan}	Enthalpy of fan discharge flow, BTU/lb
h_{pri}	Enthalpy of primary exhaust flow after heat addition BTU/lb
h_t	Throat height, in ²
K	Velocity decay coefficient, dimensionless
L	Length, in.
M	Mach number, dimensionless
P	Pressure, lb/in^2
P_r	Relative pressure; the ratio of the pressures p_a and p_b corresponding to the temperatures T_a and T_b , respectively, along a given isentrope, dimensionless
P_T	Total pressure, lb/in^2
Q	Effective heating value of fuel, BTU/lb.
q	Dynamic pressure, lb/in^2
R, r	Radius, in.
S	Nozzle centerline spacing, in.
T	Temperature, °R
V	Velocity, ft/sec

SYMBOLS AND NOMENCLATURE. (Continued)

W	Mass flow, lb/sec
W_{BX}	Bleed air removed from engine, lb/sec.
$W_C, \frac{W \sqrt{\theta}}{\delta}$	Corrected airflow, lb/sec.
W_f	Weight flow rate of fuel, lb/sec.
W_2	Weight flow rate of air, primary plus secondary, lb/sec.
W_8	Primary nozzle airflow rate, lb/sec.
x	Length, in.
α	Angle of attack; convergence angle of nozzle, degrees
γ	Ratio of specific heats, dimensionless
ϵ	Diffuser loss coefficient, $\frac{\Delta P_T}{q}$, dimensionless
η_B	Burner efficiency, dimensionless
ν	Kinematic viscosity, ft ² /sec.
ρ	Density, lb/ft ³

SUBSCRIPTS

B	Burner
b, base	Base flow region
BP	Bypass
BLC	Boundary layer bleed
$btail$	Boattail
c	Core (nozzle); capture (inlet)
DES	Design conditions

SYMBOLS AND NOMENCLATURE (Continued)

SUBSCRIPTS

e	Boattail trailing edge
EFF	Based on effective area
ENG	Refers to engine demand
f	Fuel
g	gross
GEOM	Based on geometric area
int	Interference; internal
ip	Ideal, primary exhaust flow
jet	Exhaust flow jet
max	Maximum
min	Minimum
s	Scrubbing flow region
SPILL	Spillage
T	Total condition; throat station
t_f	Total condition, fan flow
T/O	Takeoff
t_p	Total condition, primary flow
o	Local conditions ahead of inlet
2	Compressor face station
8	Nozzle throat station
9	Nozzle exit station
18	Fan discharge throat station
∞	Free-stream condition
x	Local

SECTION I

INTRODUCTION

This document presents the results from the application of PITAP procedure to two typical aircraft configurations. The two configurations used are the Lightweight Fighter (Figure 1) and the F-4J (Figure 2). The Lightweight Fighter (LWF) in the example is a study configuration used by the Boeing Company during proposal competition, for which extensive analysis and wind tunnel test data are available for comparison with predicted results. The F-4J is also a configuration that has been extensively tested during the Exhaust System Interaction Program (Contract F33615-70-C-1449). Data from these tests are used to compare with PITAP predicted results.

The main part of the PITAP calculation procedure, which is designated as Program TEM 333, has already been programmed and is operational on the Air Force computer. This program requires as input data:

- 1) the engine performance characteristics in the form of tabulated data,
- 2) flight conditions in the form of altitude, Mach number, and power setting,
- 3) geometric constants describing the inlet and nozzle/afterbody,
- 4) tabulated data representing the performance characteristics of the inlet and the nozzle/afterbody reference drag

The first three of the above inputs are readily available for most cases. The fourth input, the inlet performance characteristics, must be generated using calculation procedures described in Volume I: Engineers Manual, use of test data or other analysis methods. The calculation procedures have not yet been programmed for automatic computation, so the discussion in this document is concerned primarily with the procedures used to predict the inlet performance characteristics used as input for the TEM 333 program. From this point on, all that remains to be done is prepare the input data, submit the program, and plot up the output results.

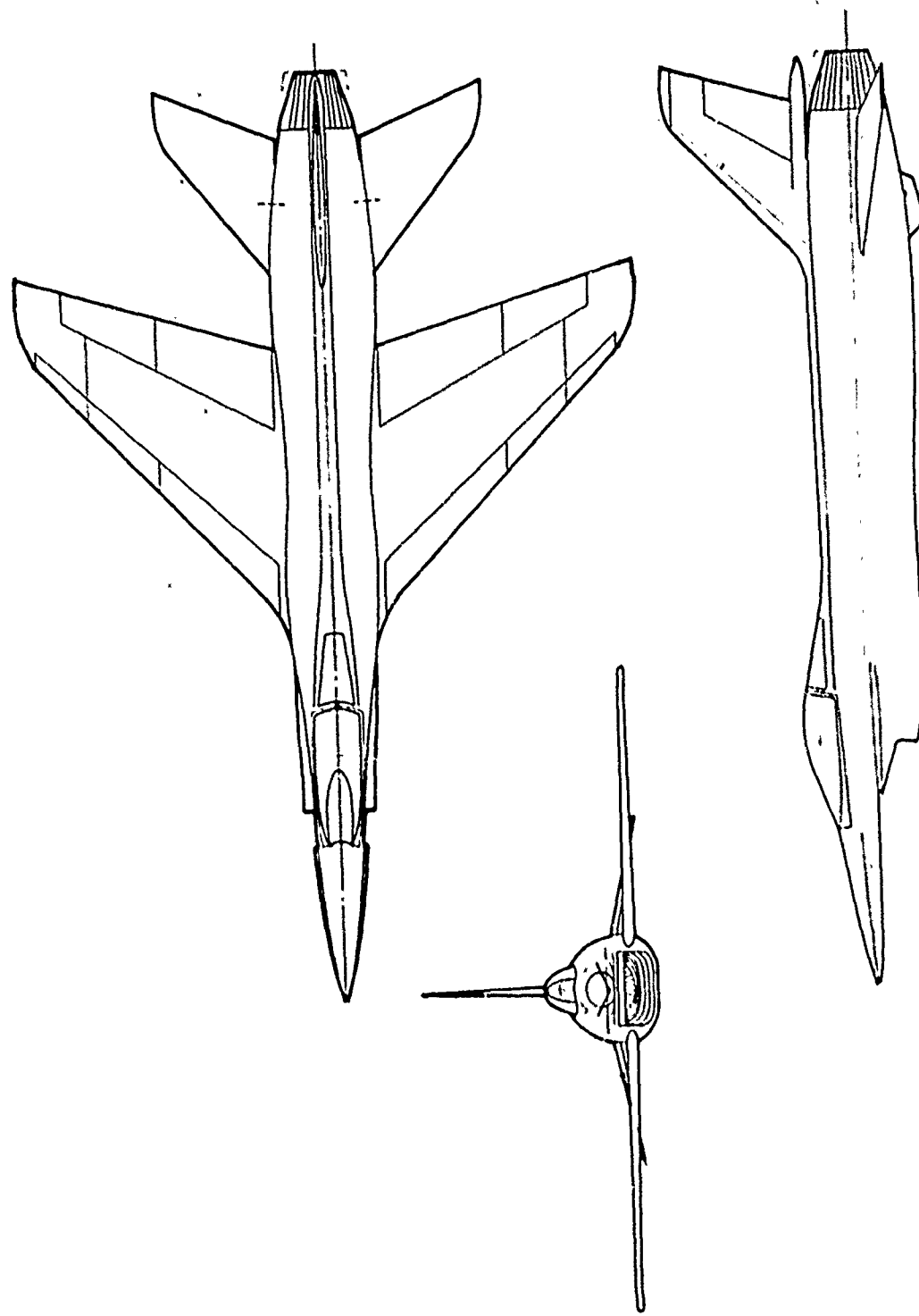


*Figure 1: GENERAL ARRANGEMENT DRAWING OF
LIGHTWEIGHT FIGHTER STUDY CONFIGURATION*

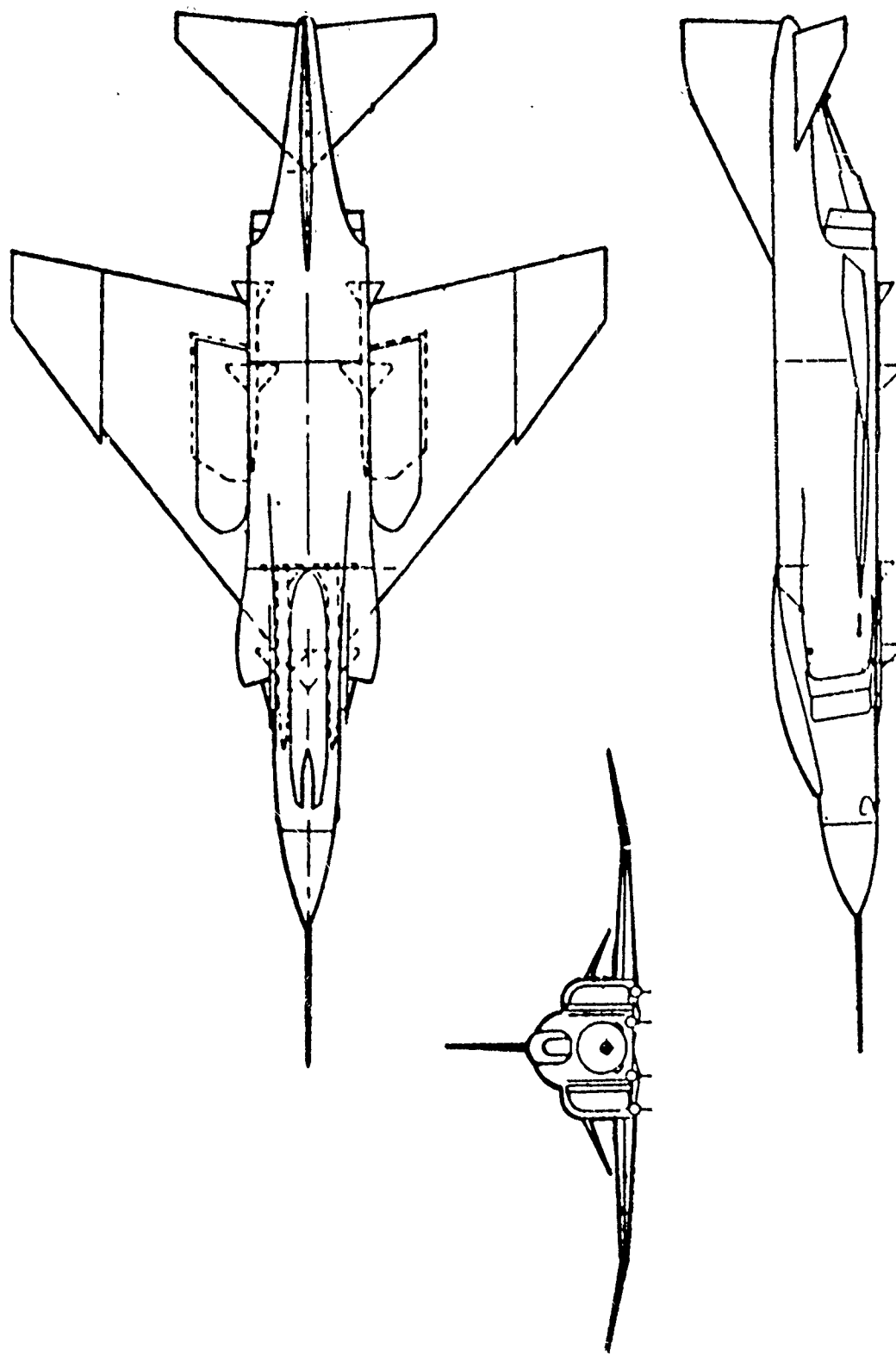


Figure 2: GENERAL ARRANGEMENT, F/A-18

Installed propulsion system performance data have been calculated for both the LWF and the F-4J sample cases. Only the input and output data from the computer run for the F-4J is presented in this document however, to avoid making the document classified.

SECTION II

LIGHTWEIGHT FIGHTER SAMPLE CASE

2.1 CONFIGURATION

The general arrangement of the LWF configuration is shown in Figure 1. It is a single-engine aircraft with an under-fuselage mounted inlet. The inlet is a two-dimensional, fixed geometry design with throat slot bleed. No bypass system is used. An advanced turbofan engine is used which has a variable geometry convergent-divergent exhaust nozzle.

2.1.1 Inlet

The geometric details of the inlet are shown in Figure 3. The critical areas required for analysis of the inlet performance characteristics are shown in Figure 3. These areas would normally be obtained from preliminary design drawings of the configuration or, if not available, reasonable engineering assumptions can be made.

The internal lines of the subsonic diffuser are shown in Figure 4, and the diffuser area variation is shown in Figure 5.

2.1.2 Nozzle/Afterbody

The nozzle/afterbody external geometry is shown in Figure 6. This drawing provides the dimensional data required to predict nozzle/afterbody drag. The full open nozzle position is used in calculating nozzle/afterbody reference drag.

2.2 PREDICTED PERFORMANCE CHARACTERISTICS

2.2.1 Inlet

The inlet performance characteristics which must be predicted to use as input to TEM 333 (existing program) include total pressure recovery, boundary layer bleed air drag, and spillage drag. No bypass system is used, therefore bypass drag is not predicted.

The LWF is designed to fly at speeds up to Mach 1.60, but the leading edge of the fixed 7 degree ramp has been positioned to keep oblique shocks out of the inlet up to Mach 2.0. The

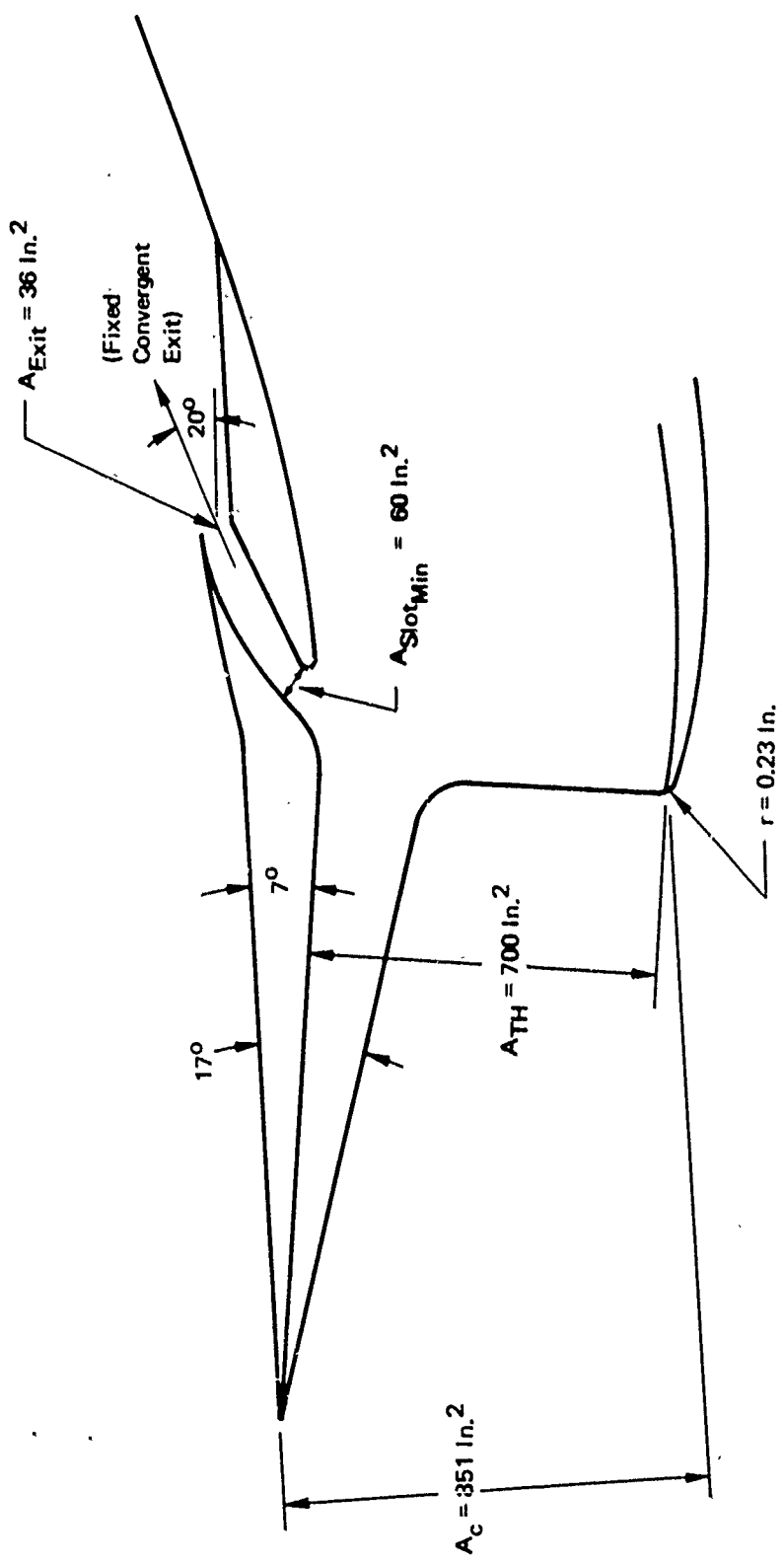


Figure 3: TWO-DIMENSIONAL INLET DETAILS

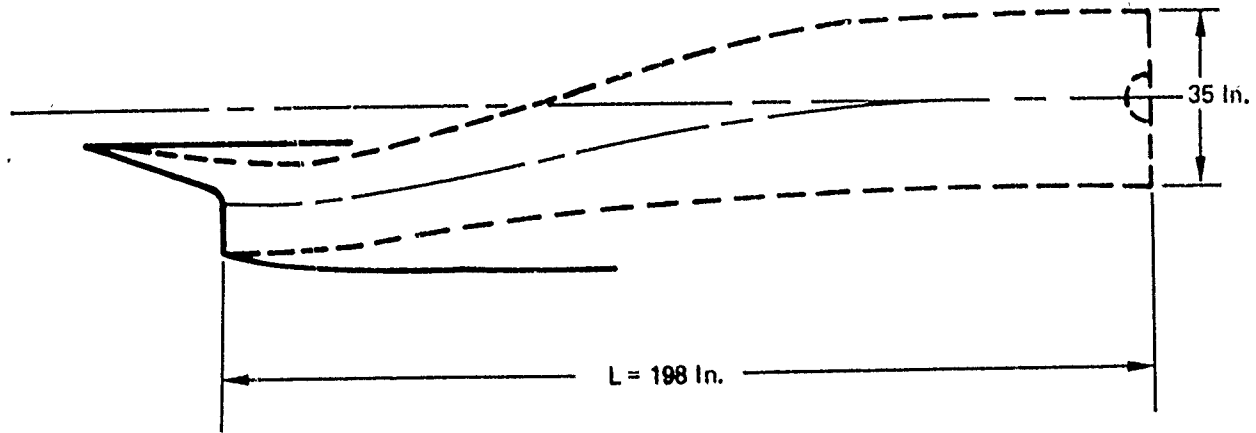
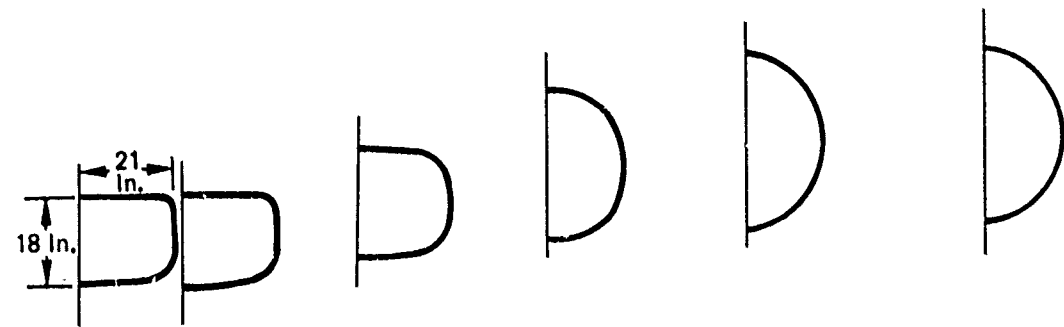
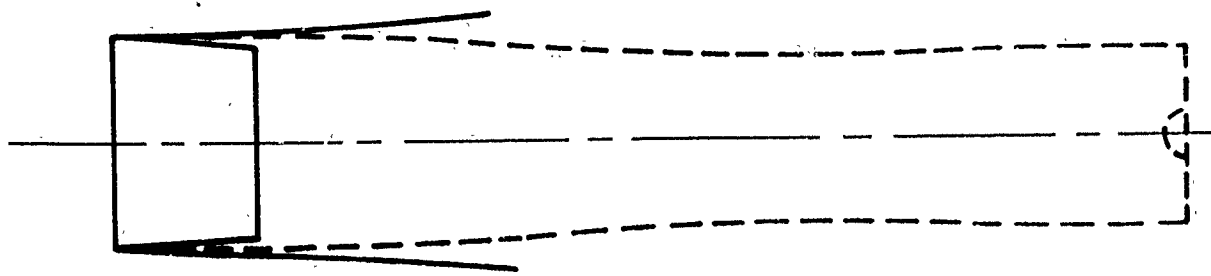


Figure 4: SUBSONIC DIFFUSER INTERNAL LINES

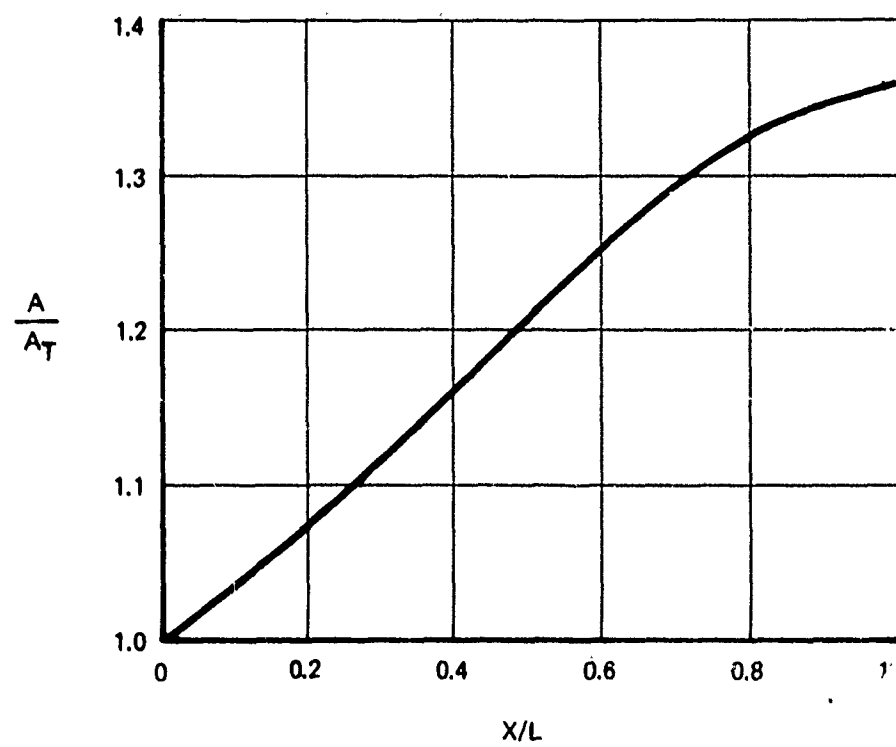


Figure 5: LWF SUBSONIC DIFFUSER AREA VARIATION

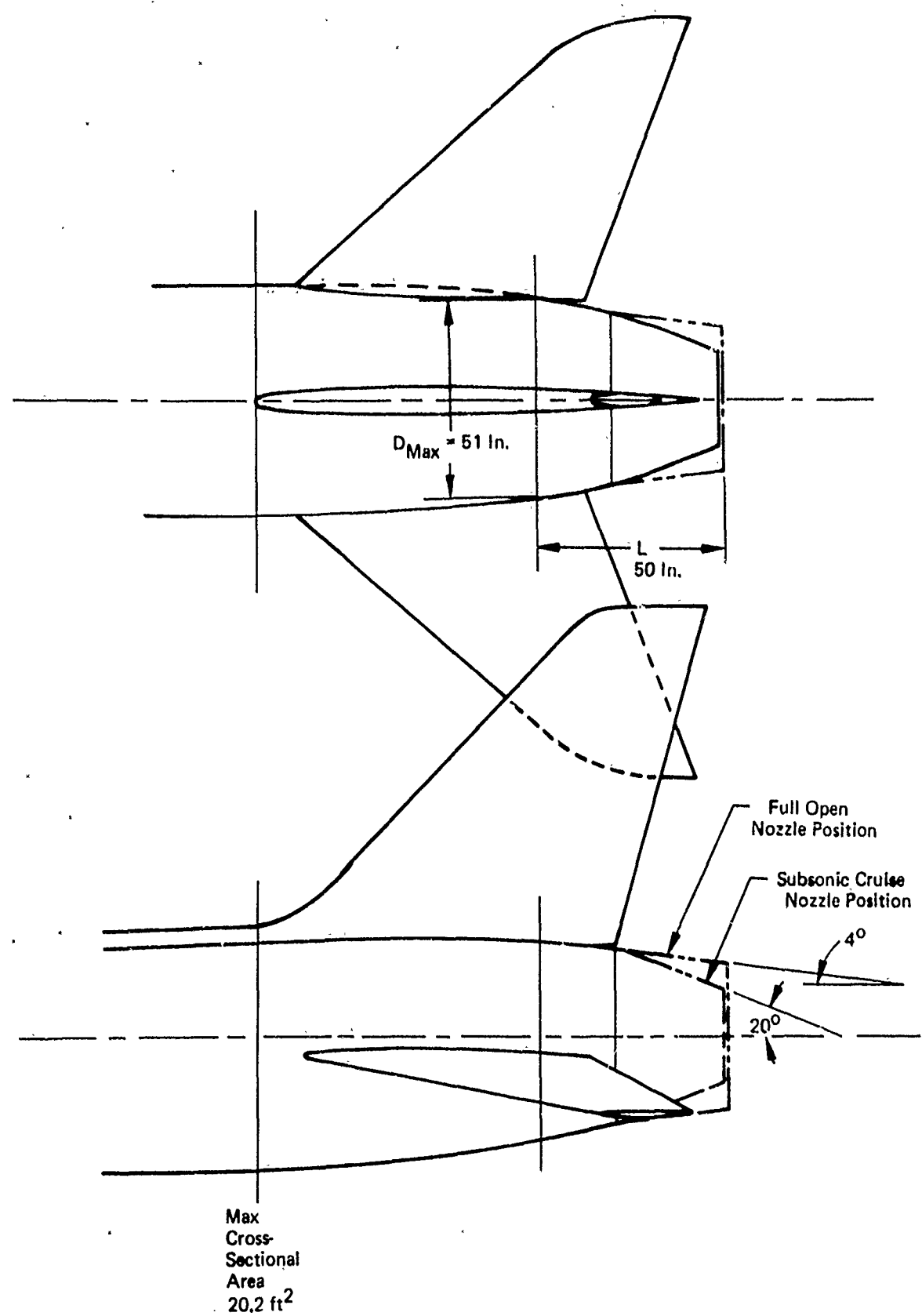


Figure 6: LWF NOZZLE/AFTERSHOCK EXTERNAL LINES

following flight conditions were selected for use in the analysis procedure:

$$M_{\infty} = 0, 0.2, 0.6, 0.8, 1.2, \text{ and } 1.60.$$

The low-speed pressure recovery for the $M_{\infty} = 0$ and 0.20 points is estimated using the procedure in Section IV, Vol. I, beginning on page 25. The calculation proceeds as follows:

The following input quantities are obtained from known geometric data, engine data, and data correlations (Vol. IV),

$$\frac{r}{D} = \frac{.23}{[(4)(700)] / [(36)+(84)]} = .01 \quad \text{Geometric data from Figure 3}$$

$$A_C = 851 \text{ in}^2 \quad \text{Geometric data from Figure 3}$$

$$M_{\infty} = 0, .20 \quad \text{Specified}$$

$$A_T = 700 \text{ in}^2 \quad \text{Geometric data from Figure 3}$$

$$A_{T.O.} = 200 \text{ in}^2 \quad \text{Assumed}$$

$$\epsilon = 0.12 \quad \begin{aligned} &\text{Subsonic diffuser} \\ &\text{loss coefficient} \\ &\text{for subsonic flow.} \\ &\text{Average value from} \\ &\text{Figures 24 \& 25,} \\ &\text{Vol. IV.} \end{aligned}$$

$$\frac{w_2 \sqrt{\theta_2}}{\delta_2} = \text{Engine Airflow} \quad \text{for } M_{\infty} = 0, 0.20$$

The above geometric and aerodynamic quantities are used as input to the low-speed calculation procedure documented in Vol. I, pages 33-41. This procedure has now been programmed as a separate subroutine, which is contained in Volume II, Programmers Manual. The results of the machine calculation are as follows:

$$M_0 \quad \frac{P_{T_2}}{P_{T_0}} \quad \frac{W\sqrt{\theta}}{\delta}$$

0	0.8137	MAX
0.20	0.8937	MAX

Low-speed total pressure recovery can also be estimated from the correlation curve of Figure 20, page 33, Volume IV. The recovery values obtained using this correlation are nearly identical to the above values.

The transonic pressure recovery ($M_\infty = 0.6, 0.8, 1.2$) is calculated from the subsonic diffuser loss coefficient and calculated throat entrance Mach number as a function of inlet airflow. Since throat Mach number is a function of engine airflow and engine airflow is a function of diffuser recovery, which depends on determine the transonic pressure recovery. This procedure is illustrated in the flow chart of Figure 16, of Volume I. Using this procedure, the following total pressure recoveries were calculated for the transonic cases:

$$M_\infty \quad \frac{P_{T_2}}{P_{T_\infty}}$$

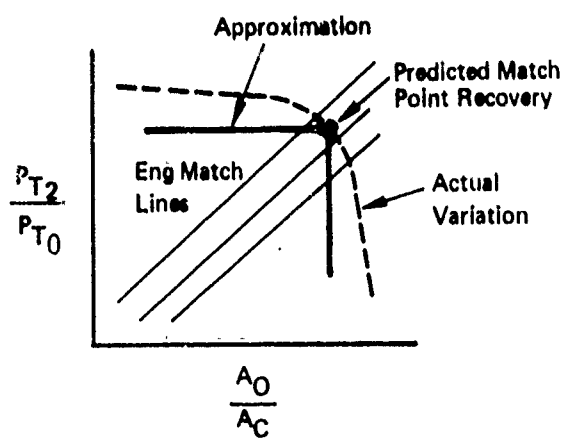
0.6	0.965
0.8	0.965
1.20	0.962

The supersonic inlet total pressure recovery through the shock system at the engine-matched condition is normally obtained from the charts of Figure 17, Volume I. To these shock losses are added the total pressure recovery losses due to the subsonic diffuser. The resulting total pressure is the normal recovery at the match point as a function of free-stream Mach number. For the LWF inlet, a two-shock supersonic diffuser design, the match point shock recoveries are obtained from Figure 17, Volume I for $N=2$. Next, the subsonic diffuser total pressure losses, calculated using a duct loss coefficient, $\epsilon = .12$ (from Figure 24 of Volume IV) and an assumed throat Mach number of .75, are added to the shock losses to obtain the design point total pressure recovery as a function of Mach number. The calculated

quantities are summarized in the following table:

	(Fig. 17, Vol. I)	(Fig. 7)	(Fig. 15, Vol. I)	
M_∞	$\frac{P_{T_{NS}}}{P_{T_0}}$	$\frac{P_{T_0}}{P_{T_\infty}}$	$\frac{P_{T_2}}{P_{T_1}}$	$\frac{P_{T_2}}{P_{T_\infty}}$
1.0	1.0	1.0	0.9625	0.9625
1.2	0.99	1.0	0.9625	0.952
1.4	0.982	1.0	0.9625	0.945
1.6	0.968	1.0	0.9625	0.93

The above recovery values can be used for most preliminary design studies where performance is required at design point conditions over a range of flight Mach numbers. To fit the format of the TEM 333 program however, it is necessary to specify recovery as a function of engine-plus-bypass mass flow ratio, A_0/A_C . This can be accomplished by using the design point recovery values calculated above as constants which do not change with mass-flow ratio below the design point and which drop straight down from the design match point. This results in a series of recovery vs. mass flow ratio plots which are different from the actual variations as shown by the following sketch:



The above method does not result in large errors for engine match lines are near the match point. However, it can result in predictions of recovery that are slightly low for off-design

airflow demands. To demonstrate the use of an alternate recovery predicting method that can be used to improve on the recovery variations at off-design mass flow ratios, an existing computer program (Reference 1), available to industry, was used for the LWF sample case, as an aid in calculating off-design recoveries. This computer program, which was originally designed to calculate theoretical additive drag, also calculates the inviscid total pressure recovery through two-shock inlet systems. The program also calculates the mass flow spilled over sideplates of various amounts of cutback. The existing version of the program, however, does not take into account the effect of the spilled mass flow on the strength of the normal shock. It is necessary, therefore, to make an adjustment to the machine computed values of inlet lip total pressure recovery to account for this effect. This approach was used for the LWF sample case. It was assumed that the airflow spilled over the sideplates resulted in a directly proportional increase in A/A^* of the supersonic flow ahead of the normal shock. The new Mach number corresponding to this A/A^* was used to obtain the normal shock total pressure recovery. The inlet lip Mach numbers from the program (as a function of mass flow ratio, A_{O_1}/A_C) were then used with a subsonic diffuser loss

coefficient of 0.12 to obtain overall total pressure recovery, P_{T_2}/P_{T_0} , as a function of inlet mass flow ratio. Using the

above described methods the plotted data shown in Figure 8 were obtained for Mach numbers 1.20 and 1.60. The subsonic values for $M_{O_1} = 0.60$ and 0.80 obtained from the previously described calculation program are also shown in the same plot for the sake of completeness. Various engine airflow demand match lines are also shown in Figure 8 to indicate where the inlet/engine combination will actually operate. The matched recovery and mass flow as a function of local inlet Mach number are shown in Figures 9 and 10 respectively. Approximate inlet buzz and stall limits are input into the TEM 333 program to give indications of those operating points where inlet/engine compatibility problems may be likely to occur. These are not required to obtain performance data, and the calculations will not be stopped if one of the limits is exceeded, however, they do serve to point out possible problem areas. The buzz and stall limits shown in Figures 11 and 12 respectively, were obtained from trends in experimental data. If reliable buzz and stall limits cannot be obtained, the best available estimate should be made, by selecting appropriate points from the recovery vs. mass flow ratio plots of Figure 8.

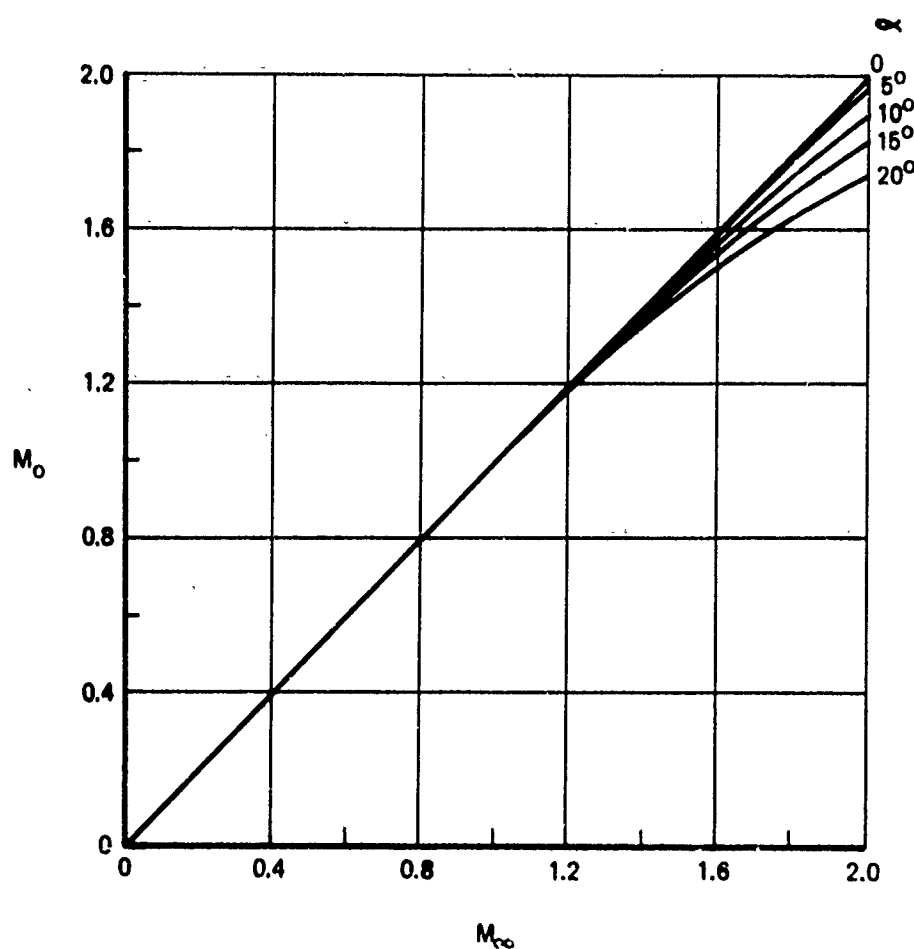


Figure 7: LOCAL MACH NUMBER VS FREE-STREAM MACH NUMBER FOR LWF

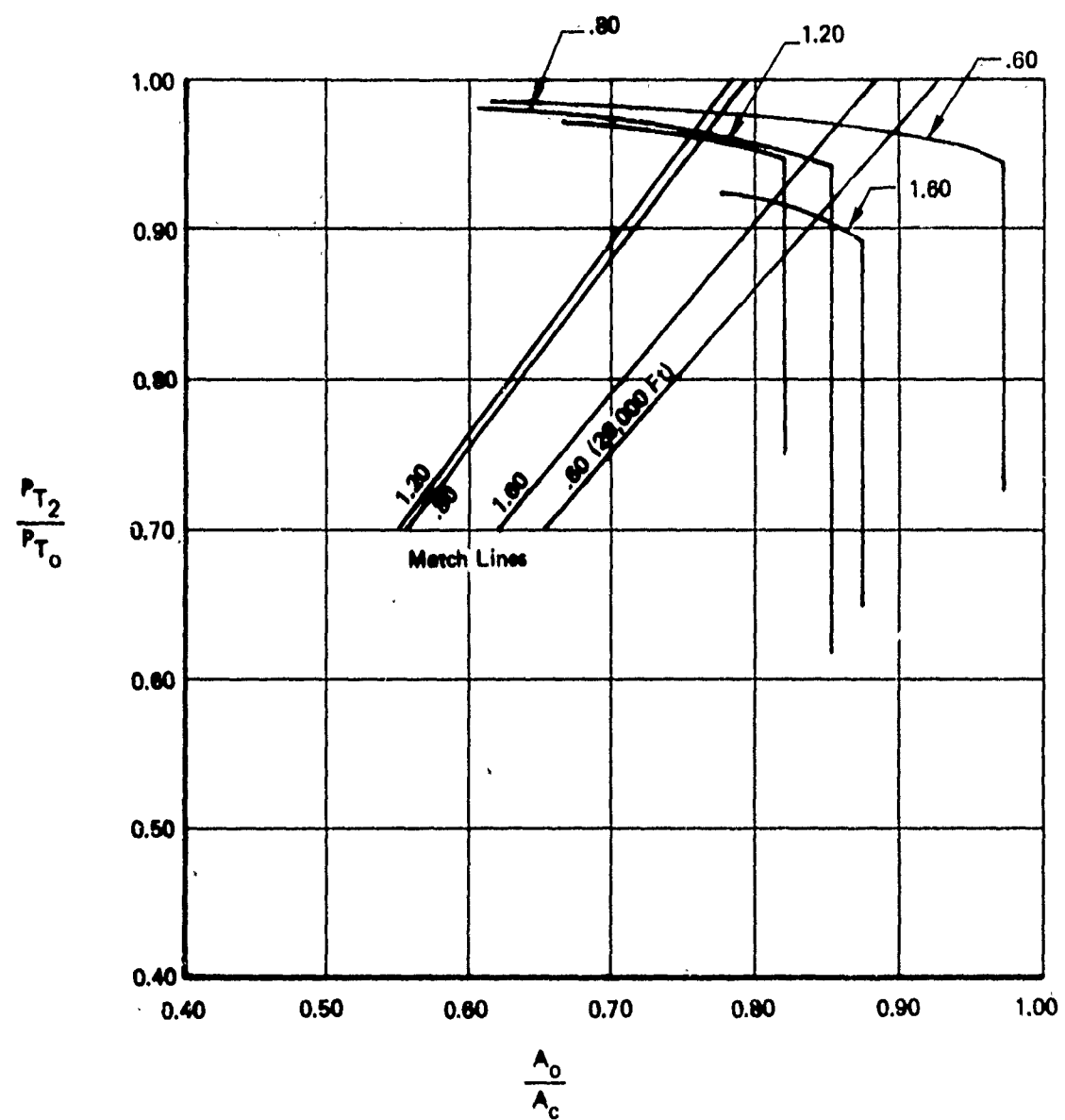


Figure 8: LWF RECOVERY VS MASS FLOW

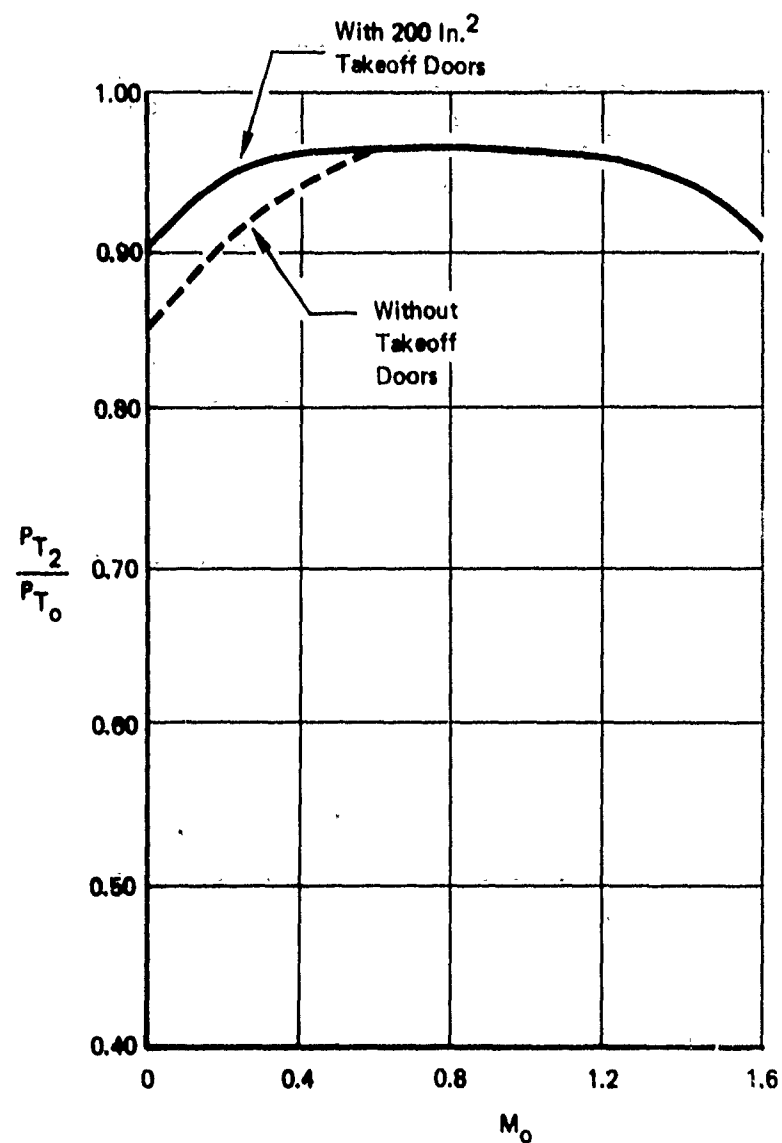


Figure 9: MATCHED INLET RECOVERY

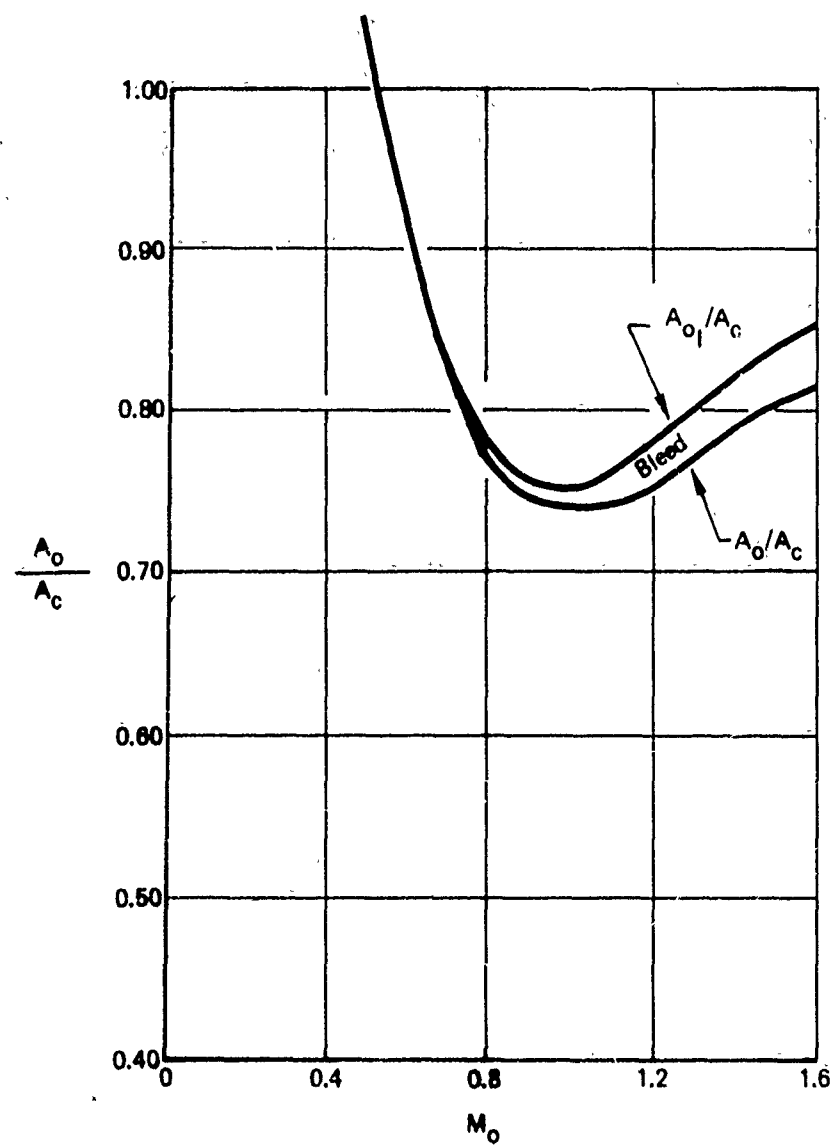


Figure 10: MATCHED MASS FLOW

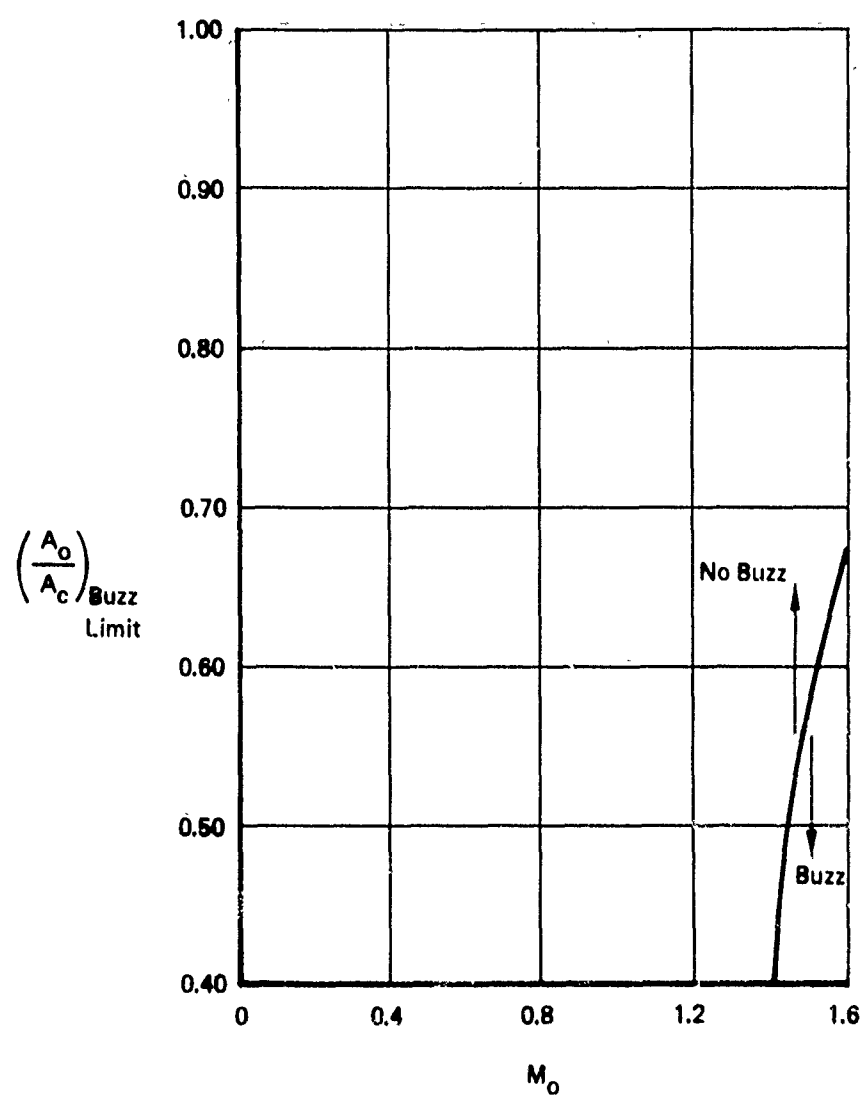


Figure 11: BUZZ LIMIT

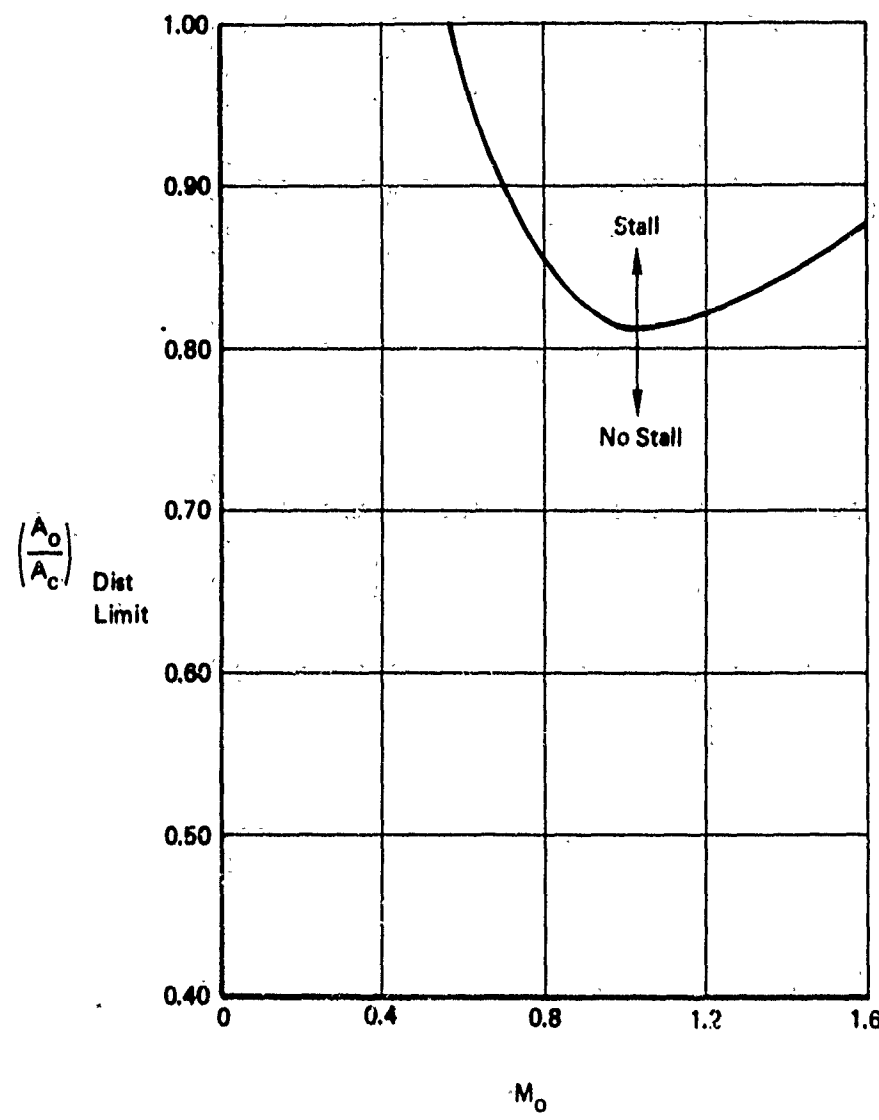


Figure 12: DISTORTION LIMIT

The first step in calculating the inlet drag is to establish an appropriate baseline mass flow ratio for use in bookkeeping aero and propulsion forces on the airplane. For subsonic Mach numbers, the baseline mass flow ratio is chosen as

$$\left(\frac{A_{O_I}}{A_C}\right)_{Ref} = \frac{A_T}{A_C}$$
. For supersonic Mach numbers, the baseline mass flow ratio is chosen as $\left(\frac{A_{O_I}}{A_C}\right)_{Ref} = \left(\frac{A_O}{A_C}\right)_{MAX}$ for each Mach number.

The maximum supersonic operating mass flow ratios for the LWF were obtained by use of the previously described computer program of Reference 1. The resulting baseline mass flow as a function of free-stream Mach number is shown in Figure 13.

The spillage drag calculation for the LWF was initiated by using the additive drag program of Reference 1 to calculate theoretical additive drag as a function of free-stream Mach number and inlet mass flow ratio. After the calculated additive drag was obtained, two adjustments were made:

- 1) The additive drags were adjusted so that the additive drag was zero at the baseline mass flow ratio condition. This resulted in plots of $\Delta C_{D_{ADD}}$ vs. A_{O_I}/A_C .
- 2) Next, the $\Delta C_{D_{ADD}}$ values were multiplied by K_{ADD} factors to correct the theoretical additive drags for configuration effects. These K_{ADD} factors (Figure 14) were obtained from the data of Volume IV. Due to the limited amount of data on K_{ADD} factors it was necessary to do a considerable amount of interpolation, extrapolation, and smoothing to obtain the K_{ADD} factors shown in Figure 14.

The final spillage drag data are presented in Figure 15.

The boundary layer bleed drag was calculated using the bleed airflow shown in Figure 16 and the bleed airflow total pressure recovery shown in Figure 17. These data were obtained from Volume IV, Section IV, "Data for Specific Configurations."

The final calculated boundary layer bleed drag is presented in Figure 18. The final bleed drag is presented as a single curve of $C_{D_{BLC}}$ vs. $A_{O_{BLC}}/A_C$ because there was little variation

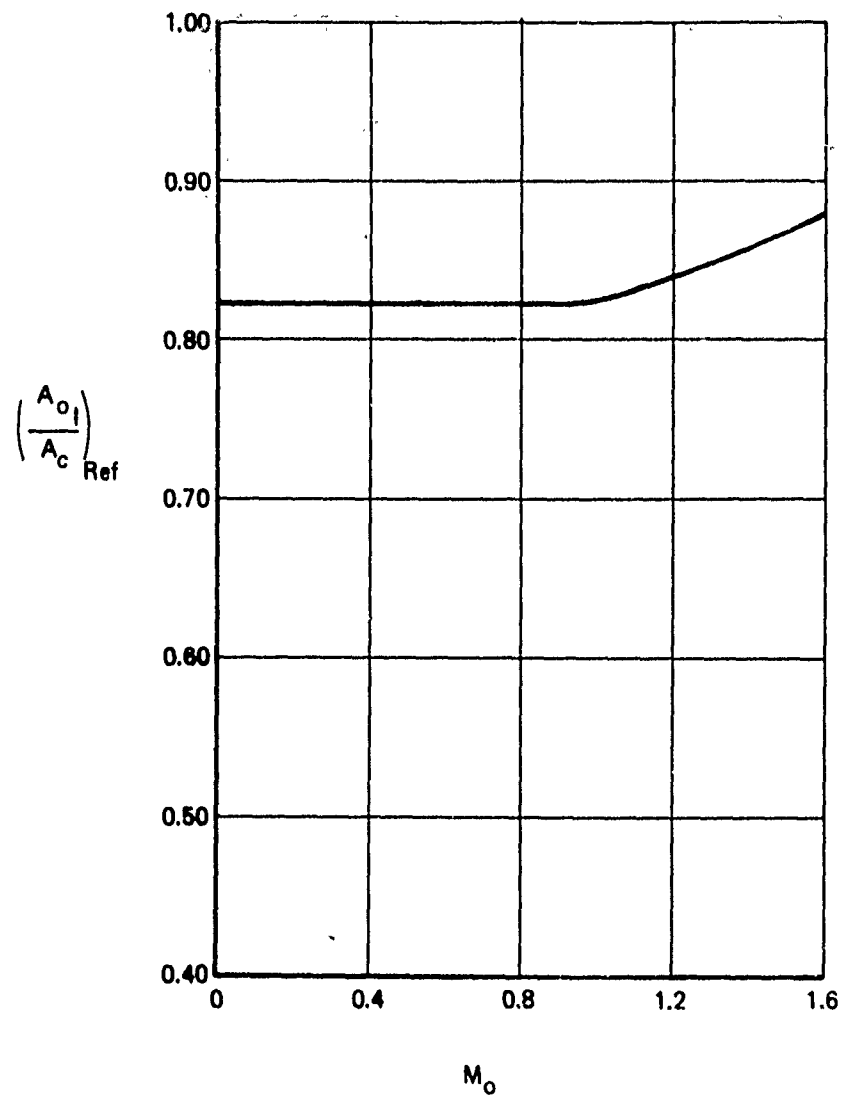


Figure 13: REFERENCE MASS FLOW

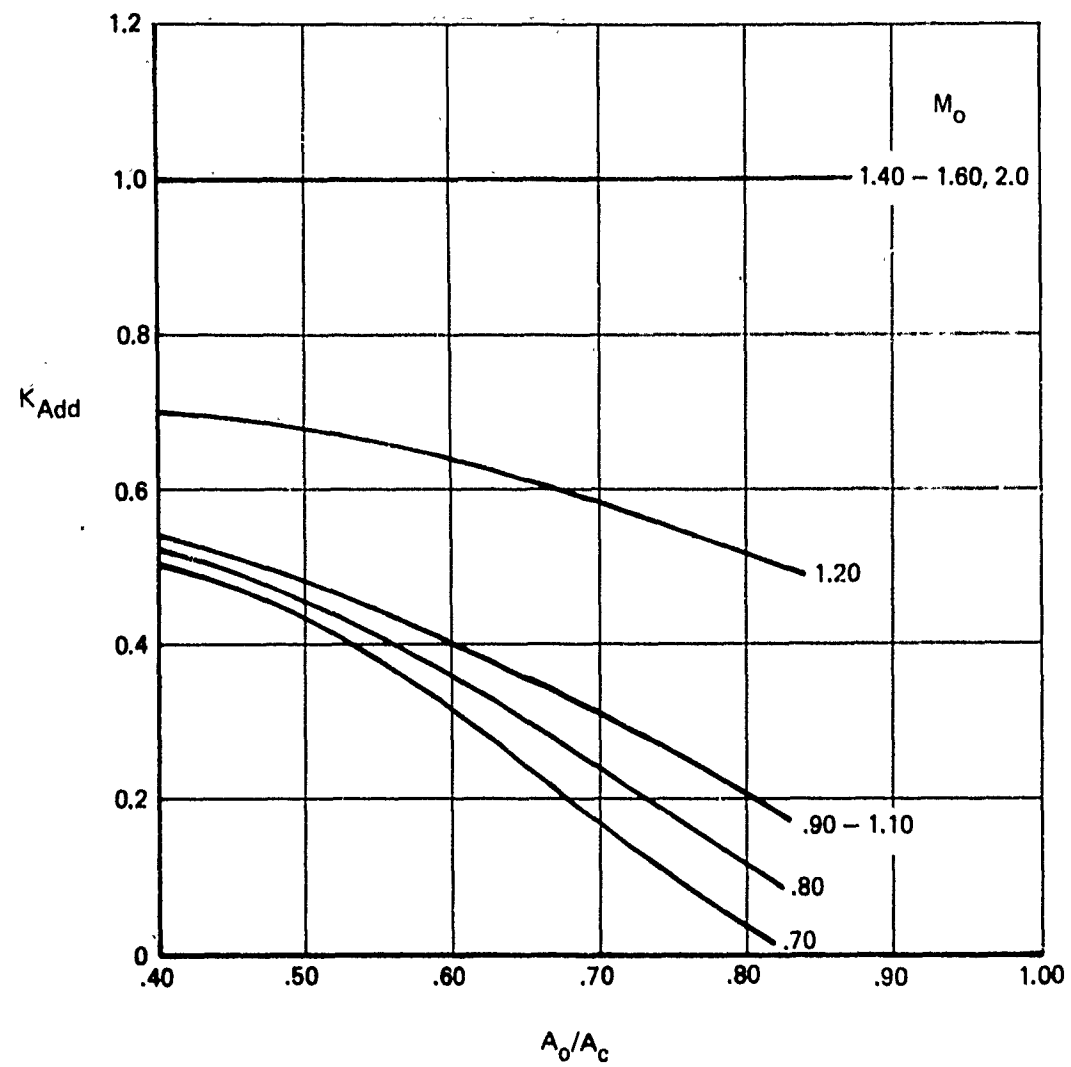


Figure 14: K_{ADD} FACTORS FOR LWF
SPILLAGE DRAG PREDICTION

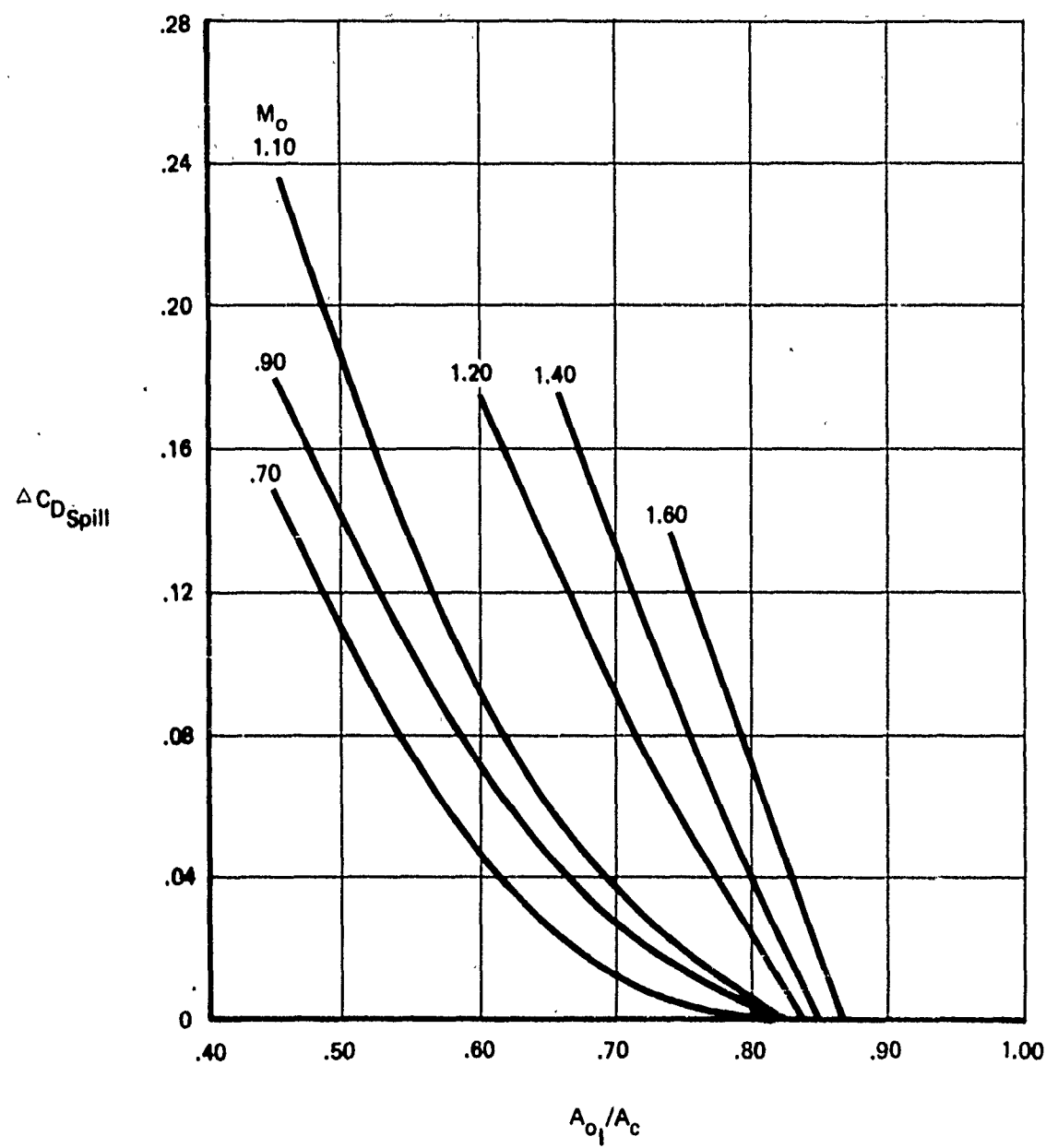


Figure 15: SPILLAGE DRAG FOR LWF

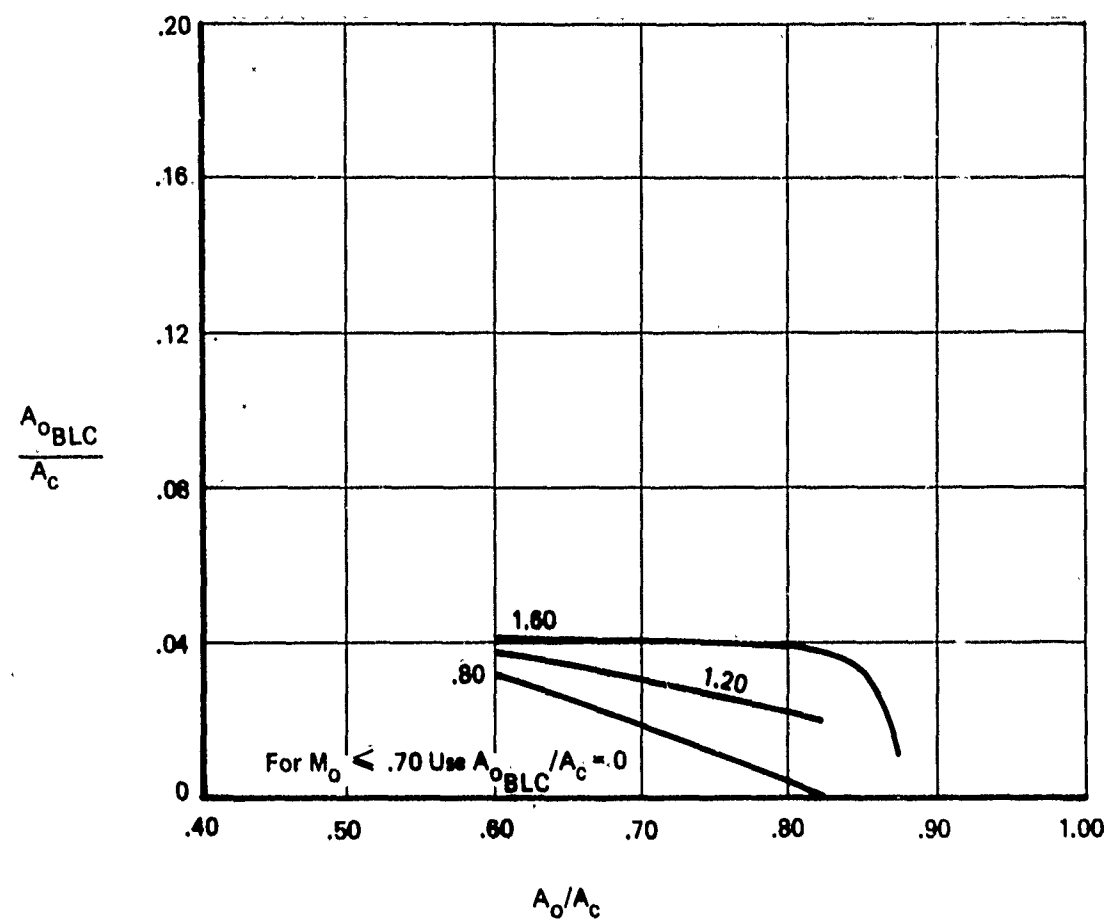


Figure 16: BOUNDARY LAYER BLEED AIRFLOW

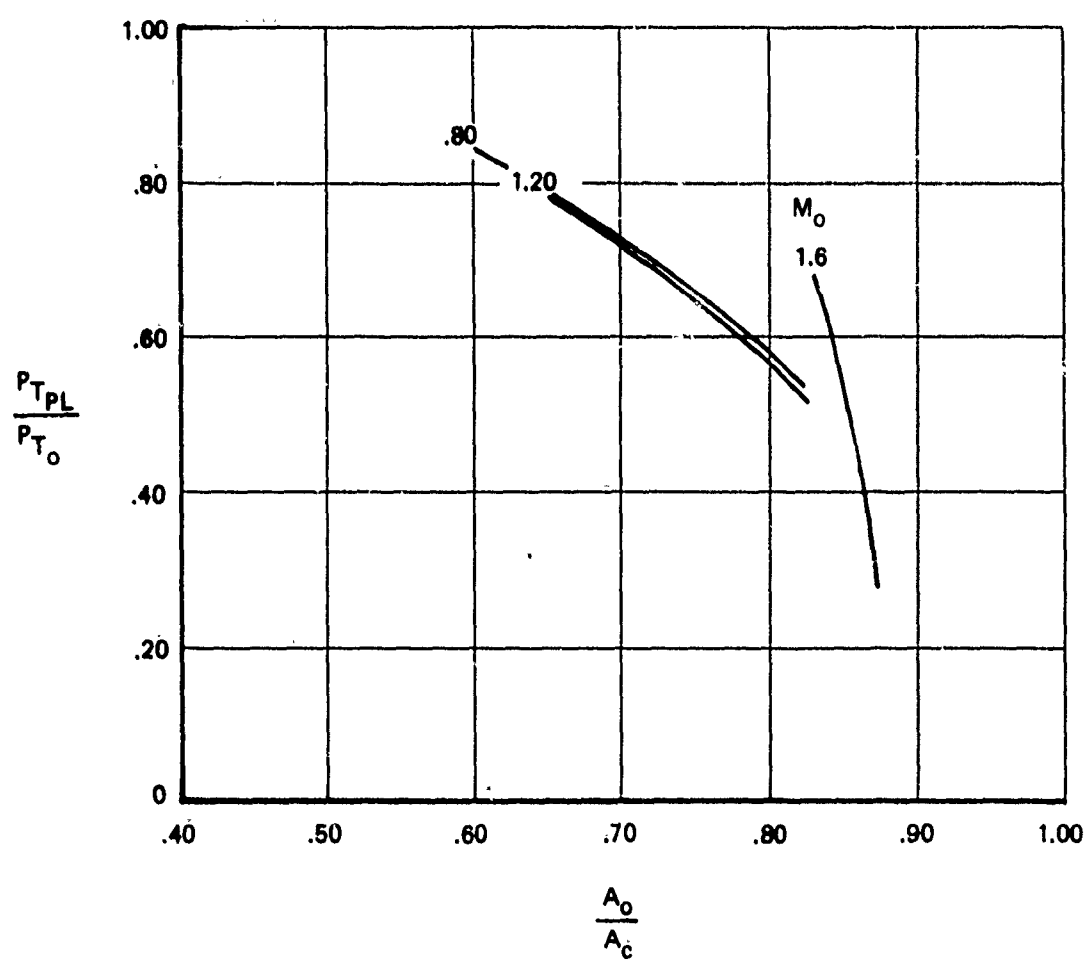


Figure 17: BOUNDARY LAYER BLEED AIRFLOW
TOTAL PRESSURE RECOVERY

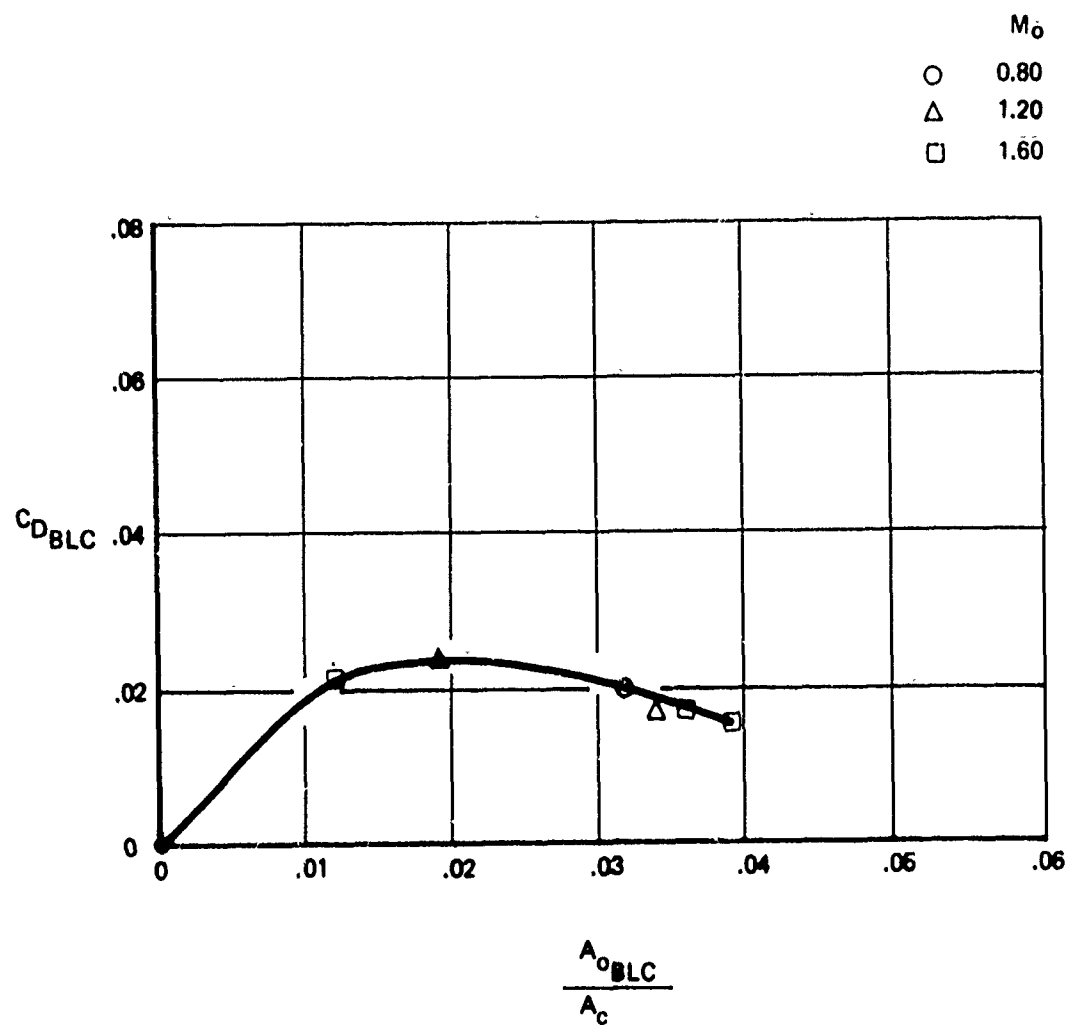


Figure 18: BOUNDARY LAYER BLEED DRAG

in the drag as a function of Mach number. Also, since the exact geometry and location of the boundary layer bleed exit was not known, the momentum drag of the boundary layer bleed air was increased by a factor of 1.25 to account for flap drag of the exit doors. This drag would normally be computed by the procedure detailed in Section IV of Volume I, if exit geometry were specified.

The drag increases to a maximum as bleed airflow is increased, then starts to decrease again. This is due to the fact that variations in bleed airflow are produced by variations in shock position. As shock position goes more supercritical, plenum pressure drops along with airflow. Conversely, as the shock goes more subcritical, the airflow goes up and so does the pressure recovery of the bleed air. These effects tend to flatten out the C_D vs. $\frac{A_0}{A_C}$ curves, as shown in Figure 18.

2.2.2 Nozzle/Afterbody

The calculation procedures for computing nozzle/afterbody drag are computerized in the TEM 333 program; therefore, the sample calculations consisted of preparing the input data for the nozzle/afterbody portion of the calculation procedure and submitting the job to the computer. These input data consist of geometric constants specifying nozzle maximum diameter, D_{MAX} , nozzle boattail length, L , nozzle-to-nozzle spacing, S , and nozzle/afterbody reference drag as a function of Mach number for the reference geometry and the reference nozzle pressure ratio. The following table summarizes the LWF geometrical constants used by the nozzle/afterbody calculation procedure in the program:

GEOMETRICAL CONSTANT	VALUE
Nozzle Spacing, S	(Single 0 Engine)
Nozzle Maximum Diameter, D_{MAX}	51 in.
Boattail Length, L	50 in.

The above constants are used, together with the nozzle pressure ratio (obtained internally by the computer program from the tabulated engine performance input data), to obtain

boattail drag from the curves of Figures 19 and 20.

It is also necessary to specify as part of the input data for nozzle/afterbody drag calculation, the variation of nozzle/afterbody reference drag as a function of free-stream Mach number. This reference drag is obtained from Figures 19 and 20 using the reference nozzle/afterbody geometry shown in Figure 6. The reference nozzle/afterbody boattail angle is 4 degrees (full open nozzle position). For this boattail angle, the subsonic reference drag is obtained from Figure 19 as a function of free-stream Mach number. The supersonic boattail reference drag is calculated from the equation shown in Figure 19. Since the reference boattail angle is only 4 degrees, no pressure ratio correction from Figure 20 is required. The final predicted reference drag for the nozzle/afterbody is shown in Figure 21.

2.3 COMPARISON OF PREDICTED AND TEST DATA

The calculated data have been compared with test results obtained from a series of aero and propulsion tests to determine their accuracy in predicting the actual inlet recovery and spillage drag and nozzle/afterbody drag.

The results of the inlet total pressure recovery comparison are shown in Figure 22. Good agreement is obtained between predicted recovery and measured recovery throughout the flight Mach number range.

A comparison of predicted and measured inlet spillage drags is presented in Figure 23. Agreement between predicted and measured drag is generally fair for most Mach numbers, and is probably adequate for preliminary studies, however, the limited amount of data available, and the scatter in the data, from which to select the K_{ADD} factor, made it necessary to spend considerable time in arriving at a suitable set of K_{ADD} factors to use. This situation could be considerably improved by the systematic gathering and analyzing of an extensive body of drag data over a wide range of configurations.

The results of nozzle/afterbody drag predictions for a 20 degree boattail angle nozzle are compared with measured data over a Mach number range from 0.40 to 1.60 in Figure 24. The predicted drags are somewhat low subsonically and slightly high supersonically. Figure 25 presents results comparing measured and predicted subsonic nozzle drags as a function of nozzle pressure ratio for a 20 degree boattail angle nozzle.

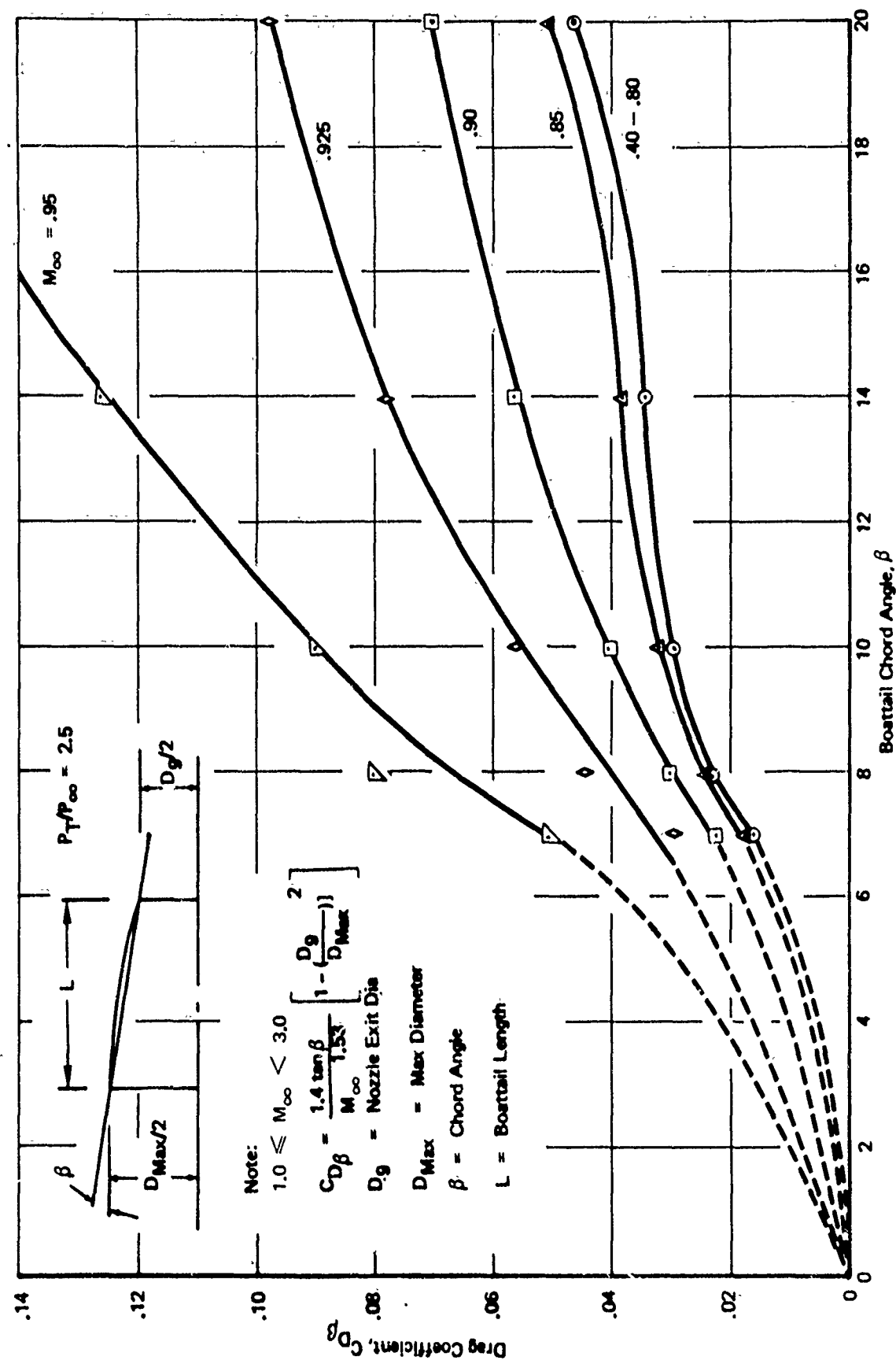


Figure 19: NOZZLE BOATTAIL PRESSURE DRAG COEFFICIENTS AS $f(\beta)$

Data Sources: 1. NASA TM X-1960
 2. Boeing Test Data
 3. Unpublished Boeing SST Data

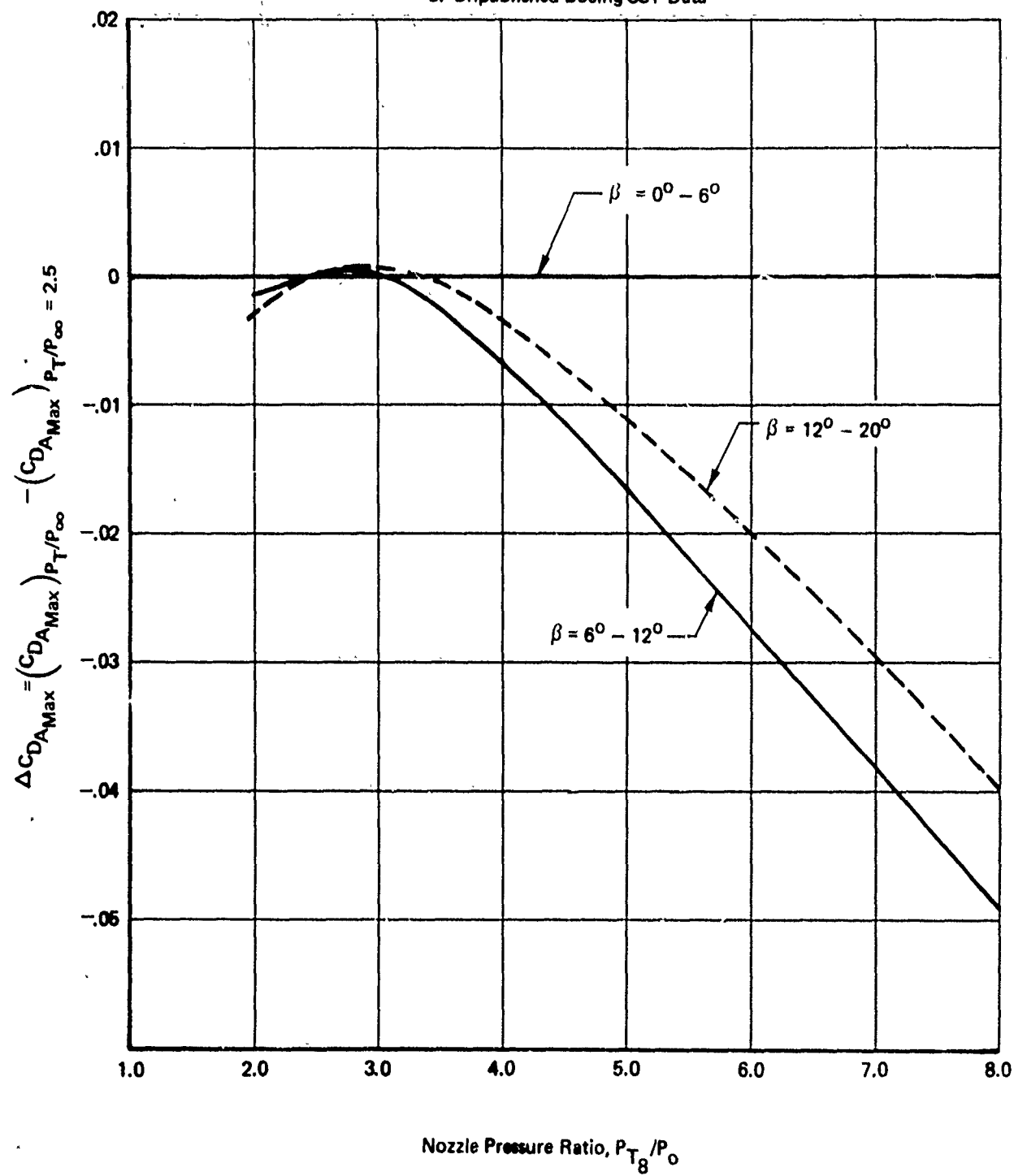


Figure 20: BOATTAIL DRAG CORRECTION
 FOR NOZZLE PRESSURE RATIOS
 OTHER THAN $P_T/P_\infty = 2.5$

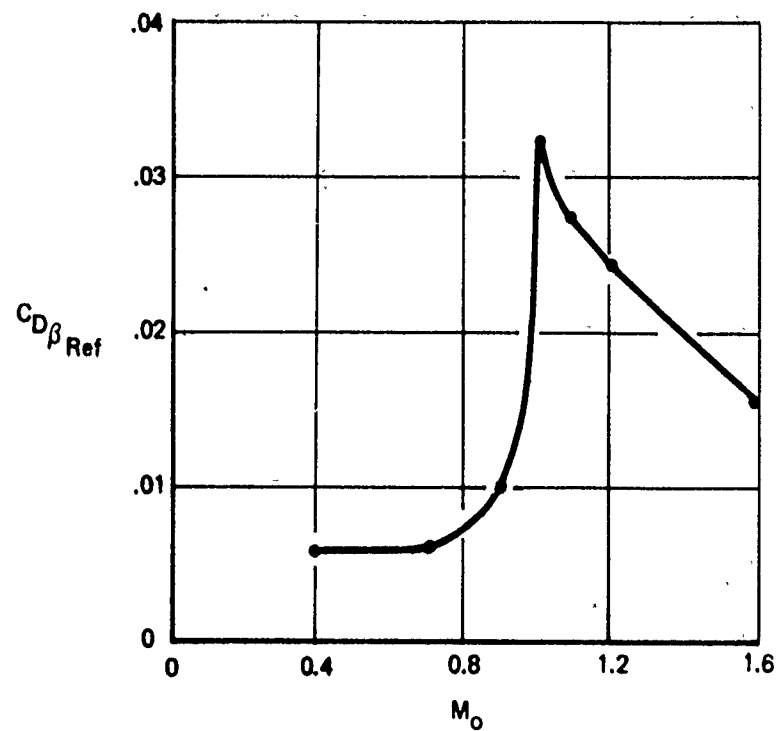


Figure 21: LWF REFERENCE DRAG FOR NOZZLE/AFTERSPOUT

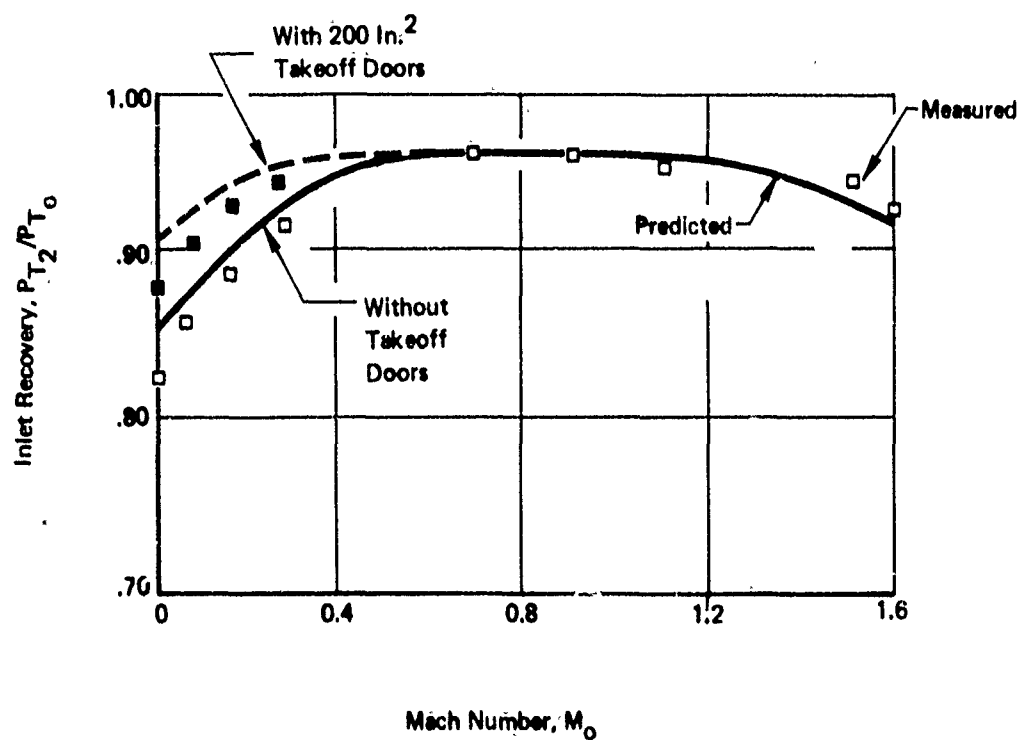


Figure 22: COMPARISON OF PREDICTED AND MEASURED INLET RECOVERY

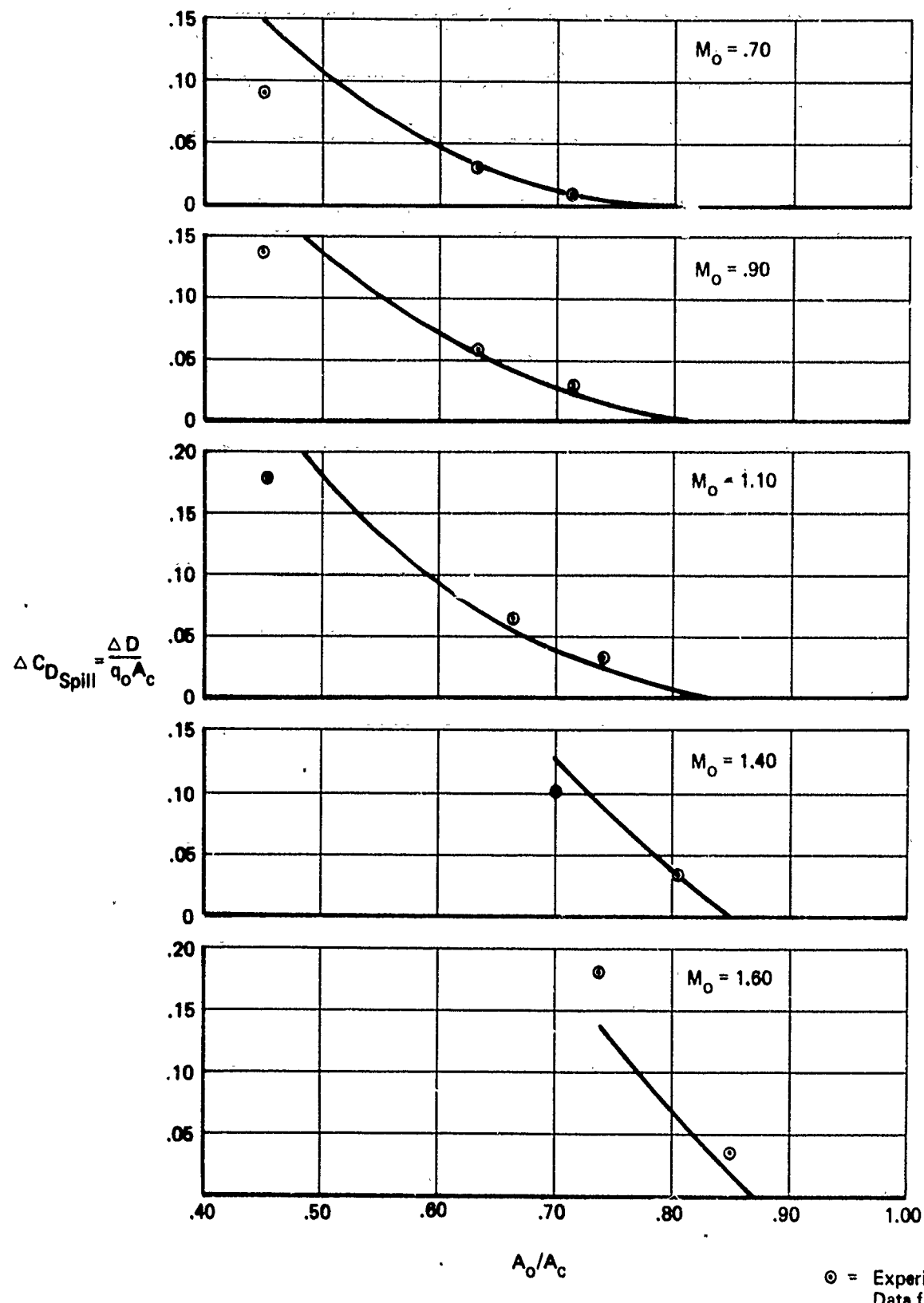


Figure 23: COMPARISON OF PREDICTED DATA AND TEST DATA FOR LWF SPILLAGE DRAG

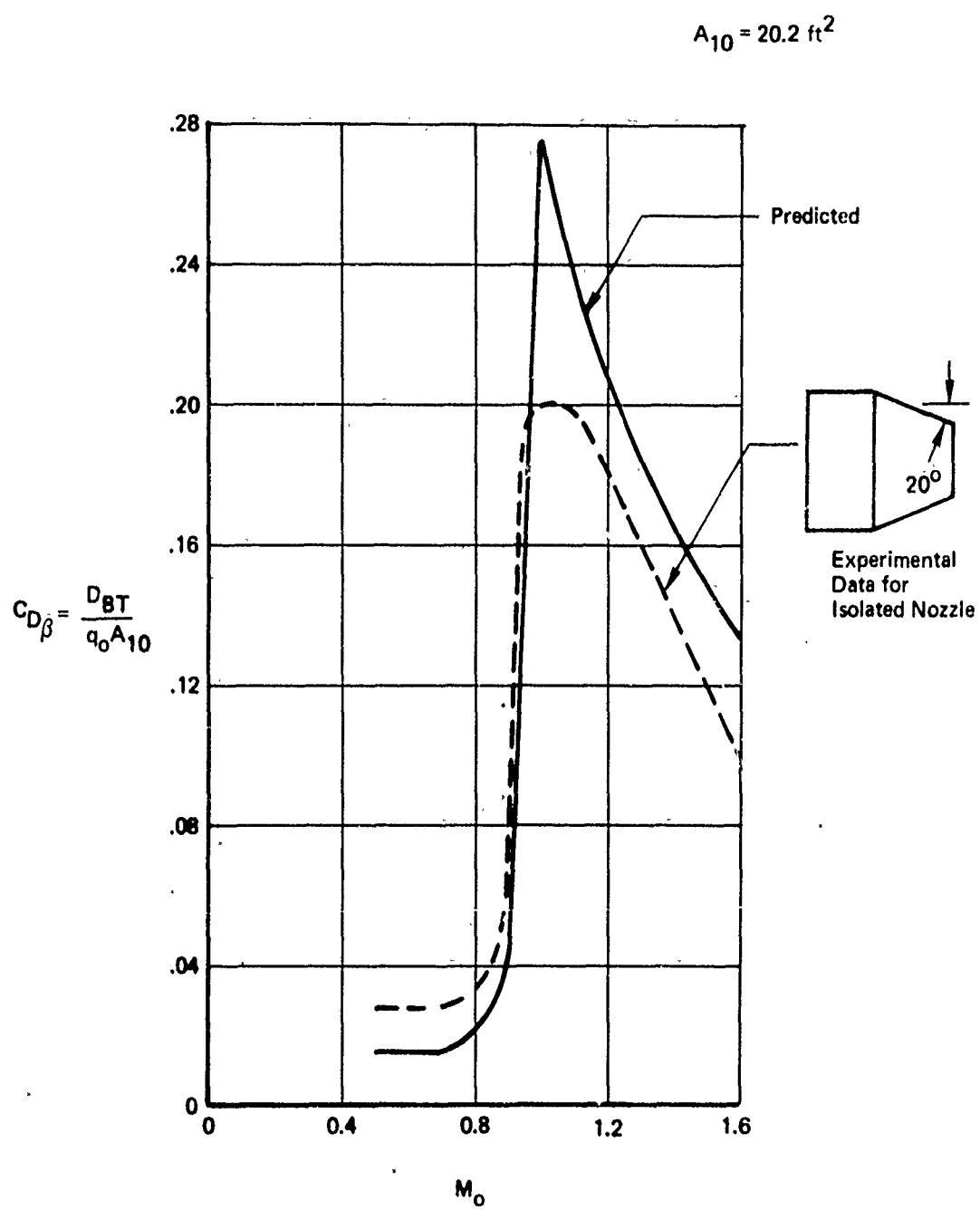


Figure 24: COMPARISON OF PREDICTED AND TEST DATA FOR NOZZLE/AFTERSPOUT DRAG

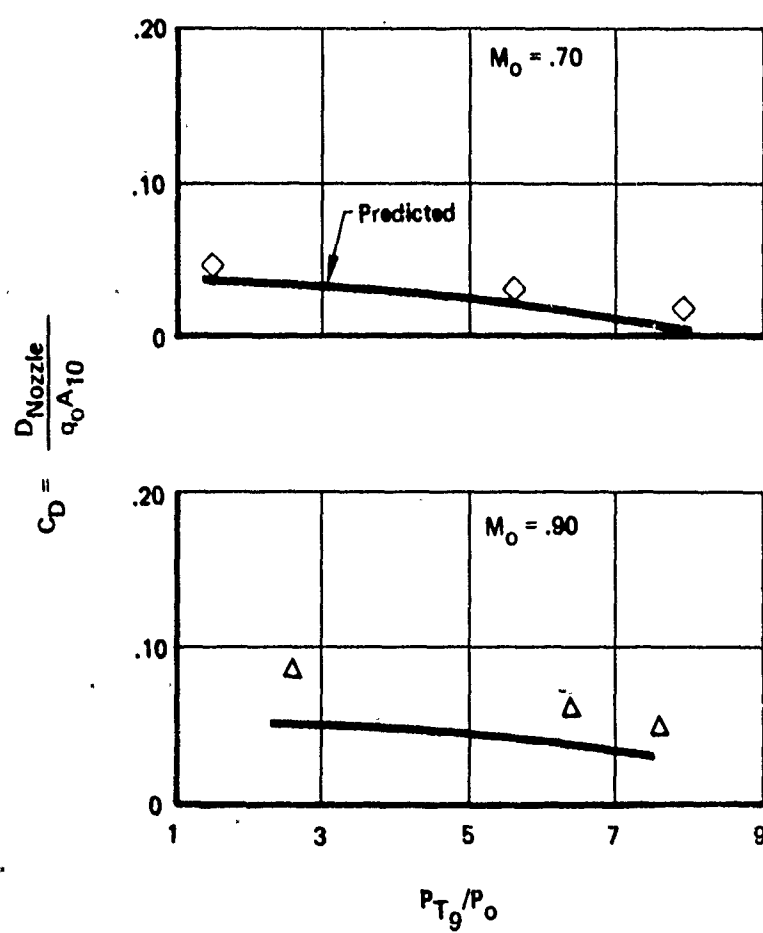
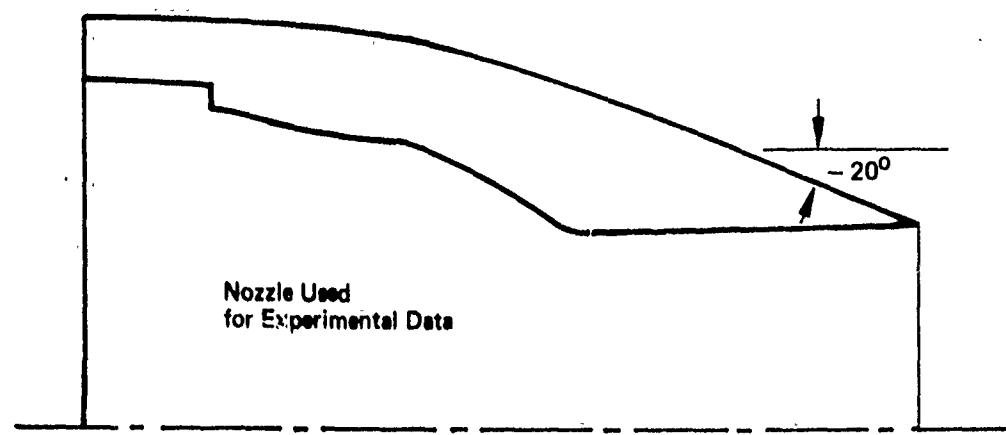


Figure 25: COMPARISON OF PREDICTED AND TEST DATA
FOR SUBSONIC NOZZLE/AFTERSPOUT DRAG AS
A FUNCTION OF NOZZLE PRESSURE RATIO

2.4 SUMMARY OF INPUT DATA FOR LIGHTWEIGHT FIGHTER SAMPLE CASE

The input data used for the TEM 333 calculation of the LWF sample case are summarized in the following table:

INLET GEOMETRY	FIGURE 3
SUBSONIC DIFFUSER GEOMETRY	FIGURE 4
NOZZLE/AFTERBODY GEOMETRY	FIGURE 6
M_O vs. M_∞	FIGURE 7
P_{T_2}/P_{T_0} vs. A_O/A_C	FIGURE 8
P_{T_2}/P_{T_0} vs. M_O	FIGURE 9
A_O/A_C vs. M_O	FIGURE 10
(A_O/A_C) BUZZ LIMIT	FIGURE 11
(A_O/A_C) DIST. LIMIT	FIGURE 12
ΔC_D SPILL vs. A_{O_I}/A_C	FIGURE 15
$A_{O_{BLC}}/A_C$ vs. A_{O_I}/A_C	FIGURE 16
C_D BLC vs. $A_{O_{BLC}}/A_C$	FIGURE 18
C_D REF. NOZZLE vs. M_O	FIGURE 21
ENGINE PERFORMANCE TABULATED DATA	CLASSIFIED (NOT INCLUDED IN THIS REPORT)

SECTION III

F-4J SAMPLE CASE

3.1 CONFIGURATION

3.1.1 Inlet

The general configuration of the F-4J is shown in Figure 2. The inlets are side-mounted, variable geometry, vertical ramp, two-dimensional, with boundary layer bleed through a porous second ramp and a small throat slot. Figure 26 shows the available details of the inlet and subsonic diffuser. These lines were taken from a drawing of a wind tunnel model used during tests reported in Reference 2. The sideplates are cut back completely ahead of the cowl lip. The initial ramp angle is fixed at 10 degrees and the second ramp angle varies from 0 degree relative to the first ramp angle relationships are shown in Figure 27.

The inlet geometry used for the analysis of the F-4J inlet performance characteristics is shown in Figures 28 and 29.

3.1.2 Nozzle/Afterbody

The nomenclature used for the nozzle afterbody drag prediction is shown in Figure 30. Typical nozzle geometries and operating pressure ratios are shown in Figure 31.

The nozzle/afterbody geometric parameters (full scale) used in the prediction method are summarized in the following table:

PARAMETER	VALUE
Max Nozzle Diameter, D_{MAX}	38.6 in.
Boattail Length, L	23.4 in.
Nozzle Spacing, S	53.8 in.

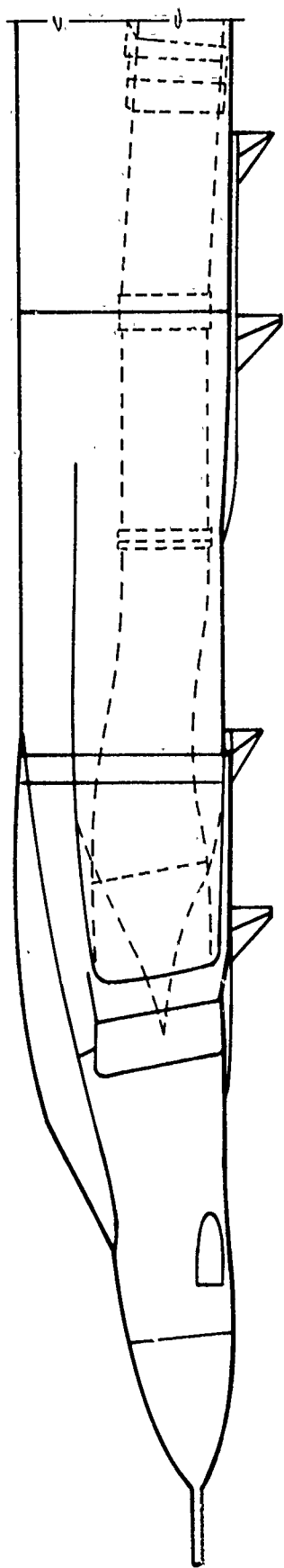
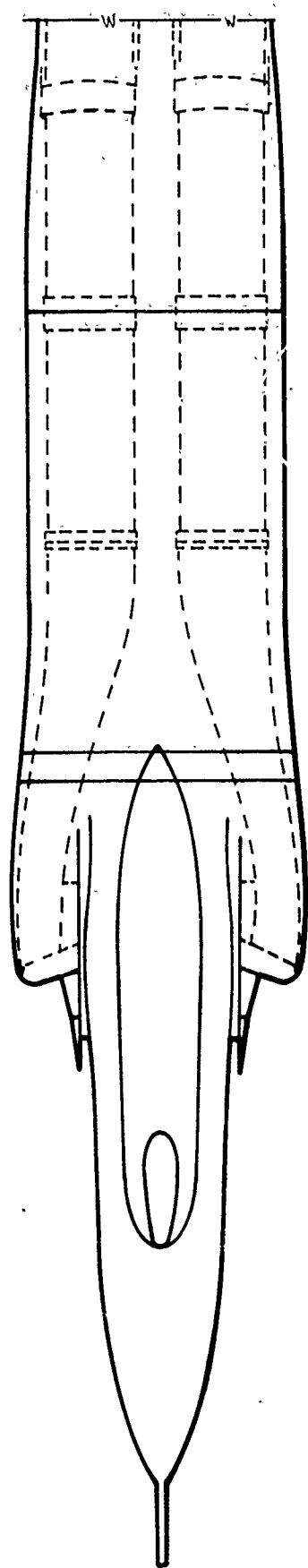


Figure 26: BASIC F/A-18 FUSELAGE, CANOPY, AND DUCT CONFIGURATION

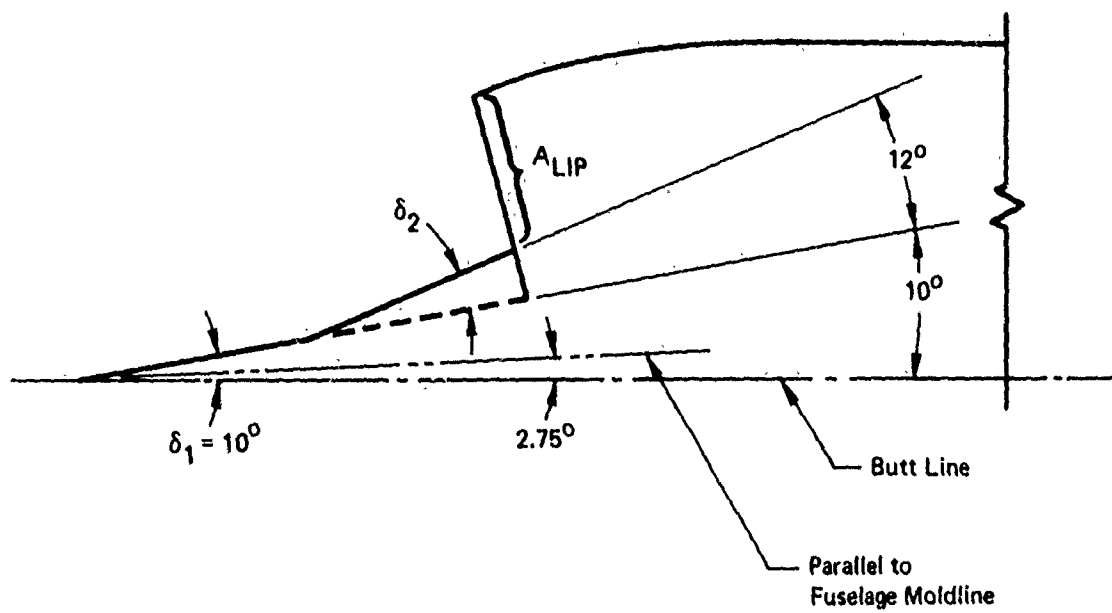


Figure 27: F-4 INLET RAMP ORIENTATION

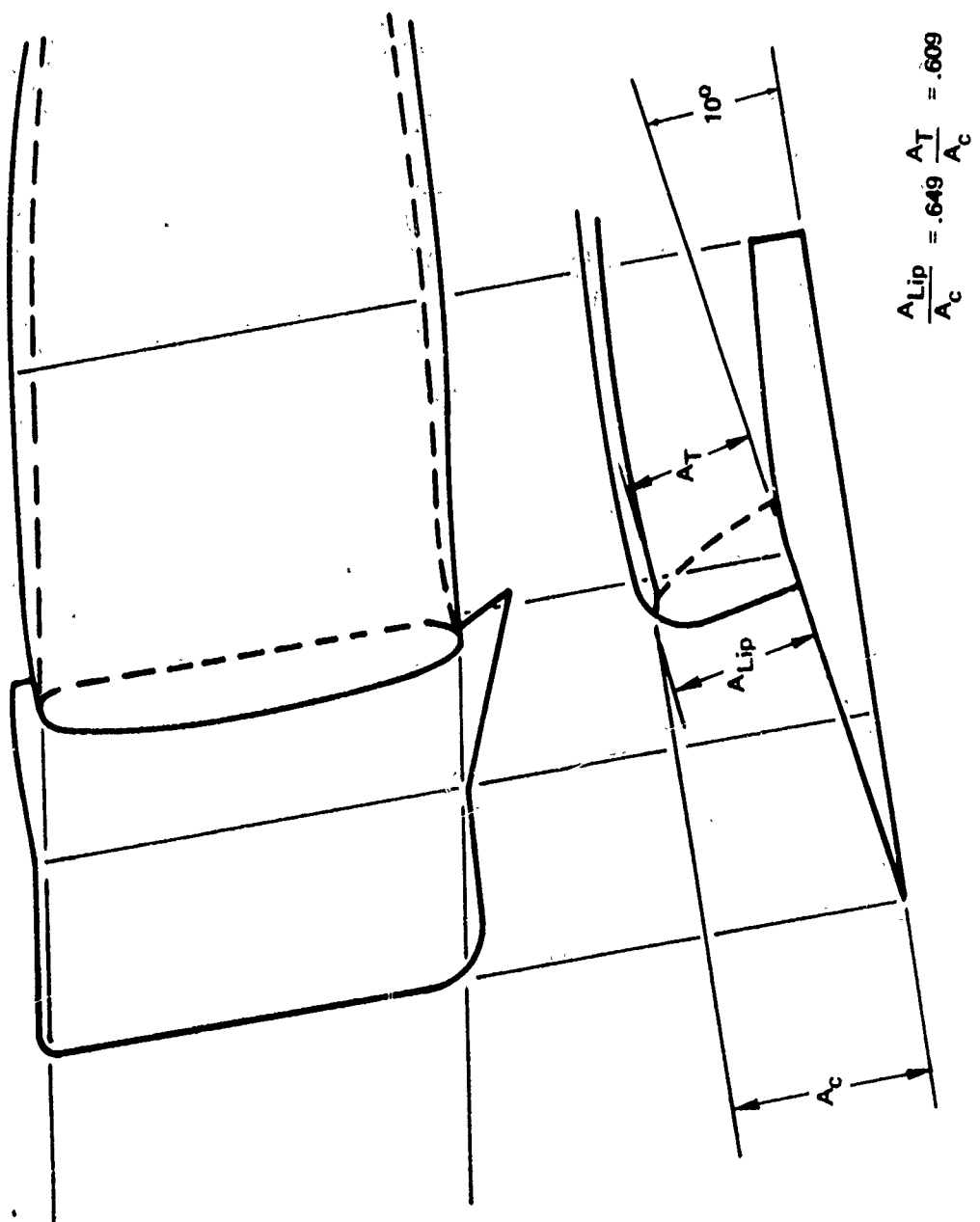


Figure 28: INLET GEOMETRY FOR $M_{\infty} = 0 - 1.20$

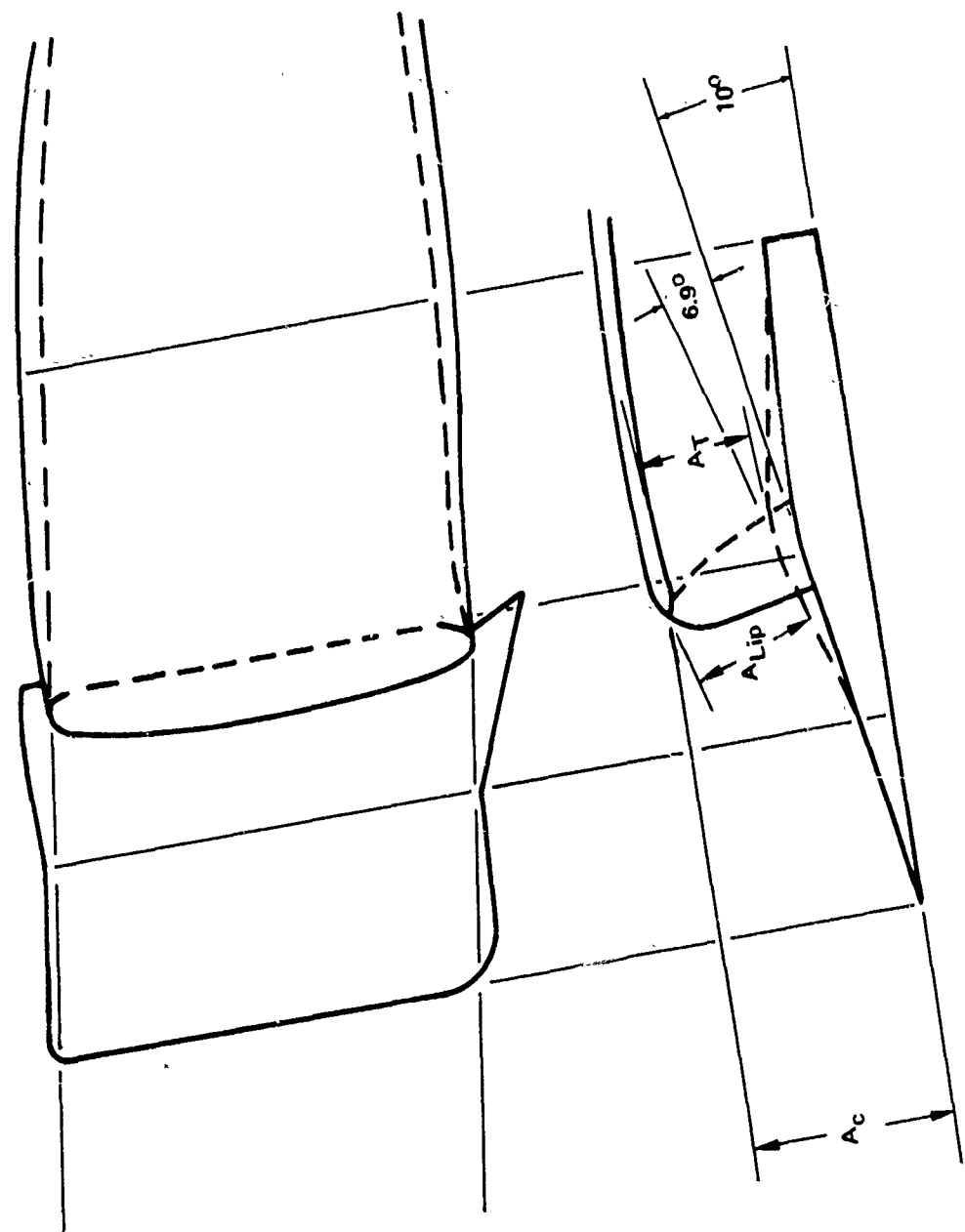


Figure 29: INLET GEOMETRY FOR $M_\infty = 1.60 - 2.0$

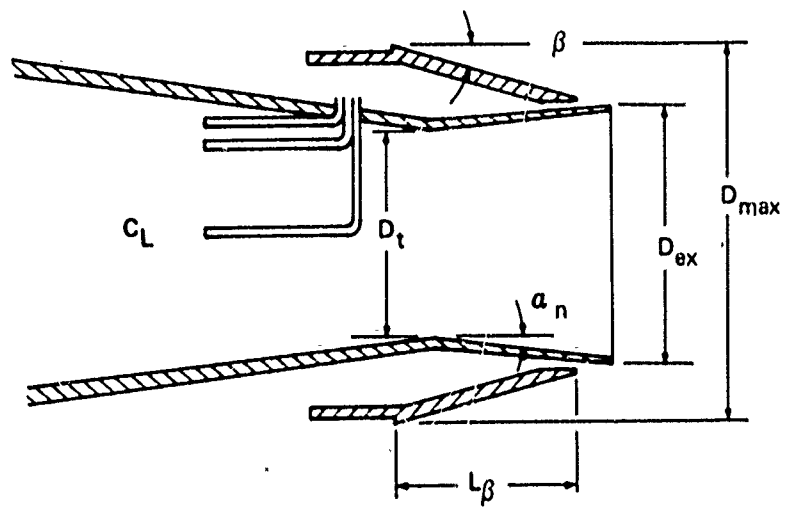


Figure 30: MODEL F-4J/B NOZZLE & SHROUD ARRANGEMENT

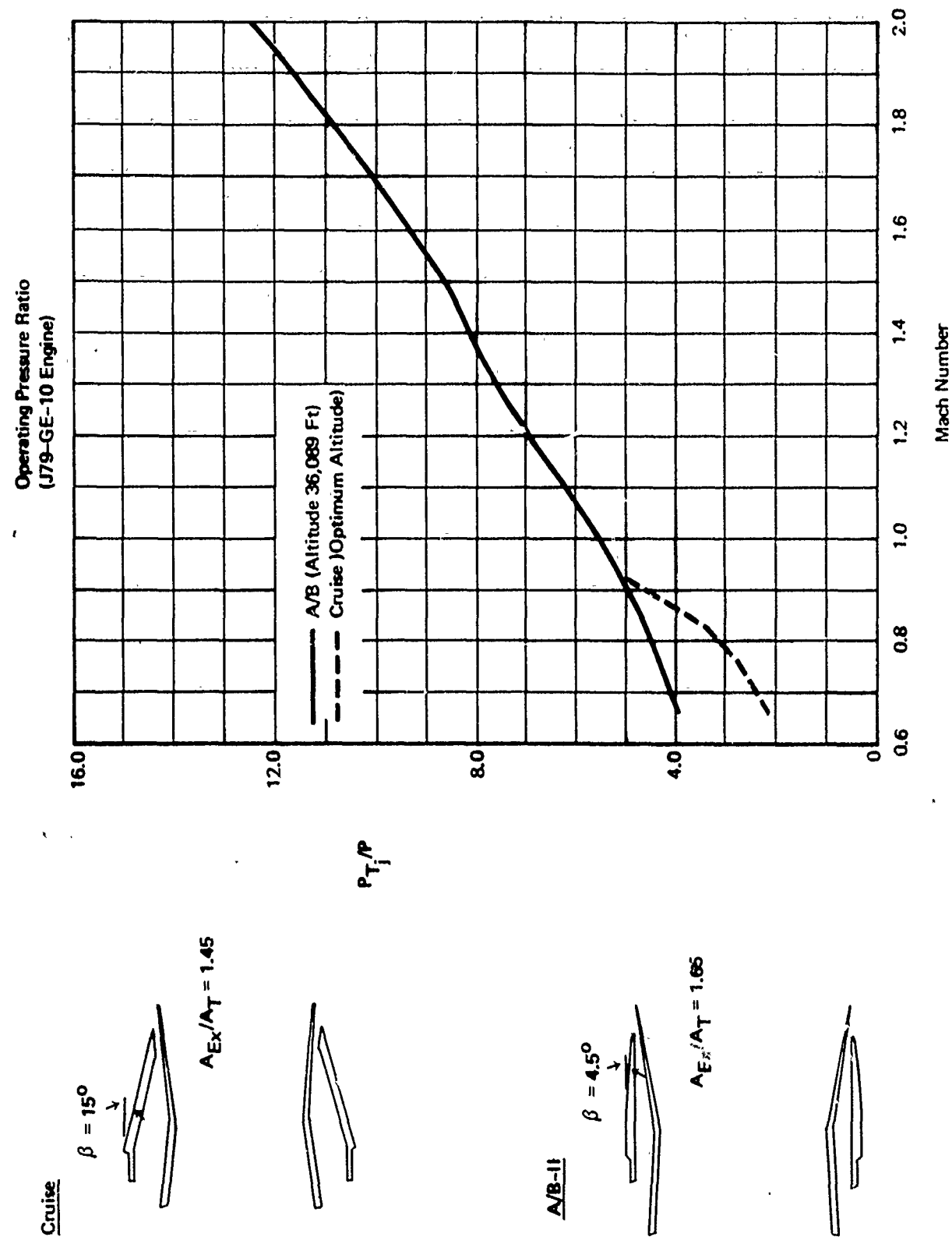


Figure 31: NOZZLE GEOMETRY AND OPERATING CONDITIONS

3.2 PREDICTED PERFORMANCE CHARACTERISTICS

3.2.1 Inlet

The same procedure was used to calculate the F-4J inlet performance that was used to calculate the inlet performance of the LWF previously discussed. The basic geometries of the two configurations are quite similar, except for the fact that the F-4J inlet is oriented with the ramp vertical instead of horizontal.

The same K_{ADD} factors were used for both the F-4J and the LWF. These factors are shown in Figure 14. The F-4J inlet geometry was used in the additive drag program (Reference 1) to obtain additive drags. These were then adjusted to the correct baseline mass flow ratio, and multiplied by the K_{ADD} factors to obtain the final spillage drags shown in Figure 39.

The predicted inlet performance characteristics for the F-4J are presented in Figures 32 through 41, in a format that is compatible with the TEM 333 program input.

3.2.2 Nozzle/Afterbody

Just as in the case of the LWF nozzle/afterbody drag calculation, the only input data required (in addition to geometric constants and engine performance tabulated data) is the nozzle/afterbody reference drag. This was determined from the data in Figure 40, 41 and 45, Volume I. The resulting reference drag is presented in Figure 42.

3.3 COMPARISON OF PREDICTED AND TEST DATA

Most of the F-4 experimental data which are available for comparing with predicted data are classified. To include these data in this report, it would be necessary to classify the report, which would limit its distribution.

Since the primary purpose of this report is to provide guidance in the use of the calculation procedure, it was decided not to include classified data, so the report could have the widest possible distribution.

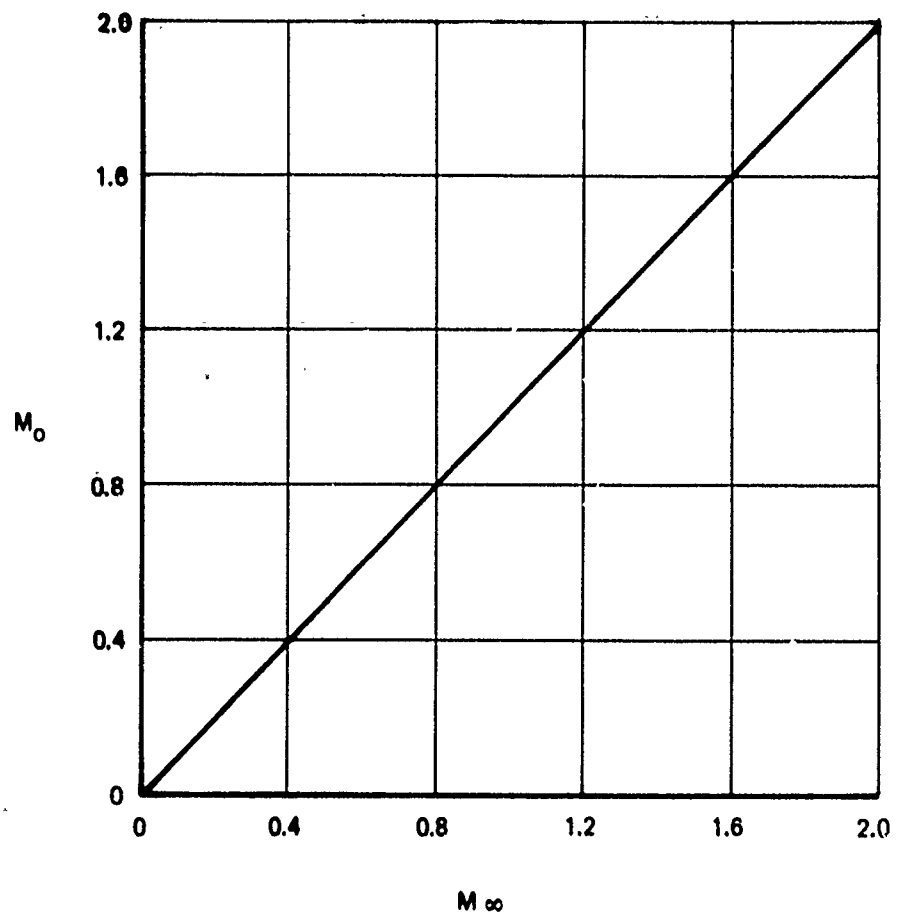


Figure 32: LOCAL MACH NUMBER VS FREE-STREAM MACH NUMBER

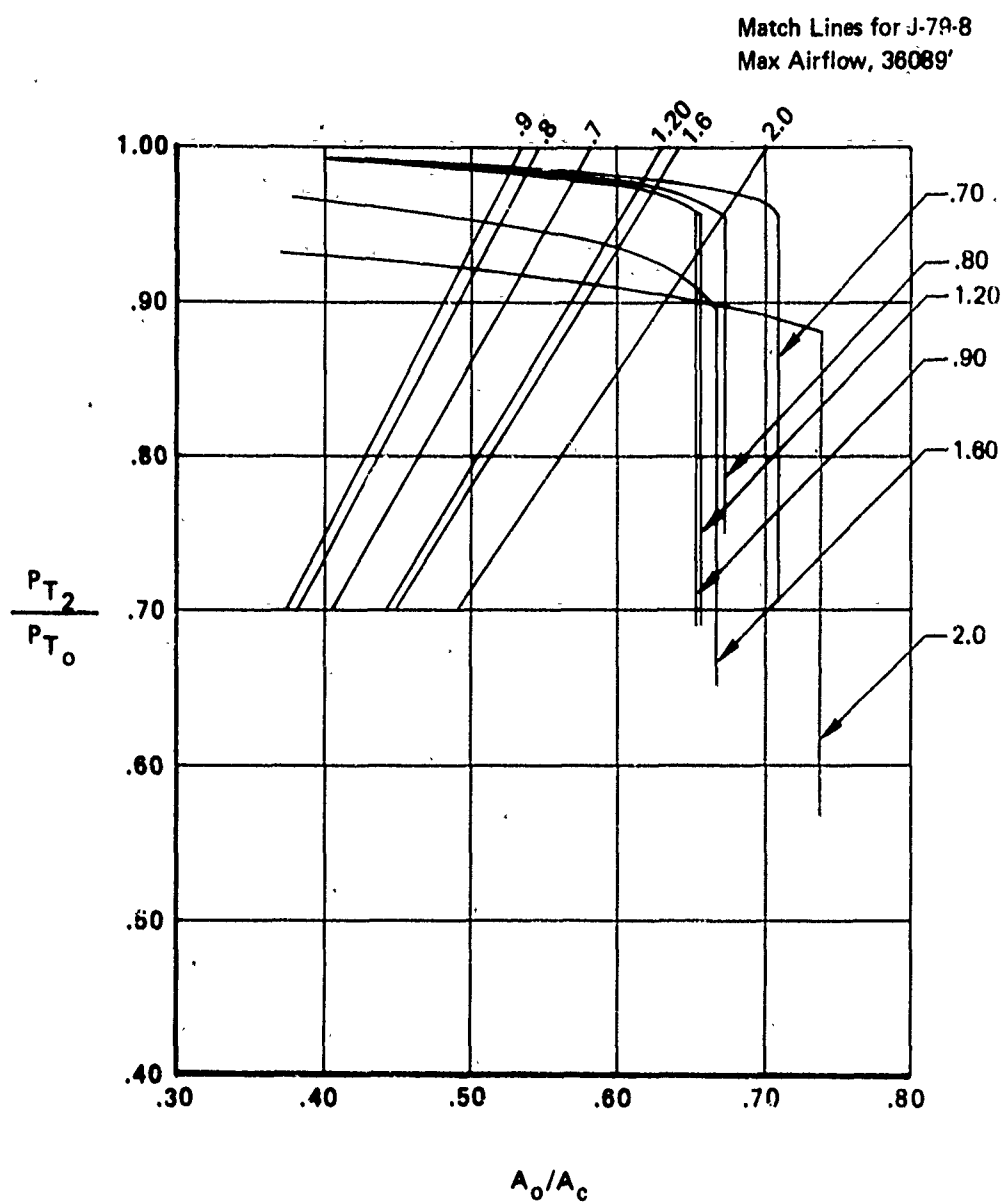


Figure 33: TOTAL PRESSURE RECOVERY VS MASS FLOW RATIO

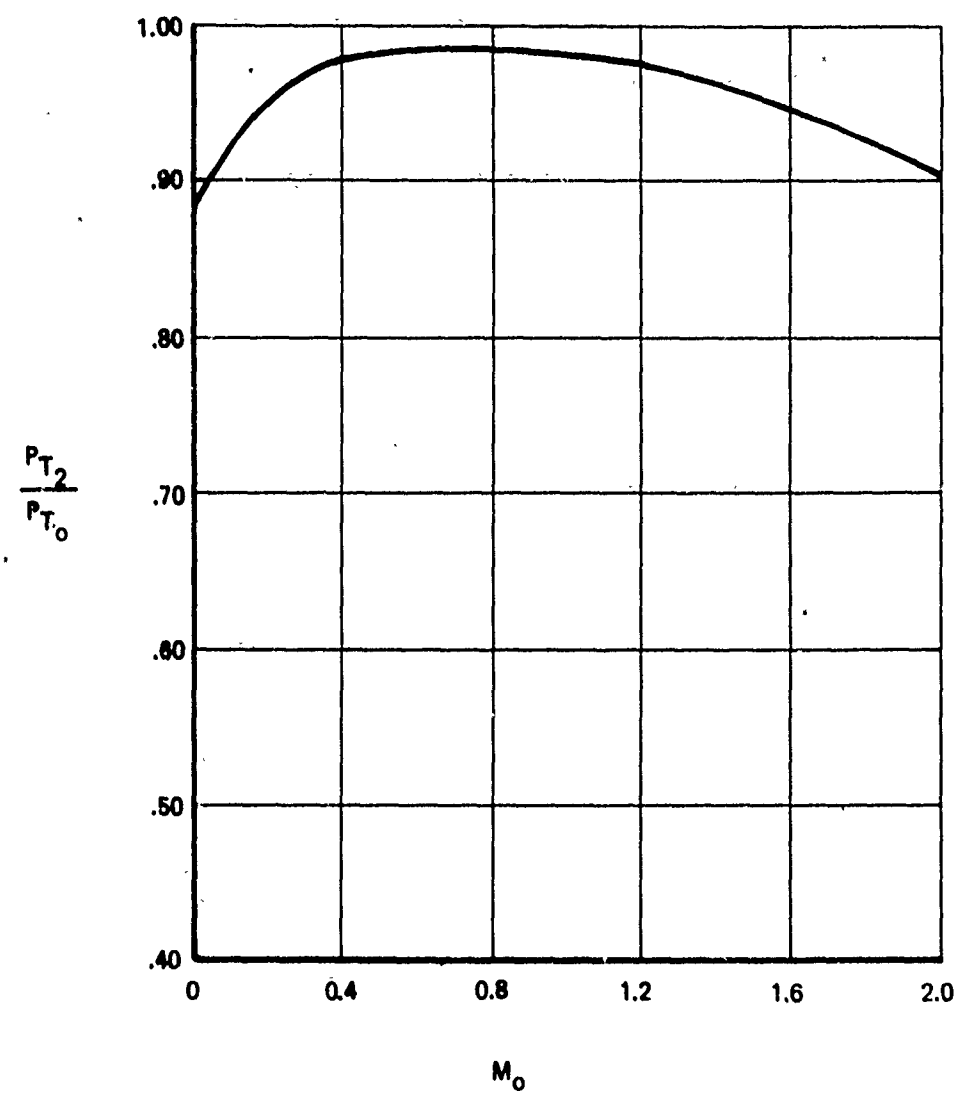


Figure 34: MATCHED INLET RECOVERY

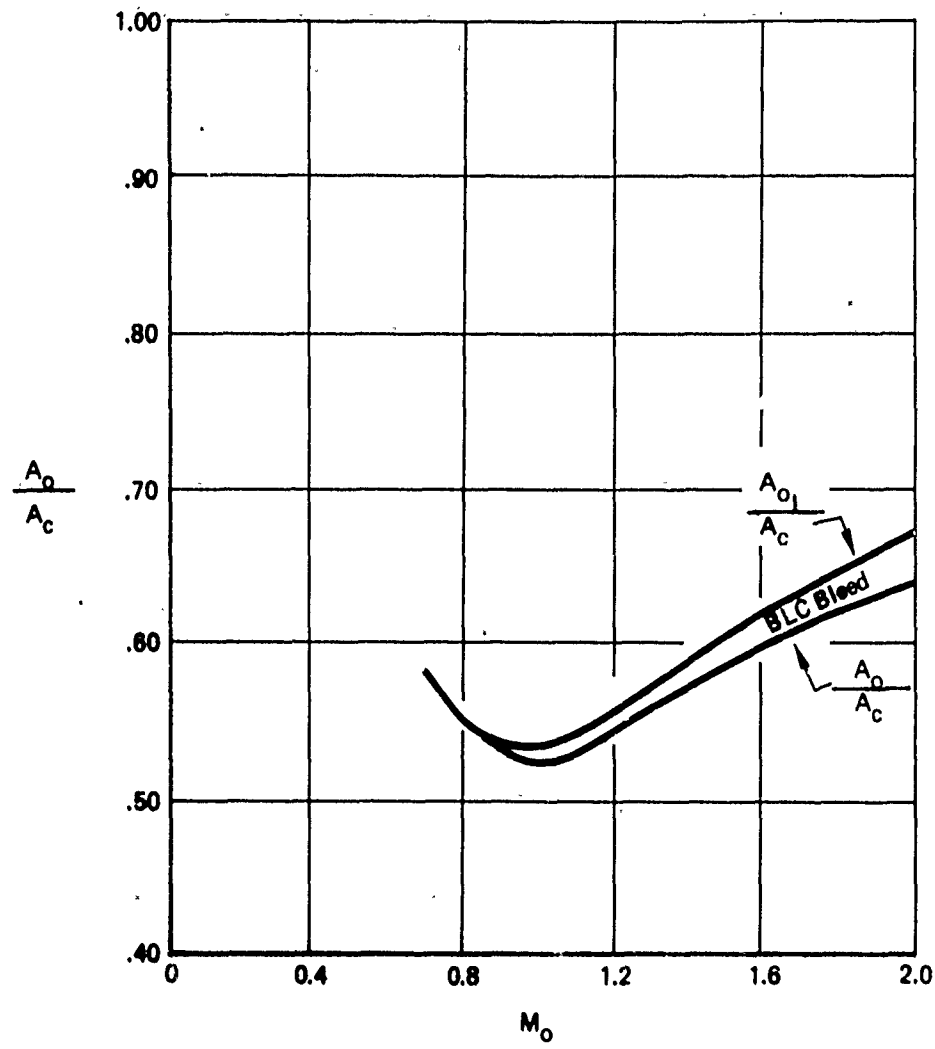


Figure 35: MATCHED INLET MASS FLOW RATIO

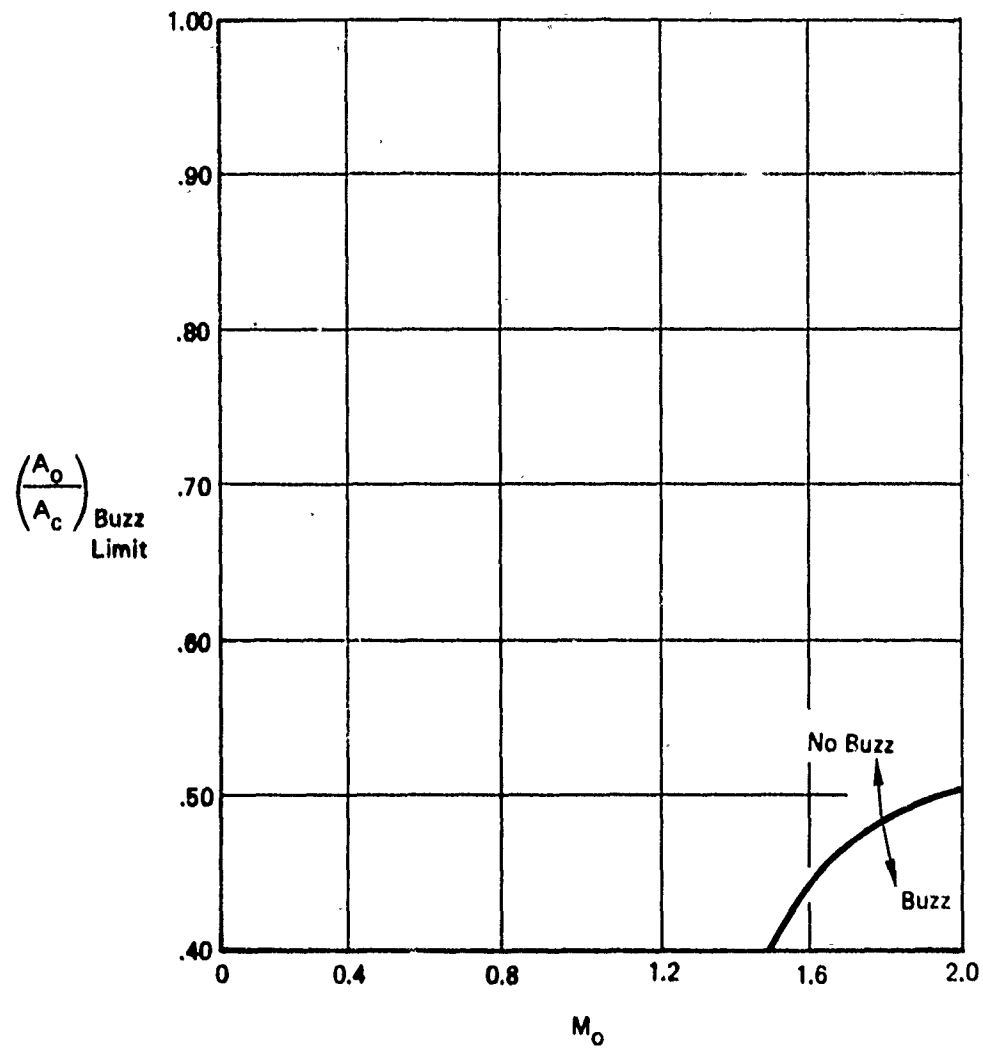


Figure 36: BUZZ LIMIT

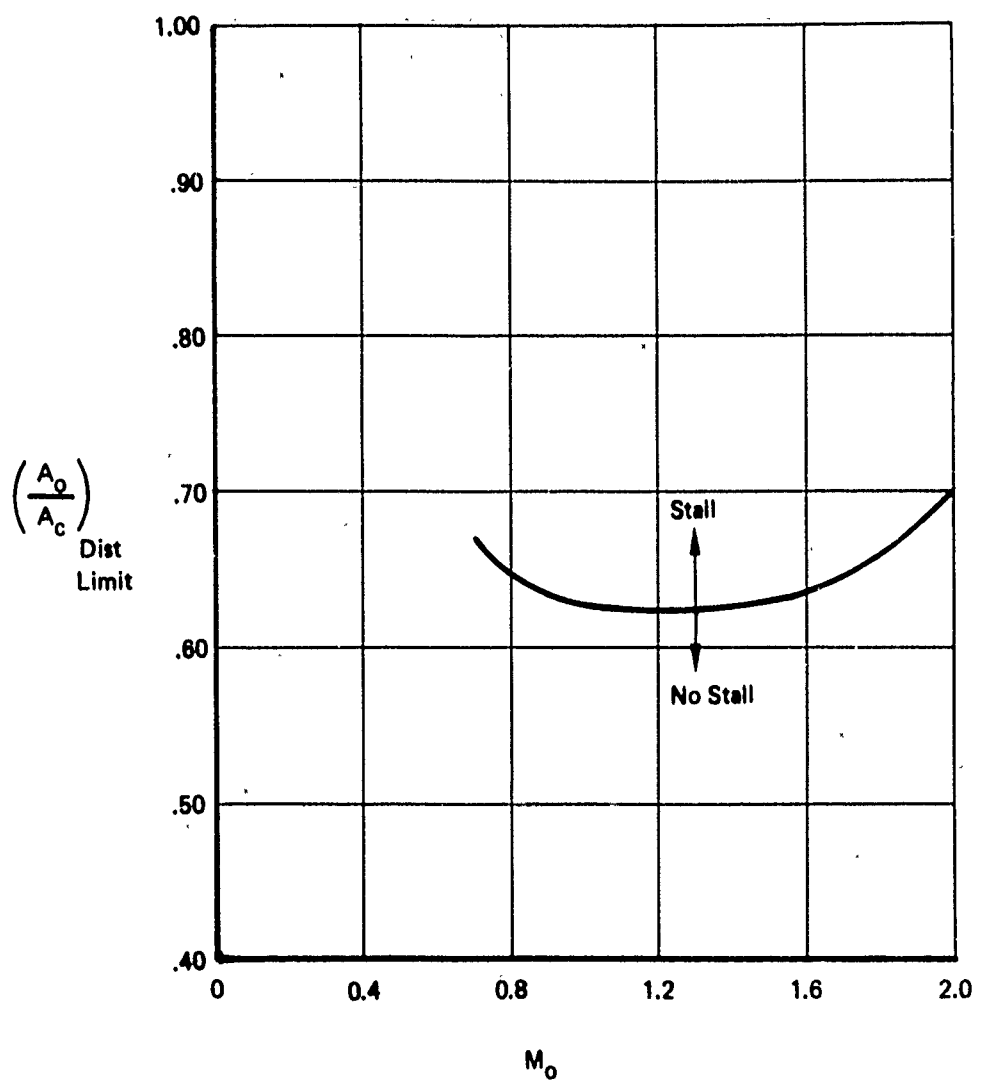


Figure 37: DISTORTION LIMIT

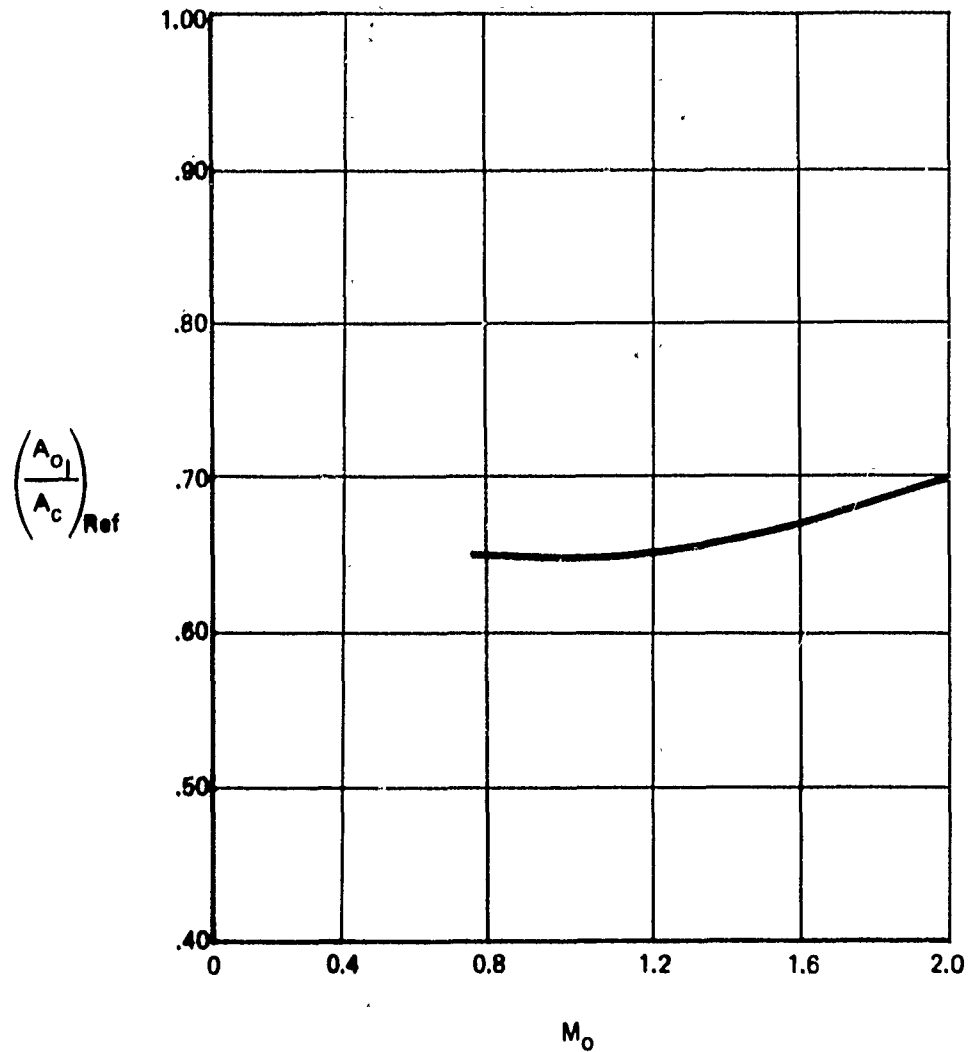


Figure 38: REFERENCE MASS FLOW RATIO

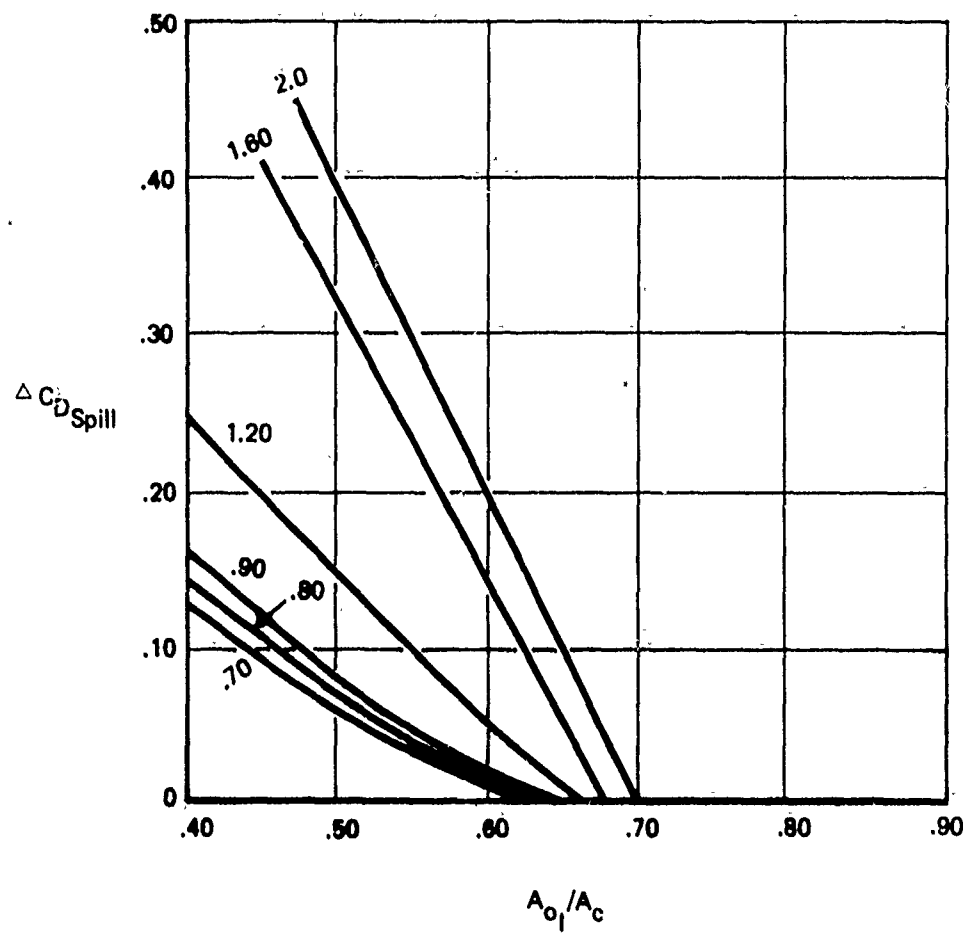


Figure 39: INLET SPILLAGE DRAG

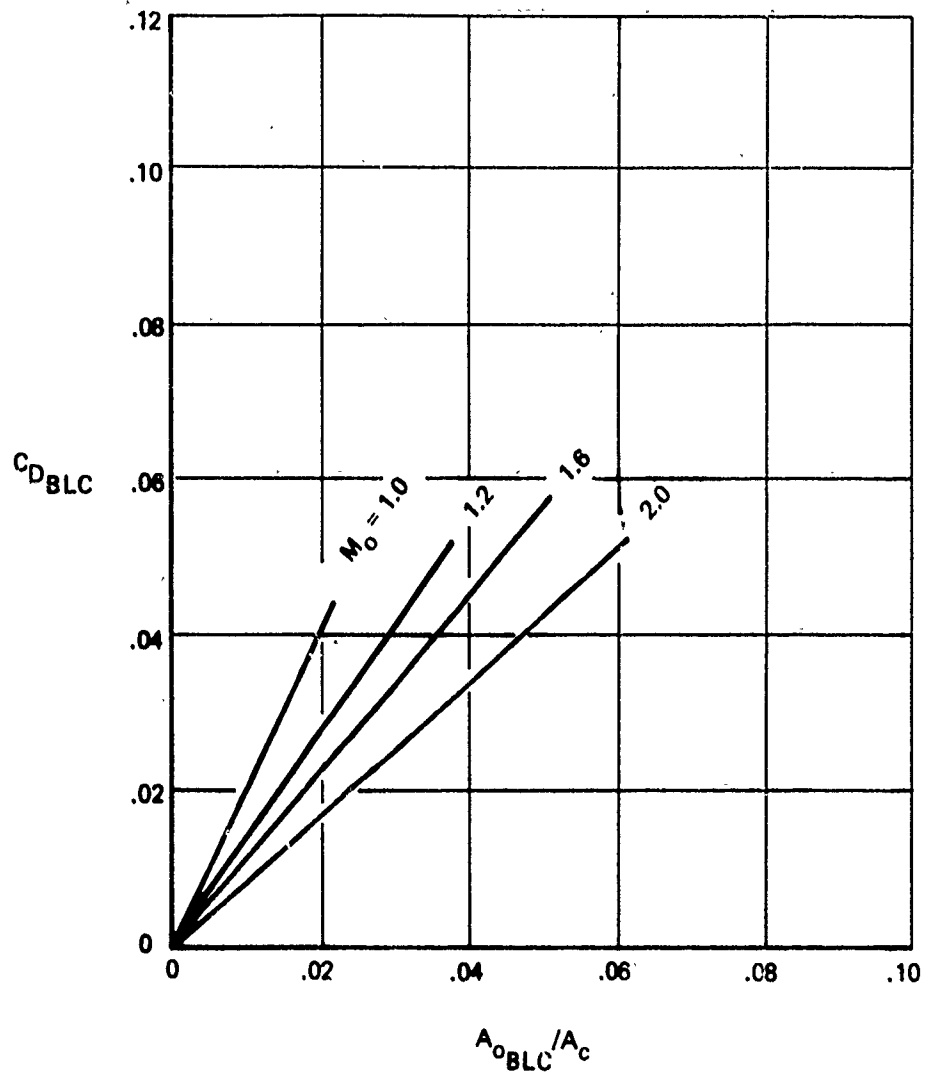


Figure 40: BOUNDARY LAYER BLEED DRAG

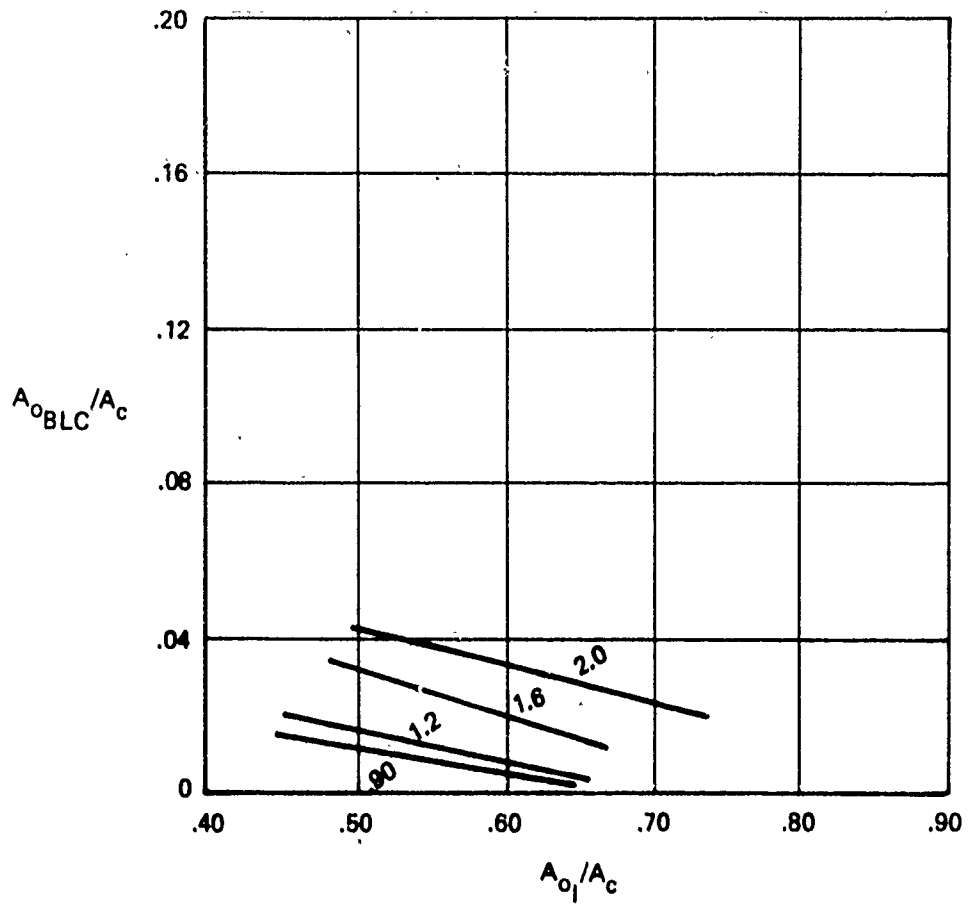


Figure 41: BOUNDARY LAYER BLEED AIRFLOW

$$A_{Ref} = .785 (D_{Max})^2 = 1,170 \text{ in.}^2$$

$$D_{Max} = 38.6 \text{ in.}$$

$$C_{D_{Ref}} = \frac{D_{Ref}}{q_0 A_{Max}}$$

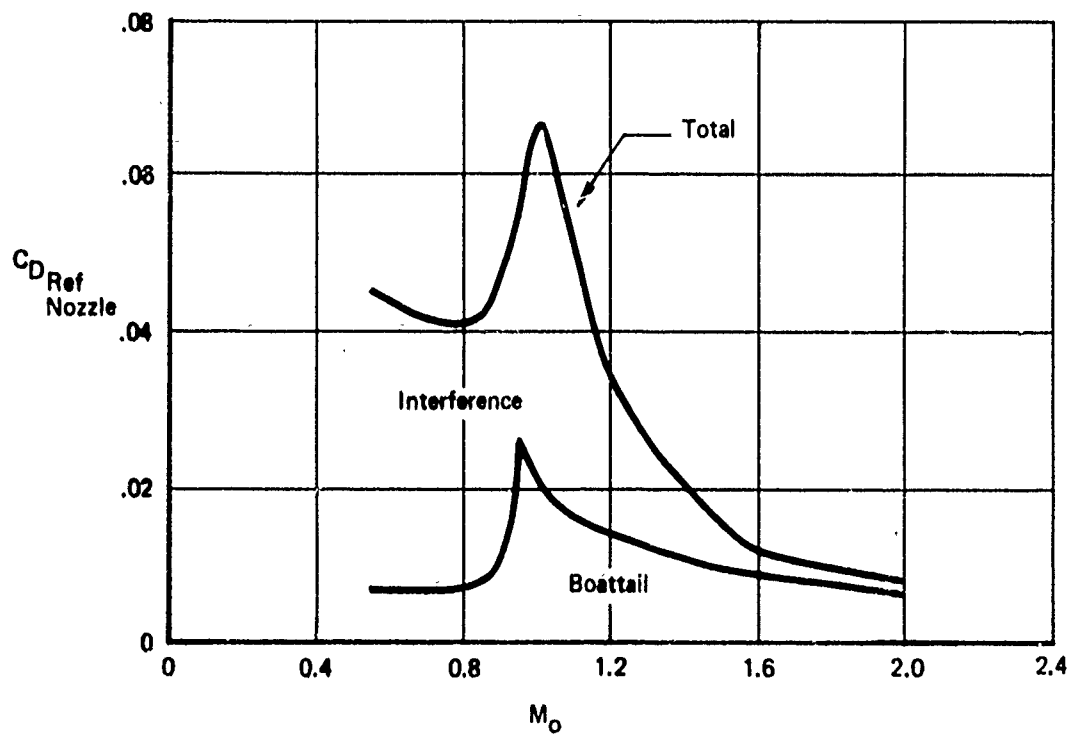


Figure 42: REFERENCE NOZZLE DRAG FOR F-4J

3.4 SUMMARY OF INPUT DATA FOR F-4J

The F-4J data used for input to the TEM 333 program to calculate installed propulsion system performance are summarized in the following table:

INLET GEOMETRY	FIGURE 26, 27 28, 29
SUBSONIC DIFFUSER GEOMETRY	FIGURE 26
NOZZLE/AFTERBODY GEOMETRY	FIGURE 30, 31
M_O vs. M_∞	FIGURE 32
P_{T_2}/P_{T_0} vs. A_O/A_C	FIGURE 33
P_{T_2}/P_{T_0} vs. M_O	FIGURE 34
A_O/A_C vs. M_O	FIGURE 35
(A_O/A_C) BUZZ LIMIT	FIGURE 36
(A_O/A_C) DIST. LIMIT	FIGURE 37
(A_{O_I}/A_C) vs. M_O REF.	FIGURE 38
ΔC_D SPILL vs. A_{O_I}/A_C	FIGURE 39
C_D PLC vs. A_{O_BLC}/A_C	FIGURE 40
A_{O_BLC}/A_C vs. A_{O_I}/A_C	FIGURE 41
C_D REF. NOZZLE	FIGURE 42
TABULATED ENGINE PERFORMANCE DATA	J79-GE-8

3.5 SAMPLE INPUT AND OUTPUT DATA FOR F-4J

This section contains sample input and output data taken directly from the computer program printout for the F-4J installed performance calculation. It is included to illustrate the format of the input and output data and to present typical results of a calculation.

OUTPUT

Standard printed output includes:

1. A "card image" listing of all input cards.
2. Labeled listing of all input fields as stored in the computer. The expanded table 2A is output as is the internally generated table of $Mach_9$ as a function of A_8/A_9 for γ_1 .
3. Output matrices including the input and output data for each of one to ten cases. A new matrix is printed whenever Mach number changes, altitude changes, or ten points have been computed at the current Mach and altitude. For each case the following are printed.

CASE	Sequential case number	
ALT	Pressure altitude - input	ft.
PS	Power setting - input	
FNA	Installed net thrust	lb.
WFT RF	Installed fuel flow corrected for recovery	
SFCA	(WFT RF)/(FNA)	
FNRF	Input thrust corrected for recovery	lb.
FRAM	Ram drag	lb.
RF	Recovery factor	
MILRF	Mil-Spec recovery factor	
DINLET	Inlet drag	lb.
CDSPL	Coefficient of spillage drag	

CDBLD	Coefficient of bleed drag	
CDBYP	Coefficient of bypass drag	
CDINL	Coefficient of inlet drag	
DNOZ	Afterbody drag	lb.
CDBT	Coefficient of boattail drag	
CDBASE	Coefficient of base drag	
DCINT	Coefficient of nozzle interference drag	
DNOZ REF	Reference afterbody drag	lb.
P8/PO	Nozzle pressure ratio - input	
A9	Nozzle exit area - input	sq. in.
A8	Nozzle throat area - input	sq. in.
CFG	Nozzle gross thrust coefficient	
BETA	Boattail angle	degrees
FN INPUT	Net thrust - input	lb.
WF INPUT	Fuel flow - input	lb/hr.
SFC INPUT	(WF INPUT)/(FN INPUT)	
W INPUT	Corrected airflow - input	lb/sec.
W ABS	Absolute airflow	lb/sec.
FN/DELTA	FNA/δ _{amb}	lb.
WF COR	WFT RF/(θ _{amb} δ _{amb})	lb/hr.
SFC COR	(WF COR)/(FN/DELTA)	
TAMB	Ambient temperature	° _R
PAMB	Ambient pressure	
TTO	Total temperature of free-stream	° _R
Q	Dynamic pressure	lb/sq. ft.

AOE/AC	Engine mass flow ratio
AOI/AC	Inlet capture mass flow ratio
AO/AC	Inlet mass flow ratio
STATUS	If equal to -99.999 a diagnostic message was written for this point.

4. Diagnostic messages. The diagnostic messages are all self-explanatory.
5. MARK II Output.

If the code on card 5.1, field 1, is 1.0 or 2.0 a MARK II engine performance deck is written on TAPE 7. The format is 80 character BCD, "card image." The MARK II deck can then be copied to PUNCH or linked to a following program.

The MARK II format is as follows:

1. Title (card image of input card 1.0)
2. Mach-alt (card image of input card 5.2)

DATA INTEGRATION IMAGES

CARD	1234567890123455789012345678901234567890123456789012345678901234567890								DEC 06, 1972
	1	2	3	4	5	6	7	8	
101	3.	1.	14300.	44181.	231.				
102	5903.	1.	16900.	36249.	193.				
103	1026.	1.	12700.	28349.	144.				
104	25000.	1.	9860.	19693.	93.				
105	35000.	1.	59300.	13114.	64.				
106	45000.	1.	3560.	6555.	43.				
107	55000.	1.	2550.	5252.	34.				
108 1.0									
109	2.	1.	21200.	47605.	272.				
110	5503.	1.	13630.	44716.	235.				
111	15000.	1.	14950.	32879.	169.				
112	25000.	1.	10230.	23611.	118.				
113	35000.	1.	7290.	15793.	73.				
114	45000.	1.	4430.	11198.	46.				
115	55000.	1.	2543.	6330.	29.				
116	55030.	1.	1463.	3791.	17.				
117 1.2									
118	5500.	1.	21200.	47215.	270.				
119	15350.	1.	17795.	38733.	232.				
120	25000.	1.	13200.	27655.	142.				
121	45000.	1.	5680.	12403.	59.				
122	55000.	1.	3263.	7772.	33.				
123	55060.	1.	1860.	4693.	22.				
124 1.4									
125	15000.	1.	20300.	44393.	235.				
126	25030.	1.	15830.	33212.	172.				
127	35020.	1.	11300.	23232.	117.				
128	45030.	1.	6932.	14952.	73.				
129	55310.	1.	4153.	9575.	44.				
130	55030.	1.	2373.	5819.	27.				
131 1.6									
132	25100.	1.	10220.	22298.	232.				
133	35050.	1.	13630.	27843.	143.				
134	45060.	1.	2450.	17650.	83.				
135	55080.	1.	5250.	11276.	54.				
136	55060.	1.	2933.	7129.	33.				
137 1.8									
138	25300.	1.	19300.	41367.	223.				
139	35000.	1.	15620.	32396.	170.				
140	45000.	1.	9395.	20682.	106.				
141	55050.	1.	5996.	13139.	55.				
142	55030.	1.	3512.	8522.	43.				
143 2.0									
144	35000.	1.	16723.	34993.	138.				
145	45000.	1.	12700.	22541.	118.				
146	55000.	1.	6610.	14284.	72.				
147	65000.	1.	3570.	9224.	44.				

TEM-333 ENGINE PERFORMANCE PROGRAM

J79-6 F4 CONFIGURATION WS/WB=.65

W8 TABLE

-0.03000	-0.00000	-0.00000	-0.00000	-0.00000	-0.00000
-0.05000	-0.00000	-0.00000	-0.00000	-0.00000	-0.00000
-0.03000	-0.00000	-0.00000	-0.00000	-0.00000	-0.00000
-0.03000	-0.00000	-0.00000	-0.00000	-0.00000	-0.00000

REFERENCE NOZZLE DRAG TABLE

0.03000	0.40000	0.75000	0.35000	0.95000	1.00000	1.25000	1.50000	1.80000	2.00000-0 NOZ REF
0.04416	0.04416	0.04103	0.04269	0.06603	0.06603	0.03500	0.01520	0.01100	0.00900-0 J79-6

INPUT DECK INPUT AC MACHS MACH DES MACH ENG. MC SEC

6.82J 2.810 -0.000 -0.0 -0.0

TABLE NUMBER 1

6.022C	3.880J	-0.00000	-0.30000	-0.00000	-0.00000	-0.00000	-0.00000	-0.00000
0.022C	3.880J	-0.00000	-0.30000	-0.00000	-0.00000	-0.00000	-0.00000	-0.00000

TABLE NUMBER 2A

• 5103C	• 7003J	• 8033J	• 9033J	• 1.2033J	1.600CJ	2.00000	-0.00000	-0.00000
• 3103C	• 5003C	• 6003C	• 7003C	• 8003C	• 9003C	• 95000	-0.00000	-0.00000
• 5252C	• 9952J	• 9952J	• 9800C	• 97200	• 96900	• 95000	-0.00000	-0.00000
• 3003C	• 5003J	• 6000J	• 5500J	• 675CJ	• 700CJ	• 72000	-0.00000	-0.00000
• 9155C	• 9900J	• 9800J	• 9750J	• 9700J	• 96500	• 95500	-0.00000	-0.00000
• 3907C	• 5307J	• 5000J	• 5250J	• 6500J	• 6750J	-0.00000	-0.00000	-0.00000
• 6159C	• 9470J	• 9300J	• 9750J	• 9680J	• 9580J	-0.00000	-0.00000	-0.00000
• 3206C	• 5306J	• 6000J	• 6250J	• 6500J	• 6550J	-0.00000	-0.00000	-0.00000
• 9375C	• 9371J	• 9780J	• 9700J	• 9600J	• 9560J	-0.00000	-0.00000	-0.00000
• 3202C	• 5003J	• 5300J	• 6250J	• 6500J	• 6500J	-0.00000	-0.00000	-0.00000
• 9155C	• 9870J	• 9790J	• 9700J	• 9600J	• 9500J	-0.00000	-0.00000	-0.00000
• 3103C	• 5003J	• 6000J	• 6250J	• 6500J	• 6550J	-0.00000	-0.00000	-0.00000
• 3003C	• 5003J	• 5303J	• 5003J	• 5250J	• 5500J	-0.00000	-0.00000	-0.00000
• 3103C	• 5003J	• 5303J	• 5003J	• 5250J	• 5500J	-0.00000	-0.00000	-0.00000
• 9155C	• 9520J	• 9352J	• 9250J	• 9120J	• 8950J	-0.00000	-0.00000	-0.00000
• 3003C	• 5003J	• 5303J	• 5003J	• 5250J	• 5500J	-0.00000	-0.00000	-0.00000
• 9155C	• 9203J	• 9190J	• 9160J	• 8850J	• 8810J	-0.00000	-0.00000	-0.00000

TABLE 2A IS EXPANDED TO +1 POINTS WITH INTERMEDIATE MACH CURVES INTERPOLATED AS DIAGNOSTIC AID

• 60	• 300C	• 3275	• 3550	• 3825	• 4103	• 4375	• 4650	• 4925	• 5205	• 5475	• 5755
• 5842	• 5933	• 6025	• 6117	• 6208	• 6300	• 6392	• 6483	• 6575	• 6667		
• 6738	• 6853	• 6942	• 7133	• 7225	• 7317	• 7308	• 7403	• 7503	• 7583		
• 7675	• 7767	• 7859	• 7950	• 8042	• 8133	• 8225	• 8317	• 8408	• 8500		
• 9955J	• 9943	• 9936	• 9929	• 9922	• 9916	• 9909	• 9902	• 9890	• 9876	• 9862	
• 9858	• 9853	• 9849	• 9844	• 9840	• 9835	• 9833	• 9826	• 9821	• 9817		
• 9812	• 9807	• 9803	• 9797	• 9790	• 9783	• 9775	• 9768	• 9761	• 9753		
• 9756	• 9739	• 9731	• 9724	• 9715	• 9714	• 9704	• 9693	• 9683	• 9676		
• 65	• 3103	• 3212	• 3485	• 3727	• 3970	• 4212	• 4455	• 4697	• 4943	• 5192	• 5425
• 5636	• 5587	• 5663	• 5748	• 5823	• 5910	• 5991	• 6072	• 6153	• 6233		
• 6314	• 6395	• 6476	• 6557	• 6638	• 6718	• 6799	• 6883	• 6961	• 7042		
• 7123	• 7293	• 7294	• 7365	• 7446	• 7527	• 7608	• 7688	• 7769	• 7850		
• 9150	• 9344	• 9339	• 9326	• 9320	• 9314	• 9308	• 9303	• 9309	• 9316		
• 9375	• 9365	• 9365	• 9359	• 9353	• 9347	• 9341	• 9336	• 9339	• 9346		
• 9313	• 9307	• 9301	• 9295	• 9287	• 9280	• 9273	• 9268	• 9273	• 9275		
• 9741	• 9739	• 9723	• 9709	• 9697	• 9685	• 9672	• 9662	• 9672	• 9677		
• 70	• 3100	• 321J	• 3420	• 3630	• 3840	• 4050	• 4260	• 4470	• 4680	• 4890	• 5100
• 5117	• 5240	• 531J	• 5380	• 5450	• 5520	• 5590	• 5660	• 5730			
• 5913	• 5943	• 6010	• 6080	• 6150	• 6220	• 6290	• 6360	• 6430	• 6500		
• 6571	• 6643	• 6713	• 6780	• 6850	• 6920	• 6990	• 7060	• 7130	• 7200		
• 9150	• 9145	• 9139	• 9134	• 9129	• 9124	• 9118	• 9113	• 9103	• 9190		
• 9133	• 9176	• 9863	• 9362	• 9353	• 9348	• 9341	• 9334	• 9327	• 9320		
• 9013	• 9206	• 9222	• 9222	• 9694	• 9666	• 9652	• 9623	• 9585	• 9550		

• 3929	• 3199	• 3397	• 3595	• 3795	• 3994	• 4192	• 4391	• 4590	• 4789	• 4987
• 5054	• 5120	• 5186	• 5253	• 5319	• 5385	• 5451	• 5518	• 5584	• 5650	
• 5715	• 5783	• 5843	• 5915	• 5981	• 6048	• 6114	• 6180	• 6246	• 6313	
• 6379	• 6445	• 6511	• 6578	• 6644	• 6716	• 6776	• 6843	• 6909	• 6975	
• 9936	• 944	• 9937	• 9931	• 9924	• 9913	• 9912	• 9905	• 9899	• 9893	• 9882
• 9378	• 9873	• 9867	• 9862	• 9856	• 9850	• 9845	• 9839	• 9833	• 9827	
• 9822	• 9816	• 9813	• 9805	• 9799	• 9793	• 9786	• 9782	• 9772	• 9762	
• 9749	• 9735	• 9723	• 9704	• 9669	• 9673	• 9653	• 9625	• 9595	• 9565	

• 80	• 3000	• 3187	• 3375	• 3562	• 3750	• 3937	• 4125	• 4312	• 4503	• 4687
	• 4958	• 5000	• 5063	• 5125	• 5188	• 5250	• 5313	• 5375	• 5439	• 5509
	• 5593	• 5625	• 5688	• 5750	• 5813	• 5875	• 5938	• 6001	• 6063	• 6125
	• 5133	• 6250	• 6313	• 6375	• 6433	• 6500	• 6563	• 6625	• 6688	• 6750
• 9950	• 9942	• 9935	• 9927	• 9920	• 9912	• 9905	• 9897	• 9890	• 9882	• 9875
• 9372	• 9370	• 9866	• 9861	• 9857	• 9852	• 9848	• 9844	• 9839	• 9835	
• 9531	• 9326	• 9622	• 9817	• 9313	• 9809	• 9804	• 9803	• 9797	• 9777	
• 9752	• 9750	• 9732	• 9715	• 9697	• 9686	• 9655	• 9630	• 9615	• 9595	

• 85	• 3000	• 3132	• 3365	• 3547	• 3730	• 3912	• 4095	• 4277	• 4461	• 4642
	• 4996	• 4947	• 5038	• 5060	• 5169	• 5129	• 5190	• 5251	• 5312	• 5373
	• 5494	• 5555	• 5615	• 5677	• 5733	• 5798	• 5859	• 5920	• 5981	• 6042
	• 6113	• 6163	• 6223	• 6285	• 6346	• 6407	• 6468	• 6529	• 6589	• 6650
• 9370	• 7913	• 9235	• 9923	• 9921	• 9913	• 9906	• 9899	• 9892	• 9884	• 9877
• 9875	• 9872	• 9863	• 9865	• 9860	• 9855	• 9851	• 9846	• 9841	• 9836	
• 9351	• 9826	• 9821	• 9817	• 9312	• 9807	• 9802	• 9797	• 9788	• 9779	
• 9753	• 9753	• 9735	• 9716	• 9693	• 9677	• 9653	• 9629	• 9604	• 9580	

• 90	• 3000	• 3179	• 3355	• 3532	• 3713	• 3897	• 4085	• 4262	• 4420	• 4597
	• 4934	• 4939	• 4953	• 5012	• 5071	• 5136	• 5189	• 5243	• 5308	• 5367
	• 5426	• 5485	• 5544	• 5603	• 5663	• 5722	• 5781	• 5843	• 5899	• 5958
	• 5613	• 5777	• 6135	• 6195	• 6254	• 6313	• 6373	• 6432	• 6491	• 6550
• 9350	• 3943	• 9936	• 9929	• 9922	• 9914	• 9907	• 9903	• 9893	• 9886	• 9879
• 9277	• 9874	• 9872	• 9869	• 9854	• 9850	• 9846	• 9842	• 9837	• 9836	
• 9832	• 9325	• 9821	• 9316	• 9310	• 9305	• 9300	• 9295	• 9289	• 9283	
• 9714	• 9755	• 9737	• 9718	• 9593	• 9675	• 9651	• 9627	• 9604	• 9586	

• 1.05	• 3000	• 3179	• 3357	• 3536	• 3715	• 3894	• 4072	• 4251	• 4430	• 4609
	• 4847	• 4907	• 4965	• 5026	• 5085	• 5145	• 5205	• 5264	• 5324	• 5383
	• 5643	• 5503	• 5562	• 5622	• 5681	• 5741	• 5800	• 5861	• 5921	• 5979
	• 5053	• 6093	• 6153	• 6218	• 6277	• 6337	• 6396	• 6456	• 6515	• 6575
• 9250	• 9943	• 9936	• 9929	• 9921	• 9914	• 9907	• 9903	• 9893	• 9886	• 9878
• 3676	• 9974	• 9871	• 9868	• 9862	• 9857	• 9852	• 9845	• 9841	• 9835	
• 9833	• 9325	• 9819	• 9814	• 9809	• 9803	• 9798	• 9793	• 9787	• 9782	
• 3753	• 9749	• 9729	• 9710	• 9689	• 9665	• 9641	• 9618	• 9598	• 9580	

• 1.20	• 3000	• 3182	• 3363	• 3543	• 3720	• 3903	• 4080	• 4260	• 4443	• 4620
	• 4920	• 4920	• 4960	• 5040	• 5100	• 5160	• 5220	• 5280	• 5340	• 5400
	• 5452	• 5520	• 5581	• 5640	• 5710	• 5780	• 5840	• 5900	• 5960	• 6000
	• 6120	• 6120	• 6180	• 6240	• 5303	• 6360	• 6420	• 6480	• 6540	• 6600
• 9950	• 9342	• 9336	• 9324	• 9321	• 9914	• 9907	• 9900	• 9892	• 9885	• 9878
• 9376	• 9373	• 9813	• 9812	• 9811	• 9861	• 9861	• 9856	• 9845	• 9839	• 9834
• 9829	• 9823	• 9823	• 9813	• 9812	• 9317	• 9802	• 9796	• 9791	• 9785	• 9780

.9761 .9742 .9722 .9703 .9680 .9656 .9632 .9608 .9592 .9580

1.40 .3000 .3162 .3365 .3547 .3730 .3912 .4035 .4277 .4460 .4642 .4825

.4836 .494 .5059 .516 .5265 .536 .5477 .5588 .5688 .5798 .589 .5981 .5933
 .5434 .555 .5616 .5677 .5738 .579 .5859 .5920 .5981 .6042
 .6113 .6163 .6224 .6285 .6346 .6407 .6468 .6528 .6589 .6650
 .9345 .9317 .9304 .9379 .9376 .9477 .949 .9539 .9574 .9574 .9546
 .9313 .9698 .9692 .9685 .9677 .9669 .9661 .9653 .9645 .9637
 .9629 .9621 .9614 .9606 .9593 .959 .9582 .9574 .9574 .9546
 .9526 .9504 .9481 .9456 .9428 .9400 .9370 .9331 .9297 .9265

1.60 .3500 .3165 .3373 .3555 .3740 .3925 .4116 .4295 .4480 .4665 .4850

.4912 .4973 .5035 .5097 .5158 .5226 .5282 .5343 .5405 .5467
 .5528 .5591 .5652 .5713 .5775 .5837 .5908 .5968 .6022 .6083
 .6145 .6209 .6268 .6330 .6392 .6453 .6515 .6577 .6638 .6705
 .9740 .9720 .9699 .9679 .9659 .9638 .9618 .9598 .9577 .9557
 .9530 .9523 .9514 .9504 .9493 .9483 .9472 .9462 .9451 .9441
 .9433 .9420 .9409 .9399 .9388 .9376 .9367 .9357 .9341 .9317
 .9232 .9267 .9249 .9208 .9176 .9144 .9107 .9055 .9002 .8950

1.80 .3000 .3232 .3405 .3637 .3810 .4012 .4215 .4417 .4623 .4822 .5025

.5093 .5165 .5228 .5295 .5363 .5530 .5498 .5565 .5633 .5700

.5736 .5835 .5903 .5970 .6033 .6105 .6173 .6240 .6308 .6375

.6443 .6510 .6578 .6645 .6713 .6786 .6848 .6915 .6983 .7050

.9545 .9527 .9508 .9493 .9471 .9453 .9434 .9416 .9398 .9379 .9358

.9351 .9364 .9336 .9327 .9318 .9309 .9300 .9291 .9293 .9274

.9254 .9252 .9240 .9228 .9216 .9202 .9191 .9179 .9164 .9145

.9126 .9106 .9086 .9063 .9039 .9014 .8987 .8952 .8916 .8880

2.00 .3900 .3223 .3440 .3660 .3880 .4103 .4320 .4540 .4763 .4980 .5200

.5273 .5347 .5423 .5493 .5567 .5640 .5713 .5787 .5860 .5933

.6007 .6080 .6153 .6227 .6300 .6373 .6447 .6520 .6593 .6667

.6740 .6813 .6887 .6965 .7033 .7107 .7183 .7253 .7327 .7409

.9350 .9333 .9317 .9300 .9284 .9267 .9251 .9234 .9219 .9201 .9180

.9173 .9165 .9155 .9151 .9143 .9136 .9129 .9121 .9114 .9107

.9099 .9085 .9071 .9057 .9043 .9029 .9015 .9001 .8987 .8973

.8959 .3945 .8932 .8918 .8902 .8884 .8867 .8849 .8830 .8810

MINIMUM MACH NUMBER FOR INLET DRAG CALCULATIONS .600

TABLE NUMBER 23
 C.00000 .20000 .40000 .60000 .90000 1.00000 1.20000 1.60000 2.00000 2.00000 -0.00000 -0.00000 -0.00000 -0.00000 -0.00000

1.01000 .57500 .54500 .53600 .52000 1.00000 1.02000 1.06000 1.08000 1.09000 -0.00000 -0.00000 -0.00000 -0.00000 -0.00000

TABLE NUMBER 24
 C.00000 .70000 .80000 .90000 1.00000 1.02000 1.06000 1.08000 1.09000 -0.00000 -0.00000 -0.00000 -0.00000 -0.00000

1.01000 .45000 .44000 .43000 1.00000 1.02000 1.06000 1.08000 1.09000 -0.00000 -0.00000 -0.00000 -0.00000 -0.00000

TABLE NUMBER 25
 C.00000 .20000 .40000 .60000 .90000 1.00000 1.20000 1.60000 2.00000 2.00000 -0.00000 -0.00000 -0.00000 -0.00000 -0.00000

1.01000 .57500 .54500 .53600 .52000 1.00000 1.02000 1.06000 1.08000 1.09000 -0.00000 -0.00000 -0.00000 -0.00000 -0.00000

TABLE NUMBER 26
 C.00000 .1.00000 1.60000 2.00000 2.40000 2.80000 3.20000 3.60000 4.00000 4.40000 -0.00000 -0.00000 -0.00000 -0.00000 -0.00000

1.01000 .45000 .44000 .43000 1.00000 1.02000 1.06000 1.08000 1.09000 -0.00000 -0.00000 -0.00000 -0.00000 -0.00000

TABLE NUMBER 3

TABLE NUMBER 3					
0.01000	-0.20000	-0.00000	-0.00000	-0.00000	-0.00000
0.02000	-0.40000	-0.10000	-0.00000	-0.00000	-0.00000
0.03000	-0.60000	-0.20000	-0.00000	-0.00000	-0.00000
0.04000	-0.80000	-0.30000	-0.00000	-0.00000	-0.00000
0.05000	-0.90000	-0.33333	-0.00000	-0.00000	-0.00000

卷之三

TABLE NUMBER 6		TABLE NUMBER 7	
6.00000	-0.00000	-0.00000	-0.00000
6.00000	-0.00000	-0.00000	-0.00000
6.00000	-0.00000	-0.00000	-0.00000
6.00000	-0.00000	-0.00000	-0.00000

NOZZLE INPUT DATA

NOZZLE TYPE DESIGNATION	0.0	ENGINE TYPE DESIGNATION	1.0
MAXIMUM DIAMETER - IN	38.6	NOZZLE BASE OUTER DIAM - IN	0.0
OVERALL PLUG LENGTH - IN	0.6	NOZZLE BOATTAIL LENGTH - IN	23.4
NOZZLE SPACING - IN	53.6	BASE FLOW AREA - SQ IN	0.0
BOATTAIL DRAG TABLE FLAG	0.6	BOATTAIL TRAILING EDGE ANGLE - DEG	10.00
PRIMARY SPECIFIC HEAT RATIO	1.35	A13 - SQ FT	-6.00

BASE DRAG TABLE

0.31000	0.33000	0.36000	0.39000	0.42000	0.46500	0.50000	0.53500	0.57000	0.60500	0.64000	0.67500	0.71000	0.74500	0.79000	1.00000	1.20000	1.60000	2.00000	-0.00000	-0.00000
0.31000	0.33000	0.36000	0.39000	0.42000	0.46500	0.50000	0.53500	0.57000	0.60500	0.64000	0.67500	0.71000	0.74500	0.79000	1.00000	1.20000	1.60000	2.00000	-0.00000	-0.00000

INTERFERENCE DRAG TABLE

0.31000	0.33000	0.36000	0.39000	0.42000	0.46500	0.50000	0.53500	0.57000	0.60500	0.64000	0.67500	0.71000	0.74500	0.79000	1.00000	1.20000	1.60000	2.00000	2.40000	2.70000	3.20000	3.60000	4.00000	4.40000	4.80000	5.20000	5.60000	6.00000	6.40000	6.80000	7.20000	7.60000	8.00000	8.40000	8.80000	9.20000	9.60000	10.00000	10.40000	10.80000	11.20000	11.60000	12.00000	12.40000	12.80000	13.20000	13.60000	14.00000	14.40000	14.80000	15.20000	15.60000	16.00000	16.40000	16.80000	17.20000	17.60000	18.00000	18.40000	18.80000	19.20000	19.60000	20.00000	20.40000	20.80000	21.20000	21.60000	22.00000	22.40000	22.80000	23.20000	23.60000	24.00000	24.40000	24.80000	25.20000	25.60000	26.00000	26.40000	26.80000	27.20000	27.60000	28.00000	28.40000	28.80000	29.20000	29.60000	30.00000	30.40000	30.80000	31.20000	31.60000	32.00000	32.40000	32.80000	33.20000	33.60000	34.00000	34.40000	34.80000	35.20000	35.60000	36.00000	36.40000	36.80000	37.20000	37.60000	38.00000	38.40000	38.80000	39.20000	39.60000	40.00000	40.40000	40.80000	41.20000	41.60000	42.00000	42.40000	42.80000	43.20000	43.60000	44.00000	44.40000	44.80000	45.20000	45.60000	46.00000	46.40000	46.80000	47.20000	47.60000	48.00000	48.40000	48.80000	49.20000	49.60000	50.00000	50.40000	50.80000	51.20000	51.60000	52.00000	52.40000	52.80000	53.20000	53.60000	54.00000	54.40000	54.80000	55.20000	55.60000	56.00000	56.40000	56.80000	57.20000	57.60000	58.00000	58.40000	58.80000	59.20000	59.60000	60.00000	60.40000	60.80000	61.20000	61.60000	62.00000	62.40000	62.80000	63.20000	63.60000	64.00000	64.40000	64.80000	65.20000	65.60000	66.00000	66.40000	66.80000	67.20000	67.60000	68.00000	68.40000	68.80000	69.20000	69.60000	70.00000	70.40000	70.80000	71.20000	71.60000	72.00000	72.40000	72.80000	73.20000	73.60000	74.00000	74.40000	74.80000	75.20000	75.60000	76.00000	76.40000	76.80000	77.20000	77.60000	78.00000	78.40000	78.80000	79.20000	79.60000	80.00000	80.40000	80.80000	81.20000	81.60000	82.00000	82.40000	82.80000	83.20000	83.60000	84.00000	84.40000	84.80000	85.20000	85.60000	86.00000	86.40000	86.80000	87.20000	87.60000	88.00000	88.40000	88.80000	89.20000	89.60000	90.00000	90.40000	90.80000	91.20000	91.60000	92.00000	92.40000	92.80000	93.20000	93.60000	94.00000	94.40000	94.80000	95.20000	95.60000	96.00000	96.40000	96.80000	97.20000	97.60000	98.00000	98.40000	98.80000	99.20000	99.60000	100.00000
0.31000	0.33000	0.36000	0.39000	0.42000	0.46500	0.50000	0.53500	0.57000	0.60500	0.64000	0.67500	0.71000	0.74500	0.79000	1.00000	1.20000	1.60000	2.00000	2.40000	2.70000	3.20000	3.60000	4.00000	4.40000	4.80000	5.20000	5.60000	6.00000	6.40000	6.80000	7.20000	7.60000	8.00000	8.40000	8.80000	9.20000	9.60000	10.00000	10.40000	10.80000	11.20000	11.60000	12.00000	12.40000	12.80000	13.20000	13.60000	14.00000	14.40000	14.80000	15.20000	15.60000	16.00000	16.40000	16.80000	17.20000	17.60000	18.00000	18.40000	18.80000	19.20000	19.60000	20.00000	20.40000	20.80000	21.20000	21.60000	22.00000	22.40000	22.80000	23.20000	23.60000	24.00000	24.40000	24.80000	25.20000	25.60000	26.00000	26.40000	26.80000	27.20000	27.60000	28.00000	28.40000	28.80000	29.20000	29.60000	30.00000	30.40000	30.80000	31.20000	31.60000	32.00000	32.40000	32.80000	33.20000	33.60000	34.00000	34.40000	34.80000	35.20000	35.60000	36.00000	36.40000	36.80000	37.20000	37.60000	38.00000	38.40000	38.80000	39.20000	39.60000	40.00000	40.40000	40.80000	41.20000	41.60000	42.00000	42.40000	42.80000	43.20000	43.60000	44.00000	44.40000	44.80000	45.20000	45.60000	46.00000	46.40000	46.80000	47.20000	47.60000	48.00000	48.40000	48.80000	49.20000	49.60000	50.00000	50.40000	50.80000	51.20000	51.60000	52.00000	52.40000	52.80000	53.20000	53.60000	54.00000	54.40000	54.80000	55.20000	55.60000	56.00000	56.40000	56.80000	57.20000	57.60000	58.00000	58.40000	58.80000	59.20000	59.60000	60.00000	60.40000	60.80000	61.20000	61.60000	62.00000	62.40000	62.80000	63.20000	63.60000	64.00000	64.40000	64.80000	65.20000	65.60000	66.00000	66.40000	66.80000	67.20000	67.60000	68.00000	68.40000	68.80000	69.20000	69.60000	70.00000	70.40000	70.80000	71.20000	71.60000	72.00000	72.40000	72.80000	73.20000	73.60000	74.00000	74.40000	74.80000	75.20000	75.60000	76.00000	76.40000	76.80000	77.20000	77.60000	78.00000	78.40000	78.80000	79.20000	79.60000	80.00000	80.40000	80.80000	81.20000	81.60000	82.00000	82.40000	82.80000	83.20000	83.60000	84.00000	84.40000	84.80000	85.20000	85.60000	86.00000	86.40000	86.80000	87.20000	87.60000	88.00000	88.40000	88.80000	89.20000	89.60000	90.00000	90.40000	90.80000	91.20000	91.60000	92.00000	92.40000	92.80000	93.20000	93.60000	94.00000	94.40000	94.80000	95.20000	95.60000	96.00000	96.40000	96.80000	97.20000	97.60000	98.00000	98.40000	98.80000	99.20000	99.60000	100.00000

PCODE 0.0 NO. ENGINES 2.0 ONE CARD INPUT/POINT 2.0

MACH NUMBER 0.0000		J79-6 F4 CONFIGURATION MS/Ms=.08	
CASE	CASE	CASE	CASE
ALT	1.000	ALT	ALT
PS	5.000	FS	
FNA	13732.990	FNA	
WFT RF	29234.480	WFT RF	
SFCA	2.121	SFCA	
FNRF	13792.990	FNRF	
FRAM	6.000	FRAM	
RF	8.800	RF	
MILRF	1.000	MILRF	
DINLET	0.000	DINLET	
CDSP1	6.000	CDSP1	
CDALD	5.000	CDALD	
CDRYP	6.000	CDRYP	
CDINL	3.000	CDINL	
DNOZ	6.000	DNOZ	
CDRT	0.000	CDRT	
CDBASE	6.000	CDHASE	
CDINT	6.000	CCINT	
DNOZ REF	6.000	DNOZ REF	
PA/P0	2.195	PA/P0	
A9	651.529	A9	
A8	650.252	A8	
CFG	1.000	CFG	
RFIA	1.000	RFIA	
FN INPUT	17000.600	FN INPUT	
WF INPUT	33221.290	WF INPUT	
SFC INPUT	1.954	SFC INPUT	
W INPUT	192.520	W INPUT	
W ABS	192.520	W ABS	
FN/DELTA	13732.990	FN/DELTA	
WF COR	29234.480	WF COR	
SFC COR	2.121	SFC COR	
TAMR	513.690	TAMR	
PAMB	2115.220	PAMB	
TT0	518.690	TT0	
Q	1.000	Q	
AGE/AC	2.000	AGE/AC	
ADIV/AC	6.000	ADIV/AC	
AD/AC	6.000	AD/AC	
STATUS	6.000	STATUS	

MACH NUMBER .250

J79-8 F4 CONFIGURATION HS/HG=.08

CASE	3.00C	CASE
ALT	3.00C	ALT
PS	1.00C	PS
FNA	14858.495	FNA
WFT RF	32224.555	WFT RF
SFCA	2.167	SFCA
FNPF	14859.391	FNPF
FRAM	1296.558	FRAM
RF	.95C	RF
WILDF	1.00C	WILDF
DINLET	3.00C	DINLET
CDSPL	3.00C	CDSPL
CDALD	3.00C	CDALD
CORYP	3.00C	CORYP
CDINL	3.00C	CDINL
DN02	42.083	DN02
COST	.03C	COST
CDBASE	3.00C	CDBASE
CDINT	.057	CDINT
DN02 RFF	21.187	DN02 RFF
PE/P0	2.218	PE/P0
A9	677.252	A9
A8	663.685	A8
CFG	1.00C	CFG
REFTA	11.154	REFTA
FN INPUT	15255.600	FN INPUT
WF INPUT	33925.655	WF INPUT
SFC INPUT	2.0394	SFC INPUT
W INPUT	192.427	W INPUT
W ARS	145.440	W ARS
FN/DELTA	14858.495	FN/DELTA
WF COR	32224.555	WF COR
SFC COR	2.167	SFC COR
TAMB	516.690	TAMB
PLMA	2116.225	PLMA
TT0	522.845	TT0
0	59.254	0
ADF/AC	3.00C	ADF/AC
ADI/AC	3.00C	ADI/AC
AD/AC	3.00C	AD/AC
STATUS	0.000	STATUS

MACH NUMBER .4000		J79-8 FL4 CONFIGURATION WS/WB=.06	
CASF	8.000	CASE	
ALT	15000.000	ALT	
PS	1.000	PS	
FI	9711.681	FIA	
AC	213a5.323	WFT RF	
SFCA	2.263	SFCA	
FNRF	9729.939	FNRF	
FRAM	15511.468	FRAM	
RF	.977	RF	
MILRF	.1.000	MILRF	
DNLE	0.220	DNLE	
CDSP	0.000	CDSP	
CDBL	0.000	CDBL	
CDYP	30.000	CDYP	
CDNL	0.000	CDNL	
DNOZ	66.031	DNOZ	
CDAT	0.030	CDAT	
CDASE	0.000	CDASE	
CDINT	0.031	CDINT	
DNOZ REF	47.773	DNOZ REF	
PSPD	2.414	PSPD	
A9	719.614	A9	
A6	693.725	A6	
CFG	10.000	CFG	
BETA	1.004	BETA	
FN INPUT	10110.600	FN INPUT	
WF INPUT	21899.000	WF INPUT	
SFC INPUT	2.168	SFC INPUT	
W INPUT	101.592	W INPUT	
W ABS	115.800	W ABS	
FN/DELTA	17228.591	FN/DELTA	
WF COR	43278.322	WF COR	
SFC COR	2.326	SFC COR	
TAMB	465.197	TAMB	
PAMB	1192.904	PAMB	
TTO	430.000	TTO	
0	133.600	0	
ACE/AC	0.000	ACE/AC	
AGT/AC	0.500	AGT/AC	
AC/AC	2.900	AC/AC	
STATUS	0.000	STATUS	

MACH NUMBER .6000 J79-8 F4 CONFIGURATION MS/M82.08

CASE	14.060	CASE
ALT	25000.000	ALT
PS	1.000	PS
FNA	7396.865	FNA
WFT RF	16533.200	WFT RF
SFCA	2.231	SFCA
FNRF	7411.908	FNRF
FRW	1713.657	FRW
RF	943	RF
MILRF	1.000	MILRF
DINLET	3.059	DINLET
CDSP1	0.005	CDSP1
CDBLD	2.050	CDBLD
COBYP	0.000	COBYP
CDINL	0.000	CDINL
DN02	62.913	DN02
COBT	0.325	COBT
COBASE	0.000	COBASE
COINT	0.326	COINT
DN02 REF	67.970	DN02 REF
P8/P0	2.677	P8/P0
A9	777.797	A9
A8	727.199	A8
CFG	1.050	CFG
BETA	0.654	BETA
FN INPUT	765C.000	FN INPUT
WF INPUT	1684C.000	WF INPUT
SFC INPUT	2.261	SFC INPUT
W INPUT	130.944	W INPUT
W ABS	9C.720	W ABS
FN/DELTA	13972.287	FN/DELTA
WF COR	48966.910	WF COR
SFC COR	2.452	SFC COR
TAMB	429.535	TAMB
PAHB	733.756	PAHB
Y10	450.452	Y10
Q	137.506	Q
AOE/AC	3.000	ACE/AC
AOI/AC	0.300	ACI/AC
AO/AC	3.000	AC/AC
STATUS	0.000	STATUS

MACH NUMBER .8000

J79-8 F4 CONFIGURATION

WS/WG=.08

CASE	22.000	CASE
ALT	35000.000	ALT
PS	1.000	PS
FNA	5673.231	FNA
WFT RF	1294.747	WFT RF
SFCA	2.275	SFCA
FNRF	5737.524	FNRF
FRAM	1671.950	FRAM
RF	984	RF
MILRF	1.000	MILRF
DINLET	37.450	DINLET
CDSP1	0.644	CDSP1
CDP1	0.013	CDP1
CDSP2	0.000	CDSP2
CDP1	0.958	CDP1
DNOZ	151.801	DNOZ
CDAT	0.013	CDAT
COBASE	0.000	COBASE
COINT	0.043	COINT
DNOZ REF	75.018	DNOZ REF
P8/P8	3.057	P8/P8
A9	855.624	A9
A9	771.312	A9
CFG	1.000	CFG
BETA	6.573	BETA
FN INPUT	5930.000	FN INPUT
WF INPUT	13114.000	WF INPUT
SFC INPUT	2.211	SFC INPUT
W INPUT	176.865	W INPUT
W ABS	69.126	W ABS
FN/DELTA	24180.239	FN/DELTA
WF COR	63117.599	WF COR
SFC COR	2.610	SFC COR
TAMB	373.874	TAMB
PAMB	496.518	PAMB
TT0	444.290	TT0
Q	222.446	Q
AOE/AC	542	AOE/AC
AOI/AC	547	AOI/AC
AO/AC	542	AO/AC
STATUS	0.000	STATUS

MACH NUMBER 1.2000

J79-6 F4 CONFIGURATION WS/WB=.05

CASE	36.000	CASE
ALT	45000.000	ALT
PS	1.000	PS
FNA	5279.403	FNA
HFT RF	123.5.503	HFT RF
SFC	2.331	SFC
FNRF	5517.351	FNRF
FRAM	2390.438	FRAM
RF	0.94	RF
MILRF	0.991	MILRF
DINLET	246.559	DINLET
COSPL	0.96	COSPL
COBAL	0.319	COBAL
COOP	0.300	COOP
COINL	0.116	COINL
DNOZ	0.0.308	DNOZ
CORT	0.061	CORT
CDRASE	0.089	CDRASE
CDINT	0.030	CDINT
DNOZ REF	0.0.620	DNOZ REF
PB/PD	4.090	PB/PD
A9	1139.512	A9
A8	867.924	A8
CFG	1.006	CFG
BETA	1.239	BETA
FN INPUT	5530.000	FN INPUT
WF INPUT	12403.000	WF INPUT
SFC INPUT	2.223	SFC INPUT
W INPUT	179.556	W INPUT
W ABS	63.723	W ABS
FN/DELTA	36144.775	FN/DELTA
WF COR	97152.437	WF COR
SFC COR	2.682	SFC COR
TAN9	399.970	TAN9
PAMB	399.102	PAMB
TT3	502.281	TT3
Q	311.574	Q
AOE/AC	0.537	AOE/AC
AOI/AC	0.756	AOI/AC
AO/AC	0.517	AO/AC
STATUS	0.000	STATUS

MACH NUMBER 1.6COC J79-8 F4 CONFIGURATION MS/MC = .88

CASE	46.000	CASE
ALT	36630.000	ALT
PS	1.333	PS
FNA	12317.271	FNA
WFT RF	27055.274	WFT RF
SFCA	2.197	SFCA
FMRF	13044.352	FMRF
FRAM	7471.331	FRA1
RF	935	RF
MJRF	962	MJRF
DINLET	795.332	DINLET
CCSPL	1.07	CCSPL
CCRD	0.623	CCRD
CCRP	0.606	CCRP
CCRL	0.130	CCRL
DNOZ	45.533	DNOZ
CDAT	0.000	CDAT
CDASE	5.052	CDASE
CDINT	0.356	CDINT
DNOZ REF	93.783	DNOZ REF
P8/P8	6.466	P8/P8
A9	1170.214	A9
A8	912.564	A8
CFG	0.998	CFG
BETA	-0.312	BETA
FN INPUT	13635.090	FN INPUT
WF INPUT	27843.515	WF INPUT
SFC INPUT	2.047	SFC INPUT
W INPUT	172.430	W INPUT
W AUS	152.448	W AUS
FN/DELTA	52497.668	FN/DELTA
WF COR	132322.357	WF COR
SFC COR	2.521	SFC COR
TAN	373.874	TAN
PAMB	416.519	PAMB
Y10	575.537	Y10
Q	819.761	Q
A0E/AC	• 598	A0E/AC
A0I/AC	• 619	A0I/AC
A0/AC	• 598	A0/AC
STATUS	5.000	STATUS

MACH NUMBER 2.0000

J79-8 F4 CONFIGURATION WS/WE=.08

DEC

CASE	55.000	CASE
ALT	35020.200	ALT
PS	1.000	PS
FNA	14972.637	FNA
WFT RF	34136.936	WFT RF
SFCA	2.284	SFCA
FNPF	15843.340	FNPF
FRAM	12273.013	FRAM
RF	.934	RF
MILRF	.925	MILRF
DINLET	947.139	DINLET
CDSP1	.073	CDSP1
COBL0	.026	COBL0
COBYP	.0.000	COBYP
CDINL	.100	CDINL
DNOZ	31.245	DNOZ
CDRT	.000	CDRT
CDASE	0.330	CDASE
CDINT	.053	CDINT
DNOZ REF	131.621	DNOZ REF
P8/PC	8.241	P8/PC
A9	1176.214	A9
A8	835.164	A8
CFG	.968	CFG
BETA	-.012	BETA
FN INPUT	16716.000	FN INPUT
WF INPUT	34990.000	WF INPUT
SFC INPUT	2.096	SFC INPUT
W INPUT	139.789	W INPUT
W ABS	2.3.340	W ABS
FN/DELTA	63915.156	FN/DELTA
WF COR	16728.493	WF COR
SFC COR	2.621	SFC COR
TAMR	393.874	TAMR
PAMR	436.518	PAMR
TT0	718.973	TT0
Q	1323.251	Q
AGE/AC	.633	AGE/AC
AOI/AC	.663	AOI/AC
AC/AC	.632	AC/AC
STATUS	5.005	STATUS

REFERENCES

1. Petersen, M. W., and Tamplin, G. C., Experimental Review of Transonic Spillage Drag of Rectangular Inlets, AFAPL-TR-66-30, May 1966.
2. Kirkbride, E. B., Wind Tunnel Test on the 5 Percent Scale F-4J Pressure Model in the McDonnell Polysonic Wind Tunnel, MDC A1045, Volume 1, 17 June 1971.
3. McVey, F. D., Rejeske, J. V., and Phillips E. J., Experimental Evaluation of Inlet Drag Characteristics in the Transonic Mach Number Regime, AFAPL-TR-68-119, November 1968.
4. Anderson, R. D., Keller, K. J., and Nieser, D. E., Exhaust System Interaction Program: Analysis of Wind Tunnel Data on a 5 Percent Scale F-4 Jet Effects Model in the McDonnell Polysonic Wind Tunnel, PSWT Test 295, MDC A1333, Volume I, January 1972.
5. Gould, D. K., and Eastman, D. W., Methods Used to Determine Aerodynamic Drag and Installed Propulsion Thrust for the Boeing Lightweight Fighter, D199-10003-1, The Boeing Company, November 1972.
6. Ross, P. A., Lightweight Fighter Propulsion System Development, D180-14475-1 TN, The Boeing Company, January 1973.

Unclassified

Security Classification

PRECEDING PAGE BLANK-NOT FILMED

DOCUMENT CONTROL DATA - R & D

(Security classification of title, body of abstract and indexing annotation must be entered when the overall report is classified)

1. ORIGINATING ACTIVITY (Corporate author) The Boeing Company P. O. Box 3999 Seattle, WA 98124	2a. REPORT SECURITY CLASSIFICATION Unclassified
	2b. GROUP

1. REPORT TITLE
Propulsion System Installation Corrections
Volume III: Sample Cases

4. DESCRIPTIVE NOTES (Type of report and inclusive dates)
Final Report 31 December 1971 to 31 December 1972

5. AUTHOR(S) (First name, middle initial, last name)
William H. Ball

6. REPORT DATE December 1972	7a. TOTAL NO. OF PAGES xii + 80 = 92	7b. NO. OF REFS 6
8a. CONTRACT OR GRANT NO F33615-72-C-1580	9a. ORIGINATOR'S REPORT NUMBER(S) AFFDL-TR-72-147	
b. PROJECT NO. 1366	9b. OTHER REPORT NO(S) (Any other numbers that may be assigned this report) d.	
10. DISTRIBUTION STATEMENT Distribution limited to U.S. Government agencies only; test and evaluation; statement applied 29 December 1972. Other requests for this document must be referred to Air Force Flight Dynamics Laboratory, (PTB), Wright-Patterson Air Force Base, Ohio 45433		
11. SUPPLEMENTARY NOTES	12. SPONSORING MILITARY ACTIVITY Flight Dynamics Laboratory Air Force Systems Command Wright-Patterson Air Force Base, OH	

13. ABSTRACT
This report presents the results of a research program to develop a procedure for use in calculating propulsion system installation losses. These losses include inlet and nozzle internal losses and external drag losses for a wide variety of subsonic and supersonic aircraft configurations up to Mach 4.5. The calculation procedure, which was largely developed from existing engineering procedures and experimental data, is suitable for preliminary studies of advanced aircraft configurations. Engineering descriptions, equations, and flow charts are provided to help in adapting the calculation procedures to digital computer routines. Many of the calculation procedures have already been programmed on the CDC 6600 computer. Program listings and flow charts are provided for the calculation procedures that have been programmed. The work accomplished during the program is contained in four separate volumes. Volume I contains an engineering description of the calculation procedures. Volume II is a programmers manual containing flow charts, listings, and subroutine descriptions. Volume III contains sample calculations and sample input data. Volume IV contains bookkeeping definitions and data correlations.

Unclassified

Security Classification

KEY WORDS	LINK A		LINK B		LINK C	
	ROLE	WT	ROLE	WT	ROLE	WT
Afterbody Drag						
Boattail Drag						
Bookkeeping Aero-Propulsion Forces						
Boundary Layer Bleed Drag						
Bypass Drag						
Inlet Performance						
Inlet Shock Losses						
Nozzle/Afterbody Installation Losses						
Nozzle Interference Drag						
Nozzle Thrust Coefficient						
Propulsion Installation Losses						
Spillage Drag						
Subsonic Diffuser Losses						
Supersonic Inlets						
Total Pressure Recovery						